



School of GeoSciences

DISSERTATION

For the degree of

MSc in Geographical Information Science

William Blomstedt

August 2014

COPYRIGHT STATEMENT

Copyright of this dissertation is retained by the author and The University of Edinburgh. Ideas contained in this dissertation remain the intellectual property of the author and their supervisors, except where explicitly otherwise referenced.

All rights reserved. The use of any part of this dissertation reproduced, transmitted in any form or by any means, electronic, mechanical, photocopying, recording, or otherwise or stored in a retrieval system without the prior written consent of the author and The University of Edinburgh (Institute of Geography) is not permitted.

STATEMENT OF ORIGINALITY AND LENGTH

I declare that this dissertation represents my own work, and that where the work of others has been used it has been duly accredited. I further declare that the length of the components of this dissertation is 5259 words (including in-text references) for the Research Paper and 7917 words for the Technical Report.

Signed:

Date:

ACKNOWLEDGEMENTS

I would like to recognize the faculty and staff of the University of Edinburgh Geosciences Department for the instruction and guidance this school year. Special acknowledgements to Bruce Gittings, William Mackaness, Neil Stuart and Caroline Nichol for sound thoughts and dissertation advice. I also extend a kind thank you to my advisor Alasdair MacArthur for agreeing to undertake this project with me.

Thanks to all my fellow students on this MSc program.

For the extensive effort learnt to providing scale-hive data I am in debt to

- Ari Seppälä, Finnish Beekeepers Association, MTT Agrifood Research Finland, Seppo Korpela, Sakari Raiskio
- Jure Justinek and Čebelarske zveze Slovenije
- René Zumsteg and Verein Deutschschweizerischer Und Rätoromanischer Bienenfreunde, Swise
- Centre Apicole de Recherche et Information

For his kindness and help starting this project I would like to distinguish Dr. Janko Božič. Thanks Janko.

I was able to undertake this year of study partly due to the support from the Eva Crane Trust. Thank you to the trustees as well as Eva Crane herself, who has been a main inspiration me on this journey.

Finally, my family, to whom I owe everything – Mother, Father, Grandpa Frank, Sister – Love and Thanks.

Mapping The Phenology of European Honey Bee Nectar Flows

Part I: Research Paper

ii. ABSTRACT

Insect pollination is vital to both the health of our ecosystem and food production. Consequently, it is important to understand how the phenology of both pollinators and plants will be influenced by global climate change. Current satellites allow a near-daily synoptic view of the entire earth, but it is difficult linking the imagery with *in situ* events because of the difference in scale between a point and pixel. Due to their generalized foraging on a variety of plants in the 100 km² surrounding their hive, honey bees operate at a scale which may be compared to satellite data. The MODIS Aqua and Terra satellites produce daily images of the earth and the Normalized Differentiation Vegetation Index (NDVI) is able to show the “green-up” or start of spring (SOS). Locally, the phenology of nectar-producing flowers can be inferred from the honey bee nectar flow (HBNF), which is measured by the weight gain of a honey bee hive. This research investigates the link between smoothed, gap-filled NDVI data, and weight gain of hives in Slovenia, Switzerland, Belgium and Finland during 2009-2012. No correlation was found between the SOS and HBNF start day, but a notable relationship ($R^2=0.73$) was seen between NDVI SOS and HBNF midpoint (50% day) within the Alps and broadleaf forests of central Europe. This indicates that HBNF can be related to continental MODIS climate models, and that nectar flows have been advancing 0.54 days per year in central Europe.

iii. TABLE OF CONTENTS

i. TITLE PAGE.....	1
ii. ABSTRACT.....	2
iii. TABLE OF CONTENTS.....	3
iv. LIST OF ABBREVIATIONS AND ACRONYMS.....	4
1. INTRODUCTION.....	5
1.1 POLLINATION.....	5
1.2 HONEY BEES.....	5
1.3 SATELLITE REMOTE SENSING.....	6
1.4 LINKING SATELLITE WITH HBNF.....	6
1.5 RESEARCH QUESTION AND HYPOTHOSIS.....	7
2. LITERATURE REVIEW.....	8
2.1 HONEY BEES.....	8
2.2 FORAGE.....	8
2.3 SCALE-HIVE.....	8
2.4 NORMALIZED DIFFERENCE VEGETATION INDEX.....	9
2.5 LINKING NDVI WITH GROUND MEASUREMENTS.....	10
2.6 CALCULATING SOS.....	10
2.7 LSP AND HONEYBEES.....	11
3. DATA AND METHODS.....	12
3.1 STUDY AREAS.....	12
3.2 DIGITAL MAP OF EUROPEAN ECOLOGICAL REGIONS.....	14
3.3 SCALE-HIVE DATA.....	14
3.3.1 SLOVENIA.....	14
3.3.2 BELGIUM.....	15
3.3.3 SWITZERLAND.....	16
3.3.4 FINLAND.....	17
3.4 HONEY BEE NECTAR FLOW METRICS.....	18
3.5 MODIS NDVI.....	18
3.6 TIMESAT.....	19
4. RESULTS.....	20
4.1 HBNF DATA.....	20
4.2 START OF SEASON – HBNF METRICS.....	21
4.3 TWO SCENARIOS.....	24
5. DISCUSSION.....	27
6. CONCLUSION.....	29
7. DATA CITATION.....	31
7.1 MODIS.....	31
7.2 SCALE-HIVE DATA.....	31
7.3 DMEER.....	31
8. BIBLIOGRAPHY.....	32

iv. LIST OF ABBREVIATIONS AND ACRONYMS

ACMF – Alps Conifer and Mixed Forests

AVHRR – Advanced Very High Resolution Radiometer

DMEER – Digital Map of European Ecological Regions

EVI – Enhanced Vegetation Index

GIS – Geographical Information Science

HBNF – Honey Bee Nectar Flow

LSP – Land Surface Phenology

LST – Land Surface Temperature

MODIS – Moderate Resolution Imaging Spectroradiometer

NDVI – Normalized Difference Vegetation Index

NF – Nectar Flow

NIR – Near-Infrared Radiation

ORNL DAAC – Oak Ridge National Laboratory Distributed Active Archive Center

QA – Quality Assurance

SOS – Start of Season

VI – Vegetation Index

VIIRS – Visible Infrared Imaging Radiometer Suite

WEB – Western European Broadleaf Forests

1. INTRODUCTION

1.1 POLLINATION

Pollination is a vital part of sustaining our ecosystems and agricultural production. Almost 90% of all plant species rely on an animal visitor to transfer pollen between individuals for fertilization and reproduction (Ollerton et al., 2011). Invertebrates are the most common pollinators and an estimated 85% of European crops depend on, or benefit from, insect pollination (Williams, 1994). A variety of reports have attempted to quantify the value of pollination (Calderone, 2012) with one estimate assigning a global annual sum of €153 billion (Gallai et al., 2009). The monetary service of pollinators in wild ecosystems is even more difficult to estimate, as they are considered fundamental contributors to global biodiversity. Without their often unacknowledged work, food-webs may be disrupted, affecting us in ways difficult to quantify. Yet many pollinators face the threat of forage and habitat reduction through land development, degradation and agricultural intensification (Tilman et al., 2001). This pressure will likely continue (Potts et al., 2010).

In recent years the majority of evidence has shown our climate is changing rapidly (Walther et al., 2002; Stocker et al., 2013). One concern is the spatial or temporal disruption of pollinator and plant phenologies, leading to trophic decoupling (Visser and Both, 2005; Parmesan, 2006; National Research Council, 2007). Several studies have shown alterations in trophic relationships or energy flows in both predator-prey and plant-herbivore interactions as a consequence of changing temperatures (reviewed by Stenseth and Myrsetrud, 2002). Others have shown a rapid change in flowering time (Fitter and Fitter, 2002). However, there are hundreds of thousands of flowering plant species and tens of thousands of pollinating insect species (Ollerton et al., 2011) many of which appear to be in decline (Biesmeijer et al., 2006). Dependencies, abundances and the response to climate change of many species are not well known. Because of the massive number of species and the rapidness of which the climate and ecosystems are changing, it is necessary to further understand these interactions. A first step is to look at a general pollinator's relationship with its changing forage.

1.2 HONEY BEES

The European honey bee (*Apis mellifera*) is often considered the most important pollinator due to its generalized foraging behaviour and relative ease in management (McGregor, 1976). Honey bees gather food in the form of nectar and pollen produced by flowers at certain times of the year. A time of profuse foraging due to high nectar availability is called a honey bee nectar flow (HBNF), which can be measured by placing a hive on a scale (scale-hive) and recording the weight daily. While the phenology of flowering and leafing has been frequently studied, (e.g. Menzel et al., 2006) little work has been done on understanding the changing of HBNFs. Certain areas of the U.S.

have shown an advancing of nectar flows in Maryland (Esaias et al., 2011) which are similar to advancing floral bloom in Washington D.C (Abu-Asab et al., 2001). Similarly, Bartomeus et al. (2011) showed phenologies of bee species advancing with their floral partners.

Advancing springs or warmer temperatures would have a significant impact on beekeepers. Bee forage would be profoundly influenced by a shift in plant species distribution due to temperature (Thuiller et al., 2005). Also, the length of nectar flows are not known to increase with earlier springs; instead bees will have longer periods of activity when they are consuming stores at a higher rate, forcing total honey yields to shrink and beekeepers to provide supplemental sugar feed. Beekeepers frequently use sub-species of honey bees adapted to their local climate, and a change in seasonal timing may make using their sub-species unmanageable. The ability to understand how HBNFs are occurring at a landscape level would benefit beekeepers, and this may be possible through the use of satellite remote sensing.

1.3 SATELLITE REMOTE SENSING

Satellite remote sensing is frequently used in large scale phenological studies and has the potential to relate to HBNFs. Remote sensing's advantages include repeated, synoptic views over a large territory, as well as the ability to analyse archival images back to the 1980s (Reed et al., 2009). The Normalized Differential Vegetation Index (NDVI) is a graphical indicator used for monitoring vegetation changes and interpreting of the impact of climatic events on the biosphere (Zhou et al., 2001; Zhang et al., 2003; Pettorelli et al., 2005). However it is difficult to translate the NDVI measurement to phenological observations on the ground due to the difference in scale between a point (single flower/tree) and a remote sensing pixel (250 x 250 metres or more) (White et al., 2009; Schwartz and Hanes, 2010).

1.4 LINKING SATELLITE WITH HBNF

Because they forage on many different floral species within 6 km of their hive, honey bees hold interesting potential to compare with the satellite data, which is collected at a similar spatial scale. Nightingale et. al. (2008) observed that a study by Zhang et. al. (2007), which analysed vegetation phenology derived from a 24 year time-series of Advanced Very High Resolution Radiometer (AVHRR), corresponded directly with an advance in peak nectar flow as measured by a scale-hive in Maryland. To investigate this further they calculated 5 scale-hive metrics (Peak, Average peak, Beginning (0.05 of weight gain), Mid point and End (0.95 of weight gain)) against Moderate Resolution Imaging Spectrometer (MODIS) NDVI phenology and found the strongest correlation between the Midpoint (50% scale-hive peak) and NDVI ($R^2 = 0.8$). Furthermore, Esaias et. al. (2011), who oversees a network of scale-hives in the United States, reported a correlation

($r^2=0.737$, $n=61$) between MODIS NDVI and 50% nectar flow in the tree-dominated Eastern North America.

1.5 RESEARCH QUESTION AND HYPOTHOSIS

In order to better understand changing phenologies of plants and bees, this research will investigate if a similar correlation exists in parts of Europe where detailed scale-hive records have been made available for research. HBNF metrics will be calculated with scale-hive data from 2009-2012 in Slovenia, Belgium, Switzerland and Finland, and a link between these and satellite data will be explored. Following research in the U.S., it is hypothesized that certain ecological zones, notably temperate forests, will show a correlation between the MODIS-derived SOS and the mid-point of the nectar flow.

Specifically this research will address the following questions:

1. Does a relationship exist between NDVI and HBNF in Europe?
 - 1.1. Is there a metric (HBNF start, HBNF 50%) which shows the strongest correlation?
2. Do certain years have a stronger relationship than others?
3. Do certain countries have a stronger relationship than others?
4. Does the relationship differ spatially depending on land cover or ecological region?

2. LITERATURE REVIEW

2.1 HONEY BEES

The European honey bee is one of seven species in the genus *Apis*. It is a eusocial insect, living a complex social system in large colonies of up to 80,000 members. Nectar and pollen comprise the complete honey bee diet, with colonies requiring 120 kg of nectar and 20 kg of pollen annually (Seeley, 1995). Bees process and dehydrate the nectar to store it as honey. Unlike many wild bee species, which have an obligate larval or adult diapause during the winter, honey bees remain active within a cluster and regulate temperature by physically generating heat with their wing muscles. Without sufficient honey collected during the spring and summer, the bees will perish from cold and starvation.

2.2 FORAGE

To gather food and water honey bees need to leave the hive and enter the surrounding environment. A colony acts as a large, connected entity which can spread in separate directions over great distances simultaneously. Scout bees must expeditiously scour the landscape to discover sources of nectar or pollen shortly after they come into bloom. They are quite effective at finding forage; a colony was shown to have a 0.5 probability of finding a small patch of flowers (100 m², equal to 1/125,000 of their average search area) within 2000 meters of their hives (Seeley, 1987).

With the flowers found, the scout bees must quickly return to recruit other foragers before the weather changes, blossoms fade or darkness descends. The scouts communicate the distance, direction and quality of the flower patch to other foragers through a precise dance language first decoded by Karl Von Frisch (1967). Honey bees are highly economical foragers and register the profitability of a nectar source by sensing the energetic efficiency of their foraging (Seeley, 1994). With the information from a number of scouts, nearly a quarter of the hive – several thousand bees – will commence in foraging on a few of these high quality patches. This process is continually evaluated throughout the day as weather and nectar conditions change (Visscher and Seeley, 1982).

2.3 SCALE-HIVE

In North America and Europe, HBNFs typically are short and profuse (a matter of weeks) where honey bees must gather as much food as possible to survive long periods of dearth (Seeley, 1995). A hive will gain weight when the bees are harvesting nectar, and a common practice for both beekeepers and researchers is to keep a hive on a stationary scale and record the daily or weekly weight to better understand the current status of the colony (McLellan, 1977; Szabo and Lefkovitch, 1991; Harbo, 1993). Weighing is fast, requires little training, does not disturb the bees and can be done at any time of the year. The daily running average, which is the average of all weights 12

hours before after that point, represents the change in food stores with a reasonable degree of confidence (Meikle et al., 2008).

Buchmann and Thoenes (1990) first proposed the use of an electronic scale, which when connected with a datalogger, provides a continuous weighing of the hive (Meikle et al., 2006). The past decade has seen a rise in use of electronic scales by researchers and beekeeping associations in Europe and North America. Weighing hives precisely and frequently can produce within-day variation and show useful information on colony dynamics and daily ecology. If shared or published, this scale-hive data becomes a historical educational record. When looked at over a number of years, it can possibly detect land-cover and/or climate-related changes. While scale-hives are collected at an *in situ* point, they reflect the status of many square kilometres – a similar scale to satellite imagery.

2.4 NORMALIZED DIFFERENCE VEGETATION INDEX

One of the most common uses of satellite imagery is to monitor the biosphere and NDVI is a frequently-used indicator of vegetation (Tucker, 1979; Sellers, 1985). Satellite-derived NDVI data has the potential to provide temporal indicators of the onset, end, peak and duration of vegetation greenness as well as the rate of growth, senescence and periodicity of photosynthetic activity (Reed et al., 1994; Myneni et al., 1997). The theoretical basis for empirical-based vegetation indices is derived from the typical spectral reflectance of leaves; reflected energy is low in the visible spectrum as a result of high absorption by photosynthetically active pigments, with maximum absorption in the blue (~470nm) and red (~678 nm) wavelengths (Jensen, 2006). Much of the near-infrared radiation (NIR) is scattered making the contrast between red and NIR a sensitive measure of vegetation quantity. Maximum red-NIR differences occur over a full canopy and minimal occur when there is little to no vegetation. NDVI is a normalized transform of the NIR to red reflectance ratio (Equation 1) designed to standardize vegetation index (VI) values to between -1 and +1 (Deering and Rouse, 1975; Solano et al., 2010):

$$NDVI = \frac{\rho_{NIR} - \rho_{red}}{\rho_{NIR} + \rho_{red}} \quad \text{Equation 1}$$

where ρ_{NIR} is infrared and ρ_{red} is red reflectance.

The MODIS algorithm calculates NDVI red and near-infrared reflectance centred at 645-nanometres and 858-nanometres respectively (Huete et al., 1999) and is computed from atmospherically correlated bi-direction surface reflectances that have been masked for water, clouds, heavy aerosols and cloud shadows. MODIS is an important part of the continuing NDVI

record begun in 1982 by AVHRR, and its products were designed to provide consistent spatial and temporal comparisons of global vegetation conditions in support of change detection and phenological and biophysical interpretations (Huete et al., 2002; Justice et al., 2002). With the ability of remote sensing to work at a regional or continental scales, modelling phenological patterns related to climate change has become possible (Schwartz and Reed, 1999; De Beurs and Henebry, 2004; Zhang et al., 2007, 2009).

2.5 LINKING NDVI WITH GROUND MEASUREMENTS

Linking traditional phenological indicators like budburst, leafing, flowering and senescence with remote sensing has great potential to enhance our ability to track the biotic response to climate change (Beaubien and Hall-Beyer, 2003). Yet finding connection has been elusive due to spatial and temporal scale mismatch, complex data interpretation and additive noise from several factors including atmospheric disturbances, solar radiation effects, cloud cover or snow cover (Reed et al., 1994; Schwartz and Reed, 1999; Zhou et al., 2001; White et al., 2005).

Because vegetation observed by satellite sensors integrates signals from abiotic and biotic surfaces, there is a distinct difference between the measurement of individual plant events and satellite-based phenology, which is often called land surface phenology (LSP) (De Beurs and Henebry, 2004). One frequently sought after measure of LSP is the start of season/spring (SOS), also known as the “green up” or “green wave.” The SOS is defined as the rapid sustained increase in remotely-sensed greenness after the longest annual period of photosynthetic senescence (White et al., 2009). SOS is an interconnected composite of biospheric events that is of special interest in the mid-latitudes, as it appears to be important for accurate computation of net primary productivity (Running and Nemani, 1991; White et al., 1999), a sensitive measure of the impacts of global change (Schwartz and Reiter, 2000; Menzel et al., 2001) and connected with springtime changes in net ecosystem exchange, sensible heat and latent heat fluxes (Wilson and Baldocchi, 2000; Schwartz and Crawford, 2001).

2.6 CALCULATING SOS

There have been many methods devised to calculate SOS (de Beurs and Henebry, 2010). However the nature of satellite data makes it difficult to extract phenological metrics directly, and the data often requires quality screening and smoothing to minimize atmospheric noise or compensate for the absence of data. A major hurdle in comparing SOS to ground measurements is the lack of observations sufficient to account for spatial heterogeneity at the landscape scale. Efforts have been made to compare satellite phenology with ground-based phenology models (Schwartz and Reed, 1999; Schwartz et al., 2002). Others have modified point sampling phenology by

upscaling high density/frequency observations (Liang et al., 2011) or supplemented medium resolution imagery (50 m) to bridge coarse resolution (500m) and plot level phenology (Fisher et al., 2006). The success of these studies suggests that sampling phenology at landscape level holds the best promise to bridge the gap between *in situ* measurements and satellite imagery.

2.7 LSP AND HONEYBEES

Because NDVI measures the greenness of the landscape generated mainly by leaves, many LSP studies have tried to link SOS with bud-burst. Leafing is an unimportant phenological event for honey bees. However Studer et al., (2007) found a multi-species index, including the flowering of several species, correlated with the SOS, and Zhang et al., (2006) showed a relationship between the mean NDVI SOS and mean flowering date of *in situ* measurements across Canada. While NDVI does not measure flowering directly, continental NDVI is best explained by temperature and precipitation variations (Los et al., 2001); two factors which are also important for flowering and nectar flow.

Unlike a flower or a tree, which is a static point representing a single species, a honey bee colony operates on a similar spatial scale as satellite data. Foraging honey bees cover 100 km² surrounding the hive and interact with a range of melliferous and pollen-producing species (Visscher and Seeley, 1982). The combination of the scale at which they operate as well as generalist foraging provide a novel form of *in situ* phenology which can be related to satellite LSP.

3. DATA AND METHODS

3.1 STUDY AREAS

Study areas were limited to locations in Slovenia, Belgium, Switzerland and Finland with available scale-hive data (Figure 1, Table 1). Three sites were selected from each country with the criteria of having precise, regularly-collected data from two or three spring seasons during 2009-2013. Certain records included notes on the species providing the nectar flow (NF) and hive manipulations i.e. feeding, adding honey supers or harvesting honey. Days with hive manipulations were adjusted to a null change. Other inconsistencies such as large weight losses (>2 kg), isolated weight gains during nectar dearth and large weight gains (>10 kg) were also removed from the data and replaced with a null change.

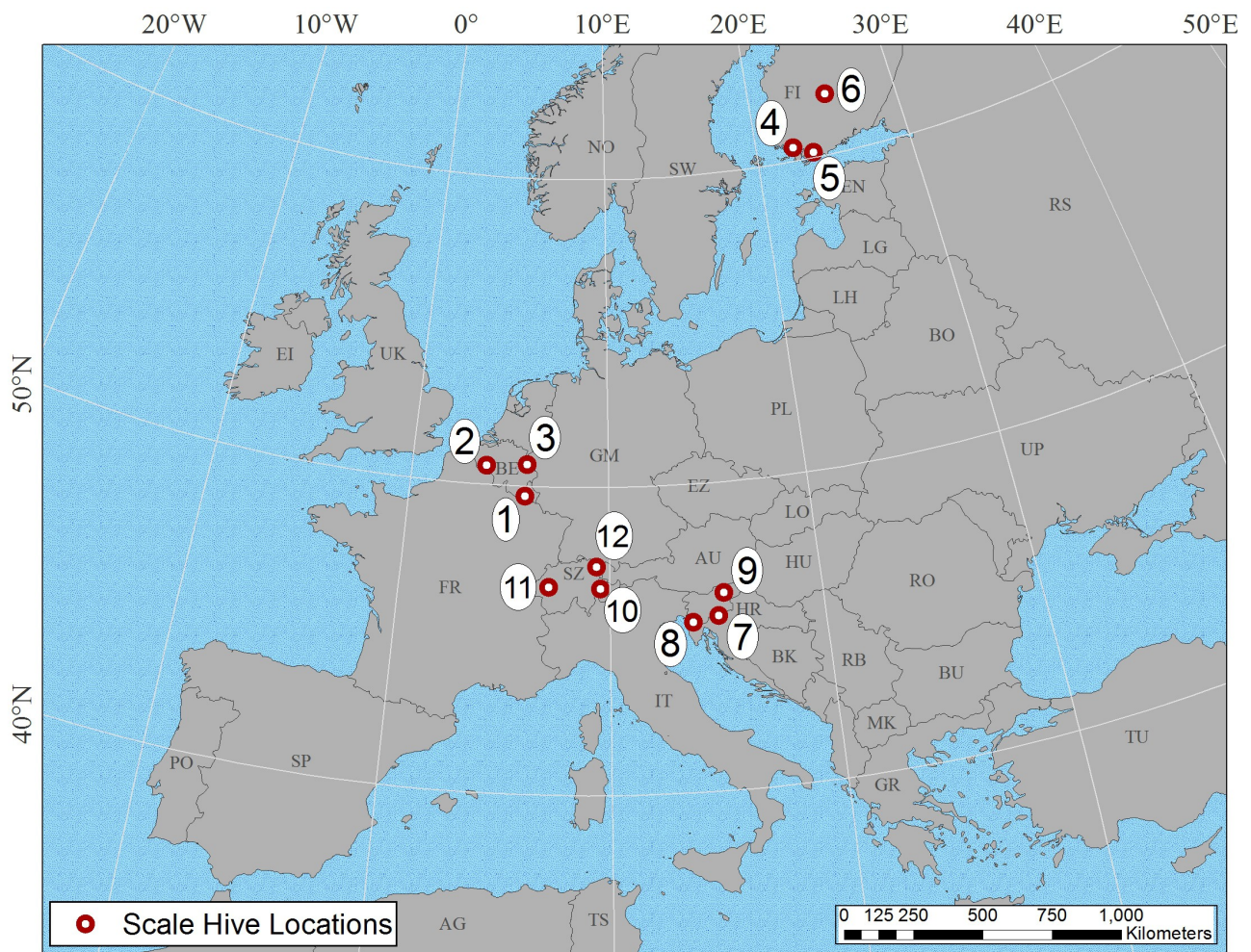


Figure 1: Locations of scale-hives

ID	Country	Hive Location	Hive Type	Y	X	Elev.(m)	DMEER	Surrounding Forage	Hive Data Availability				
									2009	2010	2011	2012	2013
1	Belgium	Arlon	Unknown	49.683265	5.799919	376	Western European Broadleaf forests	Rapeseed, urban gardens, forest		X	X	X	
2	Belgium	Ath	Unknown	50.628907	3.761358	38	Southern Temperate Atlantic	Hedgerows, urban gardens		X	X		
3	Belgium	Aubel	Unknown	50.704825	5.857697	225	Southern Temperate Atlantic	Acacia, Maize, Apple, Hawthorn		X	X		
4	Finland	Kaarina	Langstroth	60.43597	22.43225	38	Sarmatic mixed forests	Unknown			X	X	X
5	Finland	Karjalohja	Langstroth	60.18339	23.65175	53	Scandinavian and Russian taiga	Unknown			X	X	
6	Finland	Jämsä	Langstroth	61.96423	25.30072	117	Scandinavian and Russian taiga	Unknown			X	X	
7	Slovenia	Kočevski Rog – Podstenice	AŽ	45.708642	15.029349	535	Pannonian mixed forests	Oak, maple, fir, lime, spruce		X	X	X	
8	Slovenia	Koper – Dekani	AŽ	45.541377	13.832958	65	Illyrian deciduous forests	Oak, Chestnut, Ash, Acacia		X	X	X	
9	Slovenia	Zreško Pohorje	AŽ	46.440454	15.351017	1143	Alps conifer and mixed forests	Maple, fir, red pine, spruce, cherry		X	X	X	
10	Switzerland	Obervaz	CH-Box	46.715093	9.537611	1162	Alps conifer and mixed forests	Mountain flowers, Hedges, forest	X		X	X	
11	Switzerland	Posieux (Grangeneuve)	Dadant	46.764327	7.09769	630	Western European Broadleaf forests	Meadow, orchard, forest, hedgerows	X	X	X		
12	Switzerland	St. Gallen	Modified CH-box	47.425059	9.376588	671	Western European Broadleaf forests	Urban gardens, Fruit trees, Mixed forest			X	X	

Table 1: Geographical data of scale-hives. All bees are *Apis mellifera*, subspecies unknown

3.2 DIGITAL MAP OF EUROPEAN ECOLOGICAL REGIONS

The Digital Map of European Ecological Regions (DMEER) delineates and describes ecological distinct areas in Europe based on climatic, topographic and geobotanical European data. The map of ecological regions attempts to show the extent of areas with relatively homogeneous ecological conditions, within which, comparisons and assessments of different expressions of biodiversity are meaningful (Painho et al., 1996). DMEER (2000) was derived from work done by Bunce (1995) and Bohn (1994). Because no honey bee forage map of Europe exists, DMEER was used to assign hives ecological zones for means of comparison.

3.3 SCALE-HIVE DATA

3.3.1 SLOVENIA

Scale-hive data was acquired through personal communication with Jure Justinek of Čebelarske zveze Slovenije. Data was provided in the form of daily weight change and a suitable weight (30 kg) was assigned at the beginning of season. Location data was found on the website: <https://eobelar.czs.si> (Figure 2)

3.3.2 BELGIUM

Belgian scale-hive data was acquired through the Centre Apicole de Recherche et Information. Scale-hive data was collected automatically every two hours throughout the day (0600-2200), but the weight used in this research came from the day's final weigh-in (2200). Weight and location data were acquired through the website: <http://www.cari.be/balances/> (Figure 3)

3.3.3 SWITZERLAND

Swiss scale-hive data was acquired through Verein Deutschschweizerischer Und Rätoromanischer Bienenfreunde (VDRB) <http://www.vdrb.ch/service/waagvlker.html>. The hive weight was collected by datalogger every two hours from 0500-2100 and uploaded to a central server. Data contained very few notes and website stated that large variations in weight were not commented upon and the viewer must use their own judgement. Coordinates were given through personal communication with René Zumsteg of VDRB (Figure 4).

3.3.4 FINLAND

Finish scale-hive data and locations were acquired personal communication with Ari Seppälä, Beekeeping Advisor of Finland (Figure 5). Data for Finish hives was from 2011-2012, with one season in Kaarina in 2013. No notes were provided with the data.

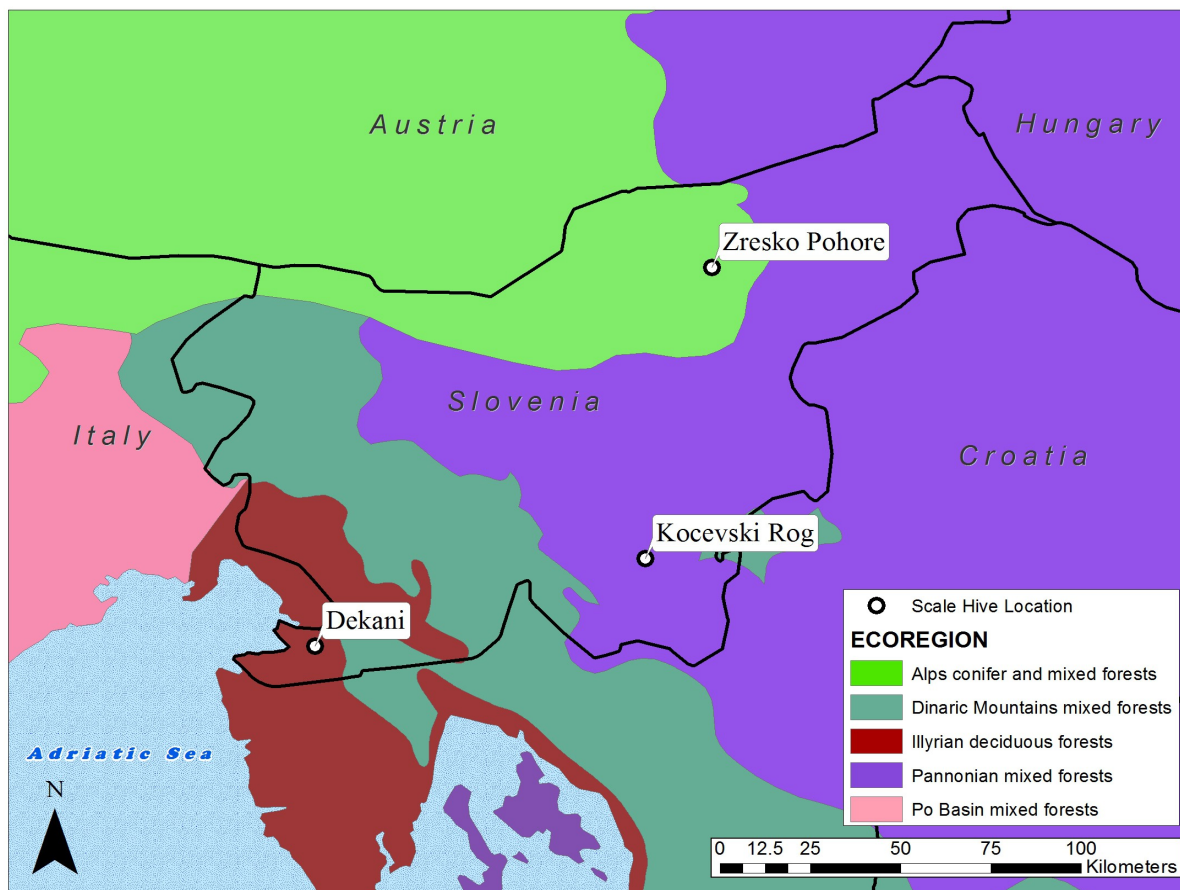


Figure 2: Slovene Hives in DMEER zones

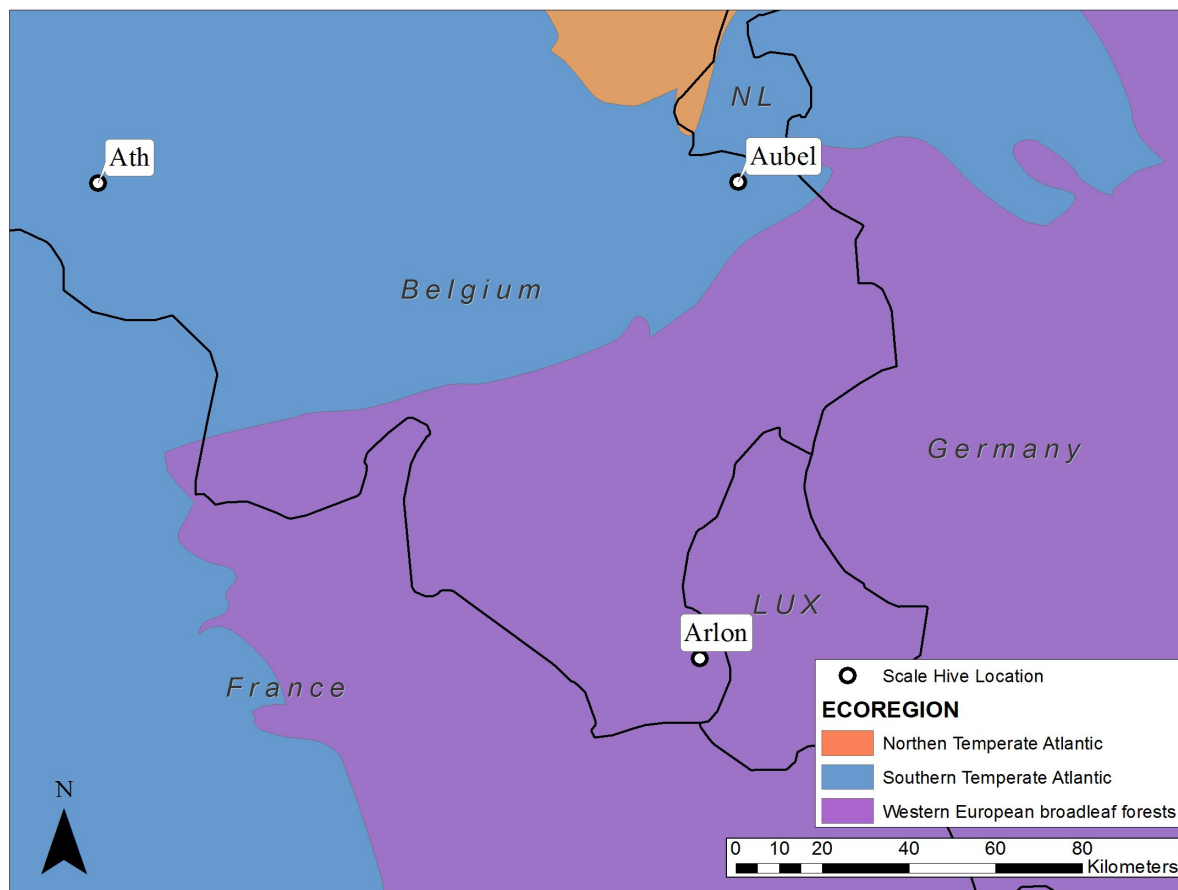


Figure 3: Belgian Hives in DMEER zones

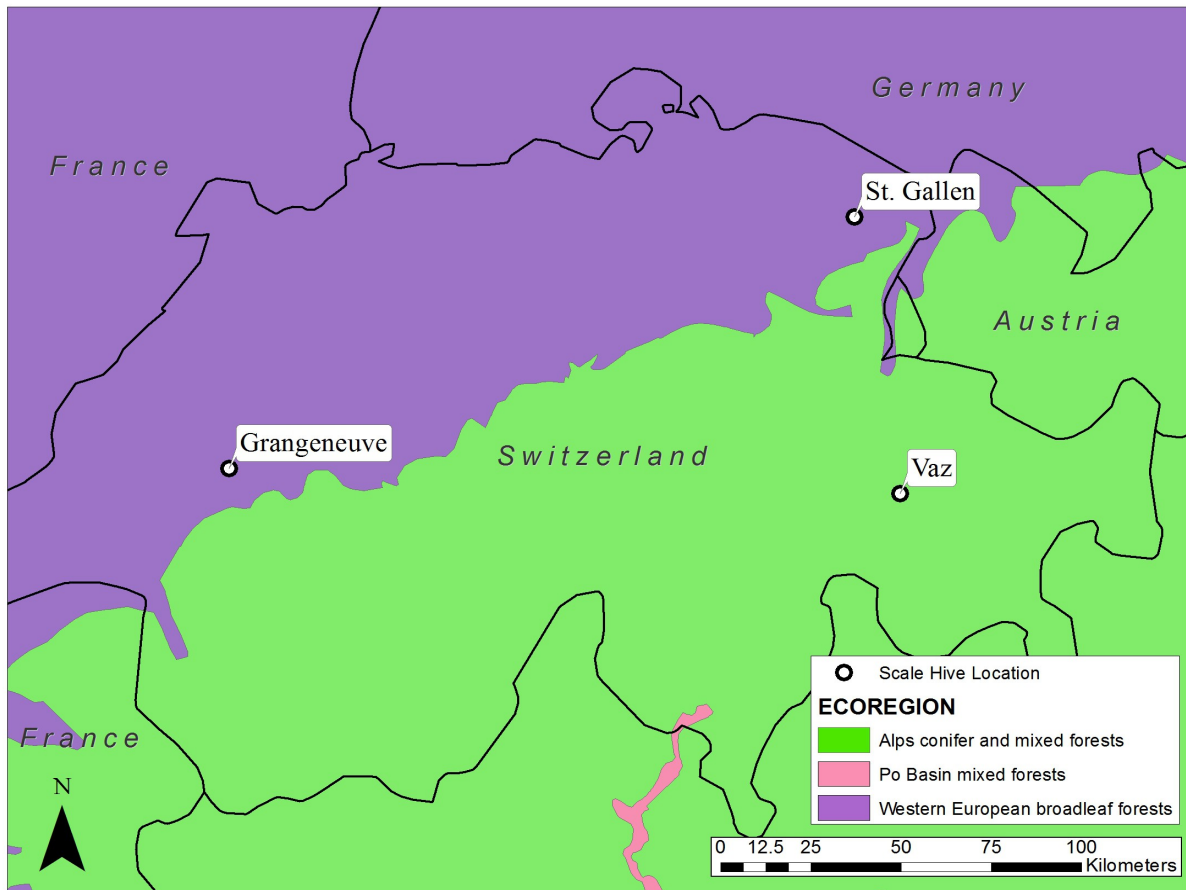


Figure 4: Swiss scale-hives in DMEER zones

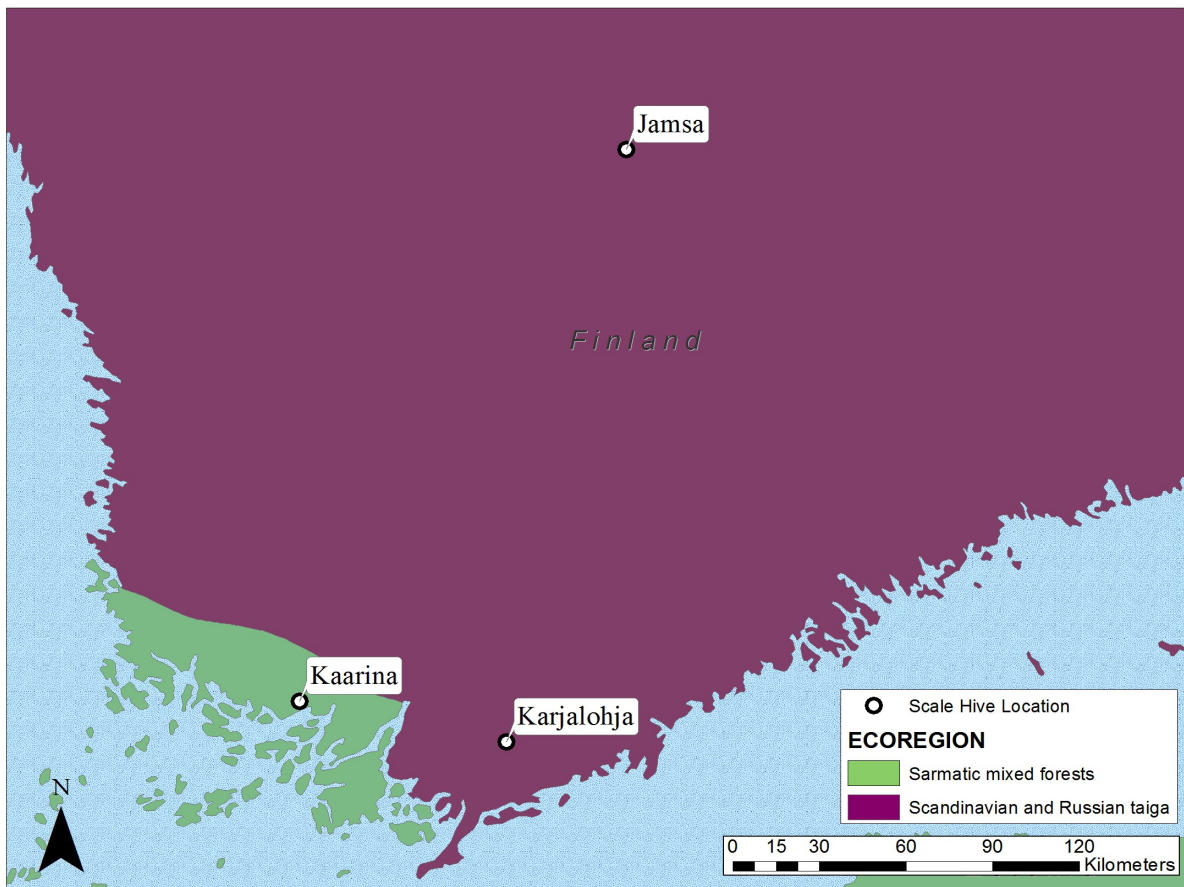


Figure 5: Finish scale-hives in DMEER zones

3.4 HONEY BEE NECTAR FLOW METRICS

For many hives, the spring HBNF was straightforward (Figure 6). The rapid gain in adjusted weight (blue line) marked the beginning of the flow (green dot), while the levelling-off indicated

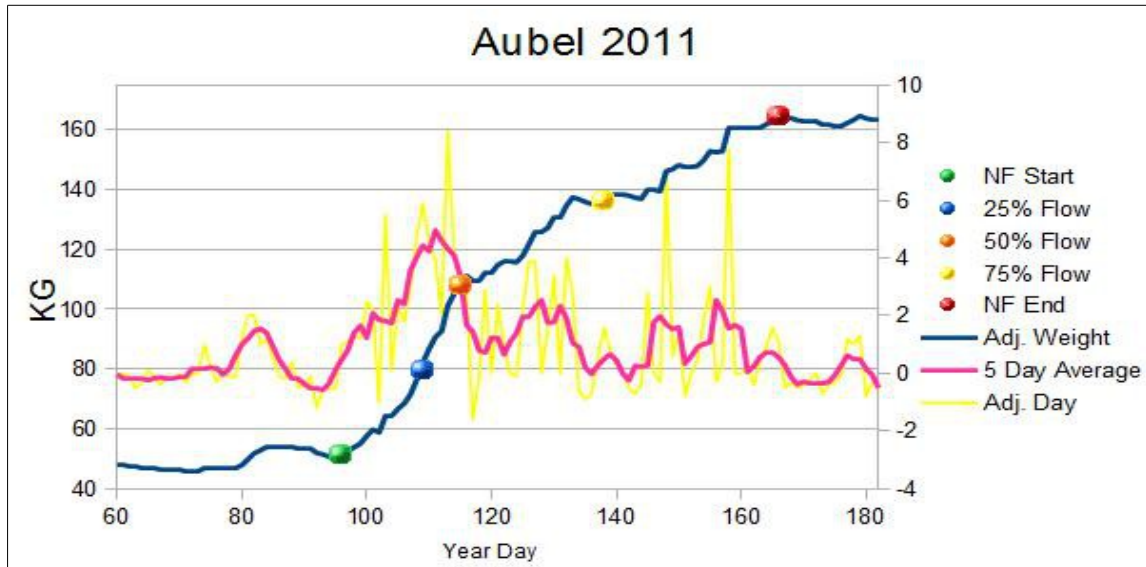


Figure 6: An example of scale-hive metrics from Aubel, Belgium in 2011

the end (red dot). Other seasons and locations had a less distinct weight gain, where, because of rainfall, variable nectar secretion or other reason, the NF fragmented. An attempt was made to identify the main spring nectar flow (at times consisting of two or three broken flows) between day 90 and day 180. Flows that began after day 180 or continued past the day 200 were considered summer NFs and not included as the spring HBNF. Exceptions were made in Finland, where flows occur much later due to their northern latitudes.

Total nectar flow weight was calculated by subtracting the weight of NF start from NF end. Duration was calculated by subtracting the NF start day from end day. Total nectar flow weight was quartered and 25%, 50% and 75% NF were calculated. The day in which the hive surpassed those weights were used for analysis.

3.5 MODIS NDVI

MODIS NDVI was from the dataset MOD13Q1 acquired at the Oak Ridge National Laboratory Distributed Active Archive Center (ORNL DAAC: <http://daac.ornl.gov>). This was collected by the Terra satellite with a ground sampling distance of 250 meters and a 16 day composite window. MODIS data with

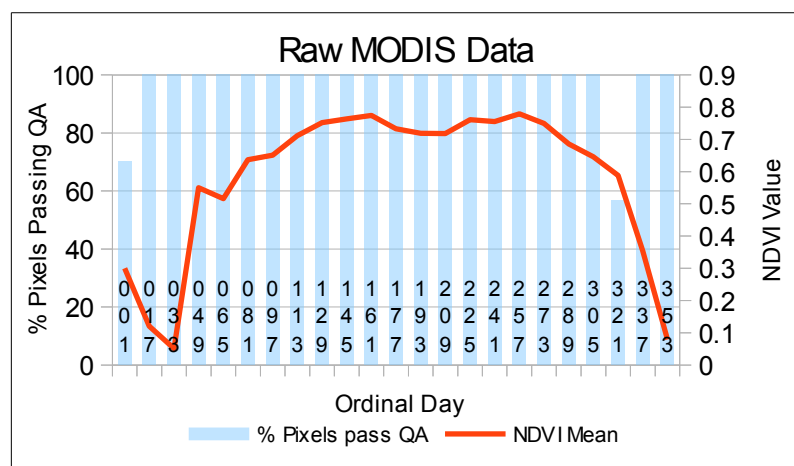


Figure 7: An example of raw MODIS data with QA information

the areal extent of approximately 6.25 by 6.25 kilometres (pixels $n=625$) was selected with the centre coordinate being the location of the hive. This area was thought to encompass the foraging range of honey bees during the spring season (Blomstedt, 2014: Section 2.4). The timespan of VI products downloaded was from January 2009 – December 2012 (except for Kaarina, Finland which included 2013). All non-vegetated pixels (Classified 13 for Urban and Built Up and 0 for Water) were removed from analysis. Each dataset included the Quality Assurance (QA) metadata describing its usability and usefulness (Roy et al., 2002). All unprocessed and cloudy pixels (ranked -1, 2 3) were removed. Following the methods of Esaias (2011) and Zhang (2006), the remaining pixels were averaged to create an overall mean for each 16 day capture.

3.6 TIMESAT

In order to extract meaningful information from NDVI data, it is necessary to suppress short term variation by using running averages, running medians or a compound smoother. TIMESAT is a software package based on MATLAB designed for extracting seasonal parameters (Jönsson and Eklundh, 2002, 2004, 2011). TIMESAT offers three smoothing functions and this research used asymmetric Gaussian method due its robustness against noise and incomplete time-series (Gao et

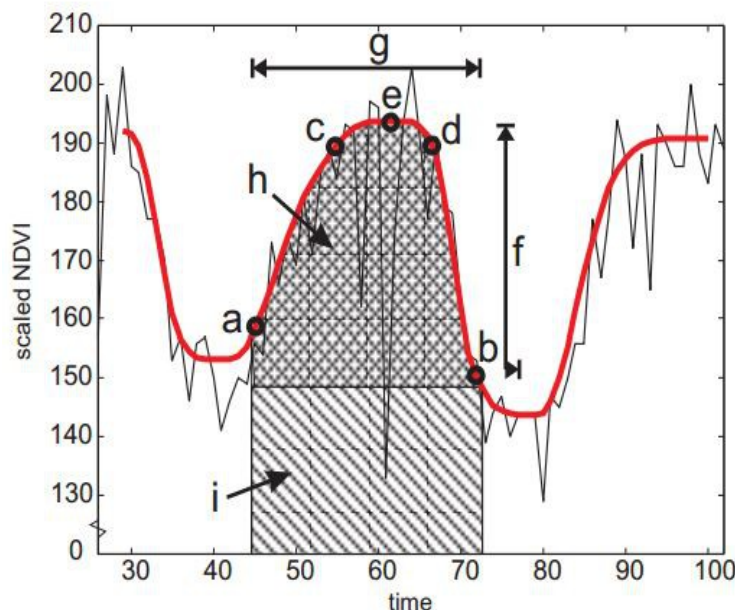


Figure 8: An example of TIMESAT phenological parameters: Black line is raw NDVI and red line is smoothed Gaussian NDVI. Points (a) and (b) mark, respectively, start and end of the season. Points (c) and (d) give the 80 % levels. (e) displays the point with the largest value. (f) displays the seasonal amplitude and (g) the seasonal length. Finally, (h) and (i) are integrals showing the cumulative effect of vegetation during the season (Jönsson and Eklundh, 2011)

al., 2008). The methodology of this research is based on Tan et al. (2011) who further enhanced the TIMESAT algorithm using night land surface temperature (LST) from MODIS product MOD11A2 to produce gap-filled NDVI time-series (Blomstedt, 2014: Section 3.8).

With a smoothed NDVI curve, the start of season can be marked by defining a threshold (amplitude or absolute value). 15% amplitude was used to designate the SOS, as this is thought to be when the majority of vegetation had revived from it's dormant state (Blomstedt, 2014:

Section 2.9). TIMESAT also offers the option to assign weight to each data capture. Data captures which contained more than half pixels ($n=315$) with a QA = 1 were only given a 75% weight. Data captures with more than 80% QA = 1 ($n=500$), or more than 10% QA = 3 were given a 50% weight.

4. RESULTS

4.1 HBNF DATA

Table 2: Scale-hive data by location. Other than columns “year” and “duration,” numbers represent ordinal dates

Country	Hive	Year	TIMESAT SOS (15%)	NF Start	NF Duration	25% Flow	50% Flow	75% Flow	NF End
Belgium	Arlon	2010	99	138	29	141	144	156	167
		2011	82	81	77	113	127	136	158
		2012	81	125	37	128	131	140	162
	Ath	2010	70	104	41	118	134	140	145
		2011	86	126	41	150	155	164	167
	Aubel	2010	64	104	40	114	118	140	144
		2011	57	96	70	109	115	138	166
Finland	Jämsä	2011	103	149	44	162	171	182	193
		2012	86	142	49	167	181	185	191
	Kaarina	2011	97	179	57	183	188	193	236
		2012	86	141	190	49	167	182	187
	Karjalohja	2013	104	149	50	180	187	191	199
		2011	99	129	64	163	180	184	193
		2012	93	141	59	161	167	184	200
Slovenia	Dekani	2010	89	124	56	134	141	161	180
		2011	75	118	17	123	127	130	135
		2012	81	121	12	126	128	130	133
	Kočevski Rog	2010	91	140	59	165	186	190	199
		2011	82	126	55	133	147	169	181
	Zreško Pohorje	2012	85	166	22	172	182	184	188
		2010	81	155	43	178	183	191	198
		2011	73	109	65	130	153	166	174
		2012	97	118	68	169	172	176	186
Switzerland	St. Gallen	2011	54	104	28	113	123	127	132
		2012	65	115	17	117	120	124	132
	Grangeneuve	2009	64	118	27	126	130	135	145
		2010	68	104	42	113	118	142	146
		2011	56	105	25	111	113	114	130
	Vaz	2009	110	124	45	135	142	148	169
		2011	114	106	48	114	129	140	154
		2012	129	142	44	156	165	179	186

Table 3: Properties of HBNF by country. Other than range column and duration rows, numbers represent ordinal date.

Country	Metric	Mean	Median	Maximum	Minimum	Range
Belgium	NF Start	111	104	138	81	57
	Duration (days)	48	41	77	29	48
	NF 50%	132	131	155	115	40
	NF End	158	162	167	144	23
Finland	NF Start	147	142	179	129	50
	Duration (days)	53	50	64	44	20
	NF 50%	179	181	188	167	21
	NF End	200	193	236	190	46
Slovenia	NF Start	131	124	166	109	57
	Duration (days)	44	55	68	12	56
	NF 50%	158	153	186	127	59
	NF End	175	181	167	133	34
Switzerland	NF Start	115	111	142	104	38
	Duration (days)	35	35	48	17	31
	NF 50%	130	126	156	113	43
	NF End	149	146	186	130	56
Total	NF Start	126	124	179	81	98
	Duration (days)	45	44	77	12	65
	NF 50%	150	144	188	113	75
	NF End	170	169	236	130	106

Table 4: HBNFs by year. 2012 not included due to Finish data available only during 2012-13. Other than range column and duration rows, numbers represent ordinal date.

Year	Metric	Mean	Median	Maximum	Minimum	Range
2010	NF Start	124	124	155	104	51
	Duration (days)	44	42	59	29	30
	NF 50%	146	141	186	118	68
	NF End	168	167	199	144	55
2011	NF Start	119	114	179	81	98
	Duration (days)	49	52	77	17	60
	NF 50%	144	138	188	113	75
	NF End	168	167	236	130	106

Tables 1-3 describe the properties of the HBNFs by location, country and year. All metrics showed large variation, with the ranges of each metric rarely under 5 weeks. Belgium had the earliest NFs while Finland the latest. Finland had the longest mean NF, while Slovenia and Belgium had the longest individual flows. Slovenian hives showed the greatest range of a minimum and maximum flow with 56 days. The mean duration of all flows is around 9 weeks in length. The curvature of nectar flows also varied greatly (Appendix A). Some HBNFs began and ended sharply while others started slowly and continued of a long period of time. In some cases a flow would be interrupted for a week or more before resuming.

4.2 START OF SEASON – HBNF METRICS

Figures 9-12 show examples of the Gaussian smoothed NDVI relative to scale hive data. For all scale-hives, the SOS began an average of 41 days before NF starts, but two seasons (Arlon 2011 and Vaz 2011) had the NF start prior to SOS. TIMESAT SOS (15%) showed a weak positive relationship to all HBNF metrics ($R^2 = 0.2$ to 0.33) with HBNF start and 50% seen in figures 13-14. However the regression lines have similar slopes and figure 14 shows a group of points following a linear pattern below a less-formed upper group. HBNF metrics for the year 2011 showed similar low correlation ($R^2 = 0.25$ to 0.42 , Appendix B). Belgium and Switzerland exhibited the strongest relationships (Figures 15-16) while Slovenia ($R^2 = 0.24$) and Finland ($R^2 = 0.00$) were insignificant.

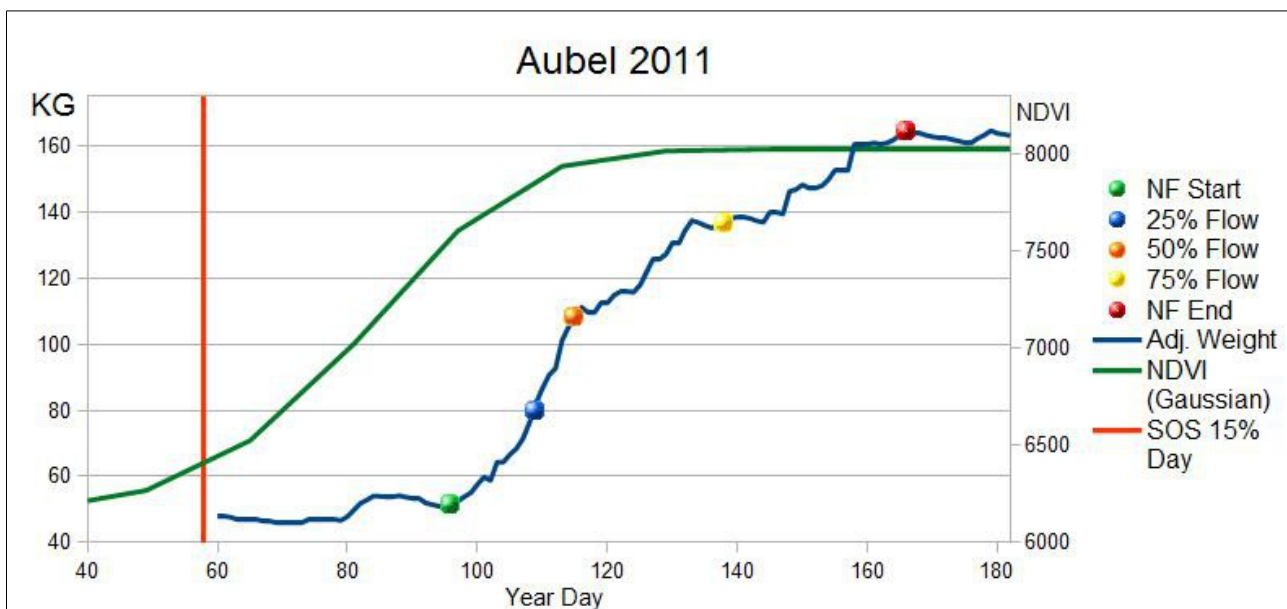


Figure 9: Belgian example of Gaussian smoothed NDVI and scale-hive data.

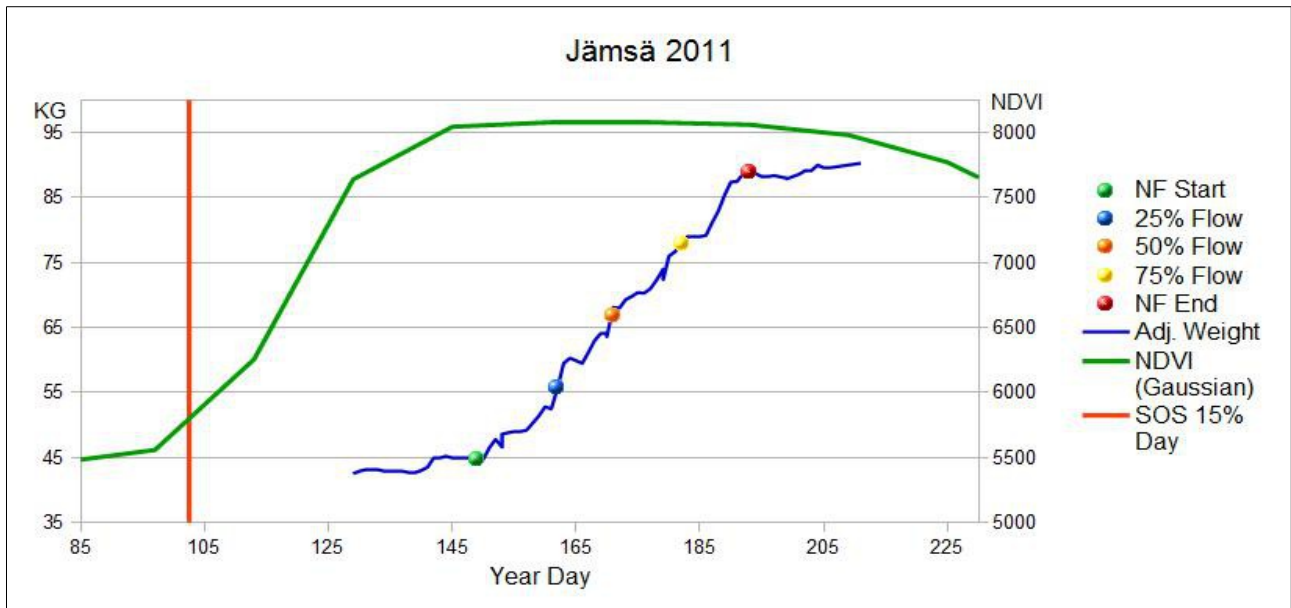


Figure 10: Finish example of Gaussian smoothed NDVI and scale-hive data

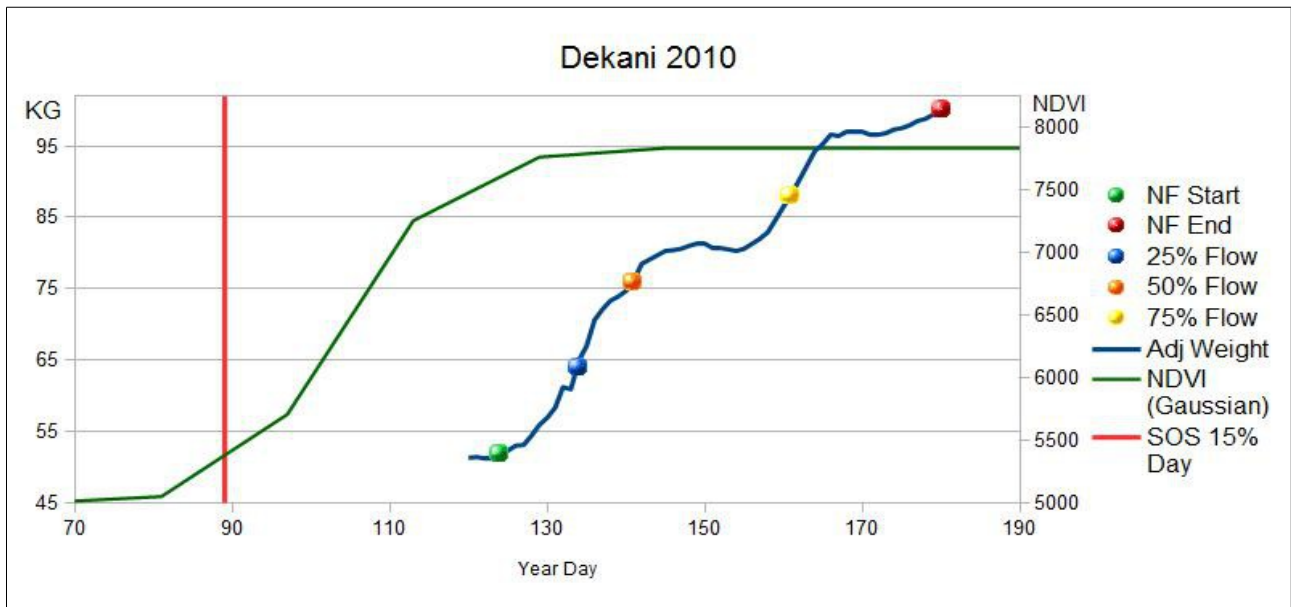


Figure 11: Slovene example of Gaussian smoothed NDVI and scale-hive data

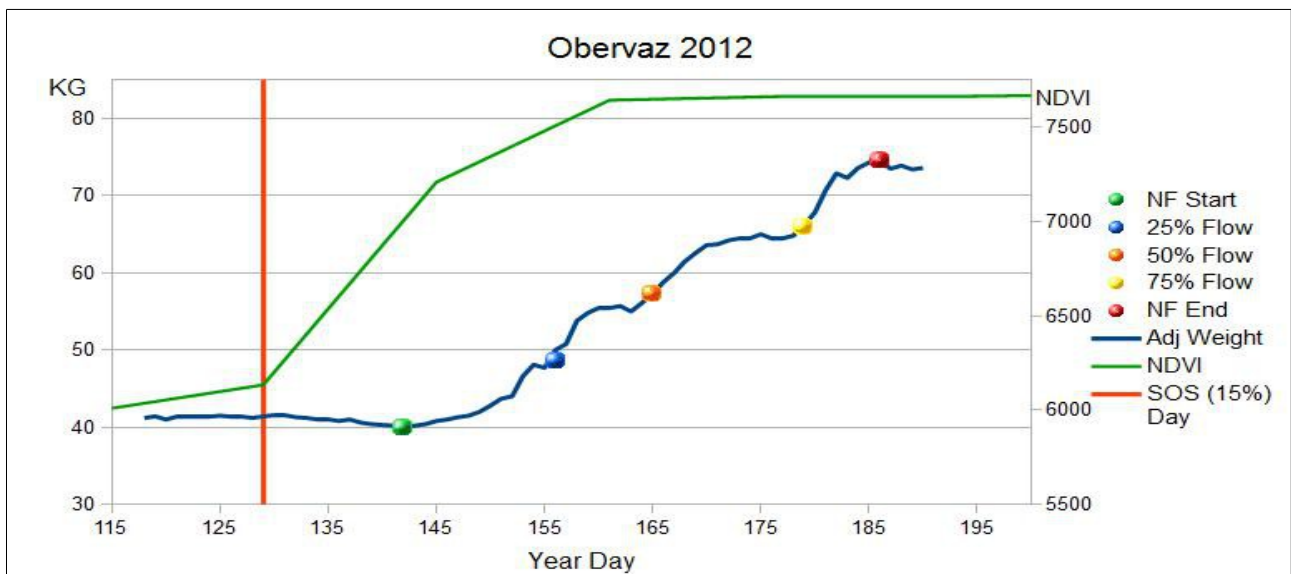


Figure 12: Swiss example of Gaussian smoothed NDVI and scale-hive data

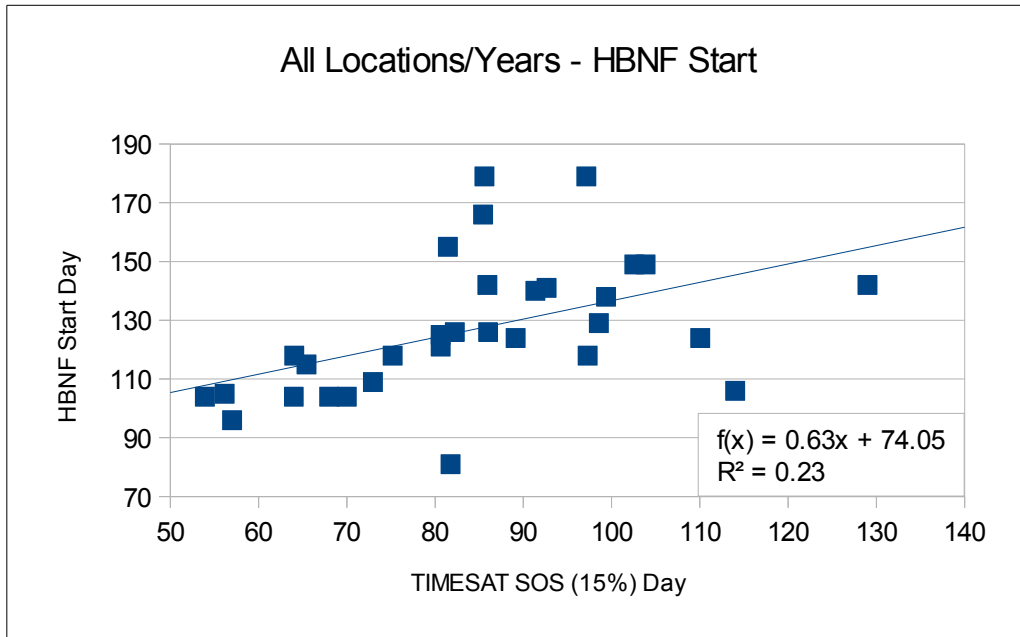


Figure 13: All Locations/Years – HBNF Start, n=31

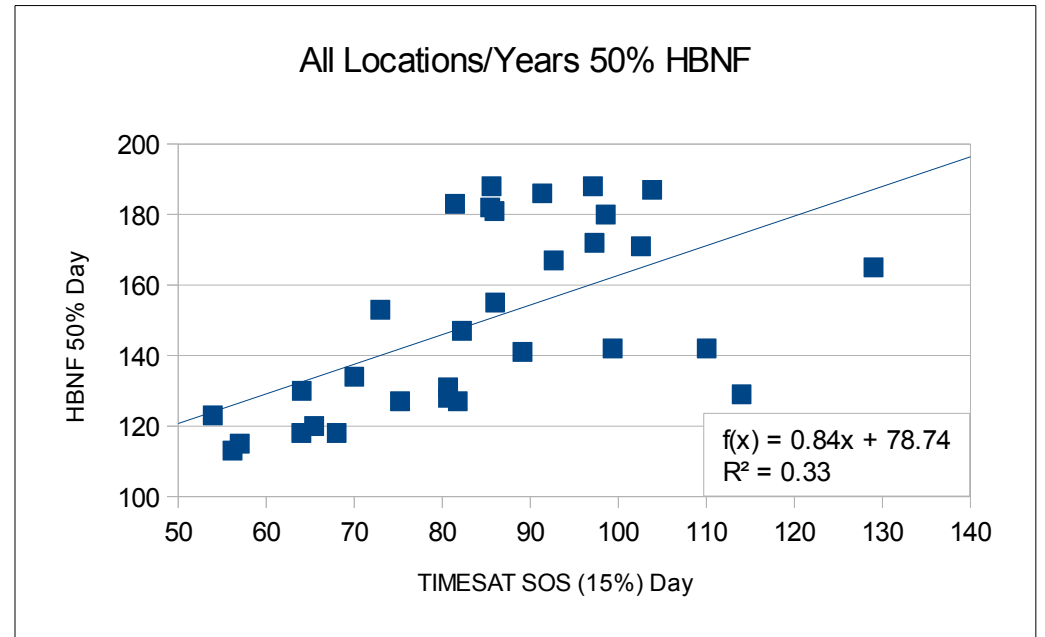


Figure 14: All Locations/Years – HBNF 50%, n=31

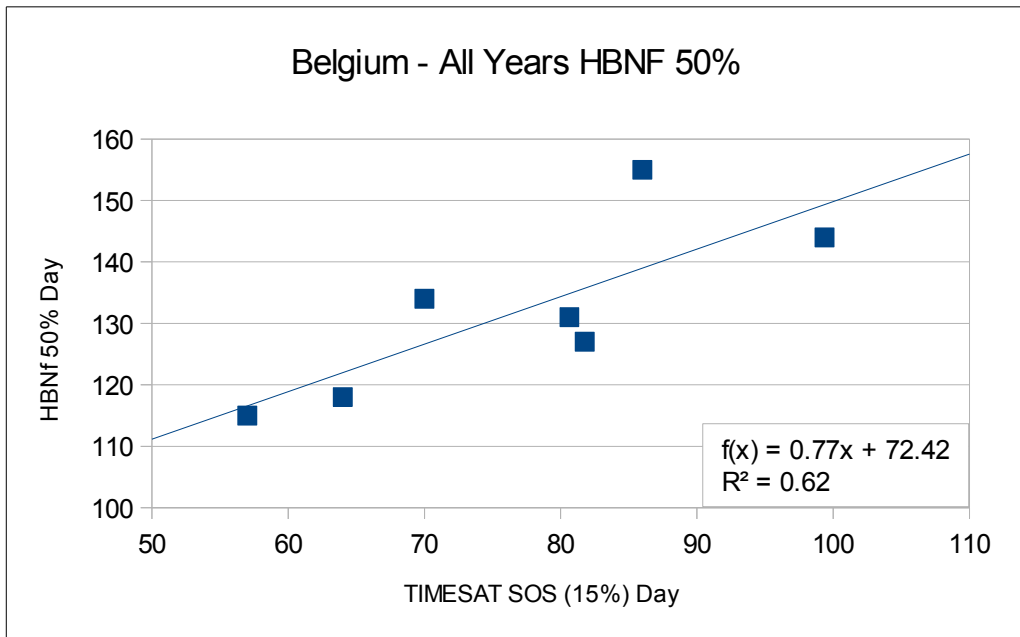


Figure 15: Belgium – All Years HBNF 50%, n=7

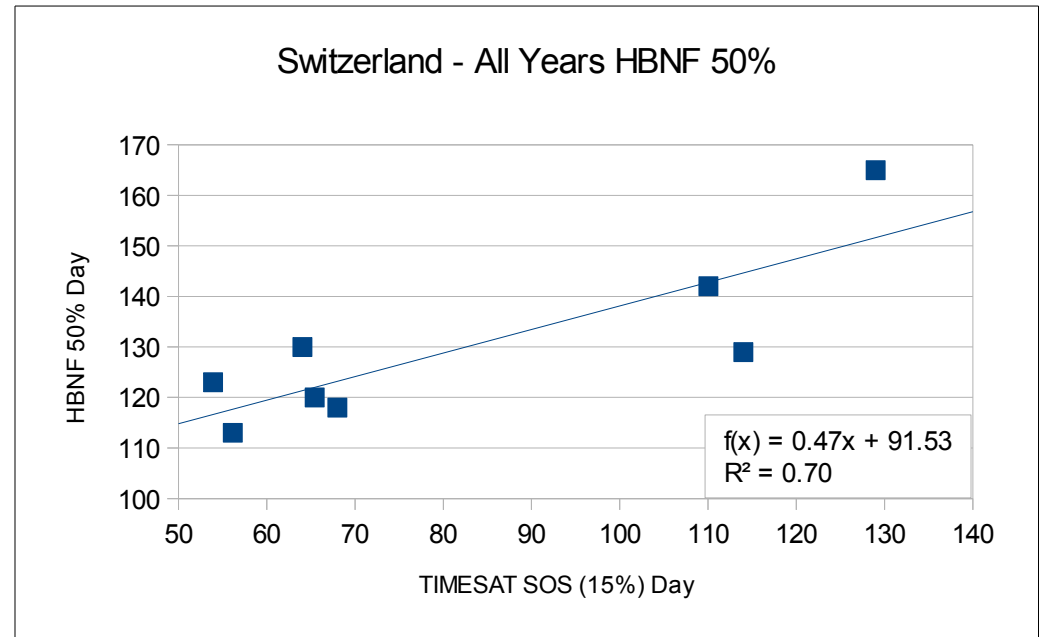


Figure 16: Switzerland – All Years HBNF 50%, n=8

4.3 TWO SCENARIOS

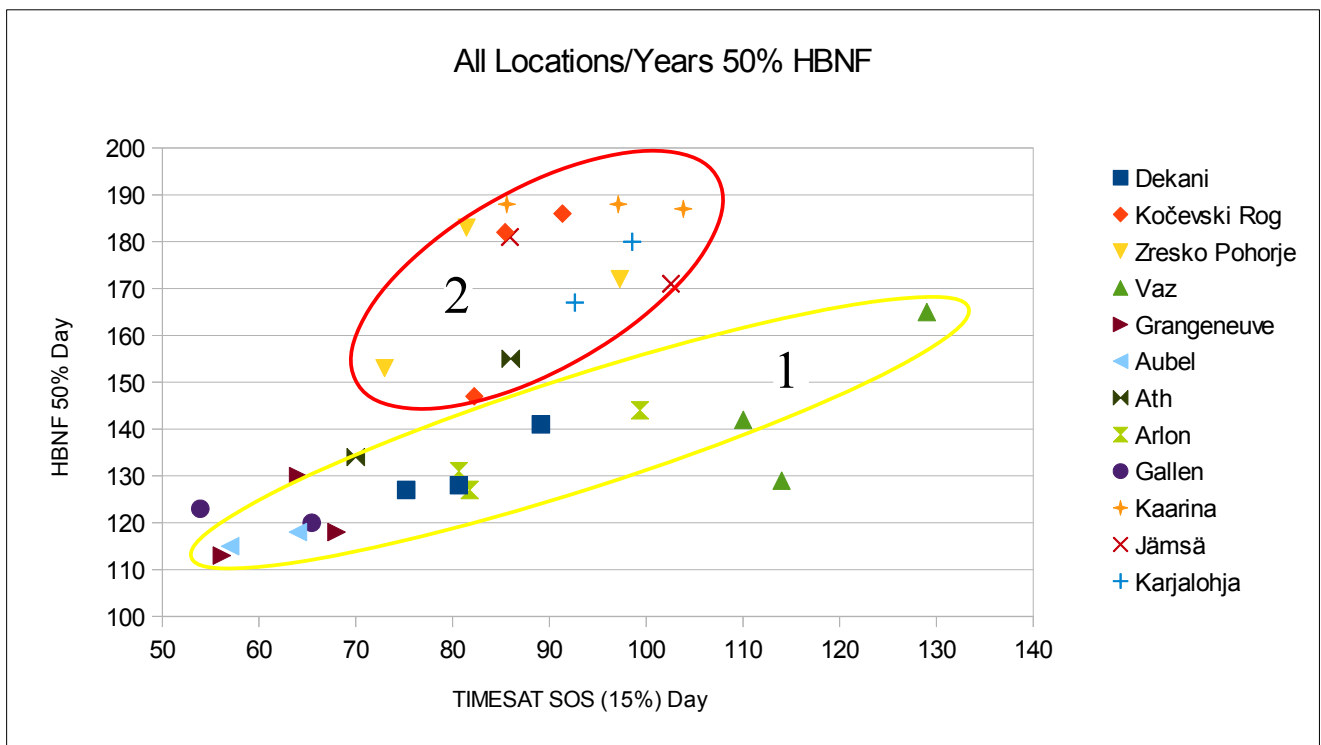


Figure 17: All locations/years shown by location. The lower group, circled in yellow is deemed scenario 1 while the upper group, circled in red, is scenario 2.

Figure 17 shows scale-hives by location with two point clouds: a lower group (1) generally following a linear trend beneath an upper block (2). The scale-hives are divided evenly and are seen by DMEER in table 5.

Table 5: Hive locations by scenario

Scenario	Location	Country	DMEER Zone
1	Aubel	Belgium	Southern Temperate Atlantic
	Arlon	Belgium	Western European Broadleaf
	Dekani	Slovenia	Illyrian Deciduous Forests
	Grangeneuve	Switzerland	Western European Broadleaf
	St. Gallen	Switzerland	Western European Broadleaf
	Vaz	Switzerland	Alps Conifer and mixed forests
2	Ath	Belgium	Southern Temperate Atlantic
	Kaarina	Finland	Sarmatic Mixed Forests
	Jämsä	Finland	Scandinavian and Russian taiga
	Karjalohja	Finland	Scandinavian and Russian taiga
	Kočevski Rog	Slovenia	Pannonian Mixed Forests
	Zreško Pohorje	Slovenia	Alps Conifer and mixed forests

The first scenario contained the hives from Switzerland, one Slovene and two from Belgium. All hives in DMEER zone Western European Broadleaf (WEB) are in scenario 1. Looking at the locations in Figure 18, it's possible to see that all locations in the first scenario are in a spatially continuous region, mainly consisting of the DMEER WEB and Alps Conifer and Mixed Forests (ACMF).

The second scenario contained two locations from Slovenia, all three hives from Finland and one Belgian hive. This Belgian hive straddled the line between the two scenarios in Figure 17, but was included in the second due to its DMEER zone and geographical location outside the contiguous scenario 1 area.

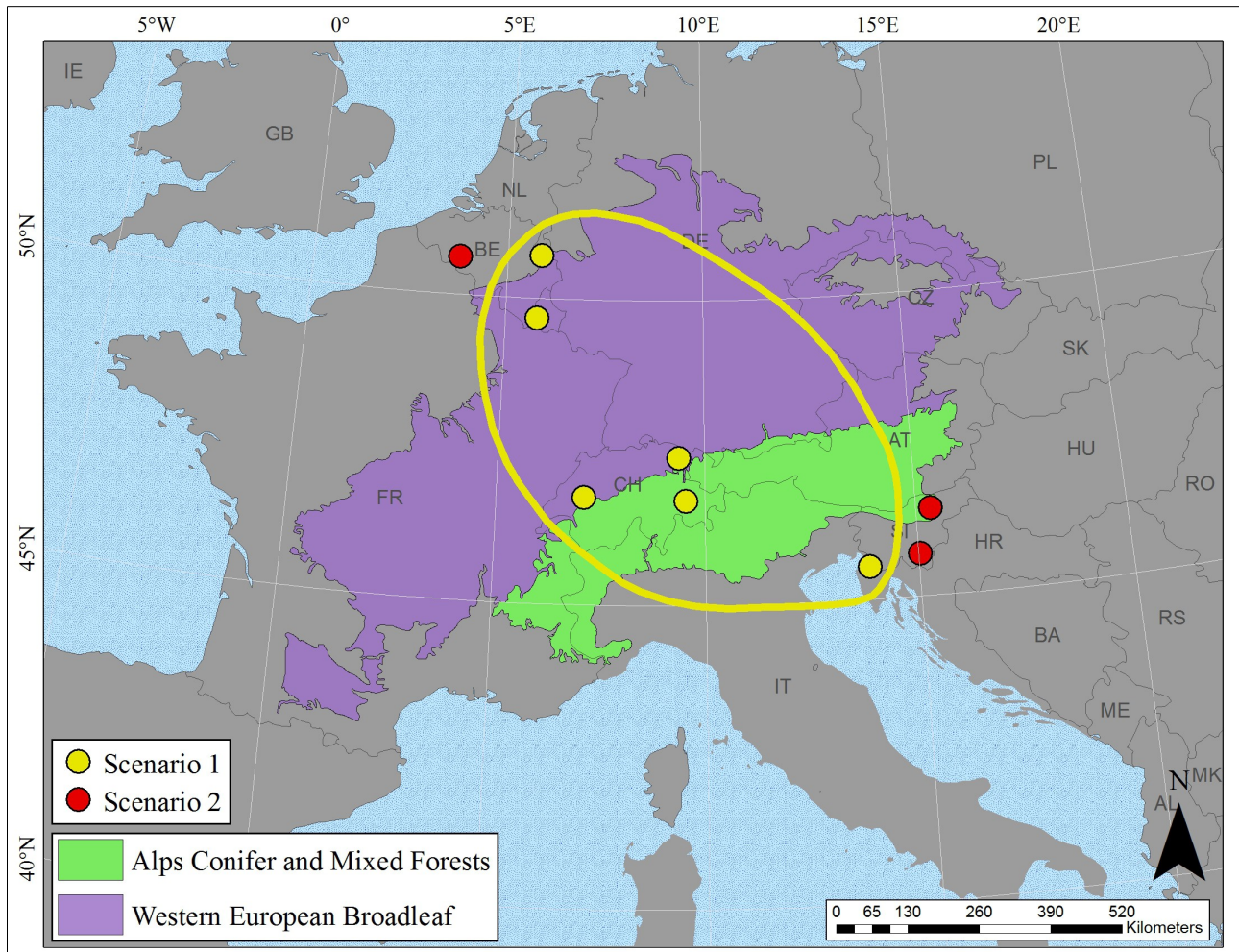


Figure 18: Hive locations by scenarios in DMEER. Yellow polygon denotes contiguous area.

When separated, the correlation for SOS and HBNF metrics become much stronger for the first scenario, while remaining weak for the second (Figures 21-22). The HBNF start continues to have a weak relationship (Figure 19) but the strongest correlation is found with HBNF 50% first scenario (Figure 20, $R^2 = 0.73$).

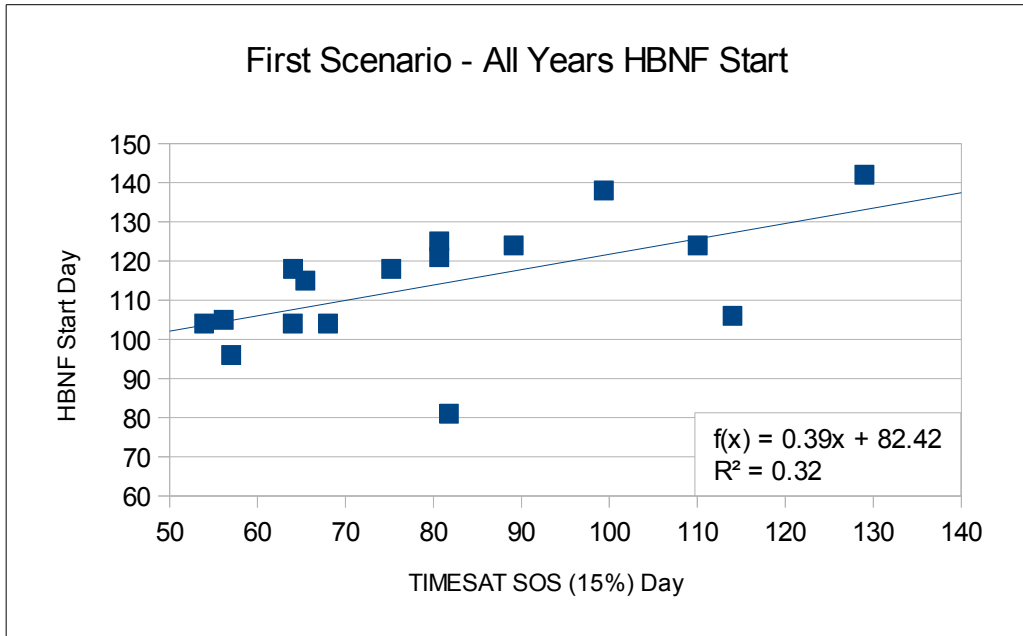


Figure 19: First Scenario – All Years HBNF Start, n=16

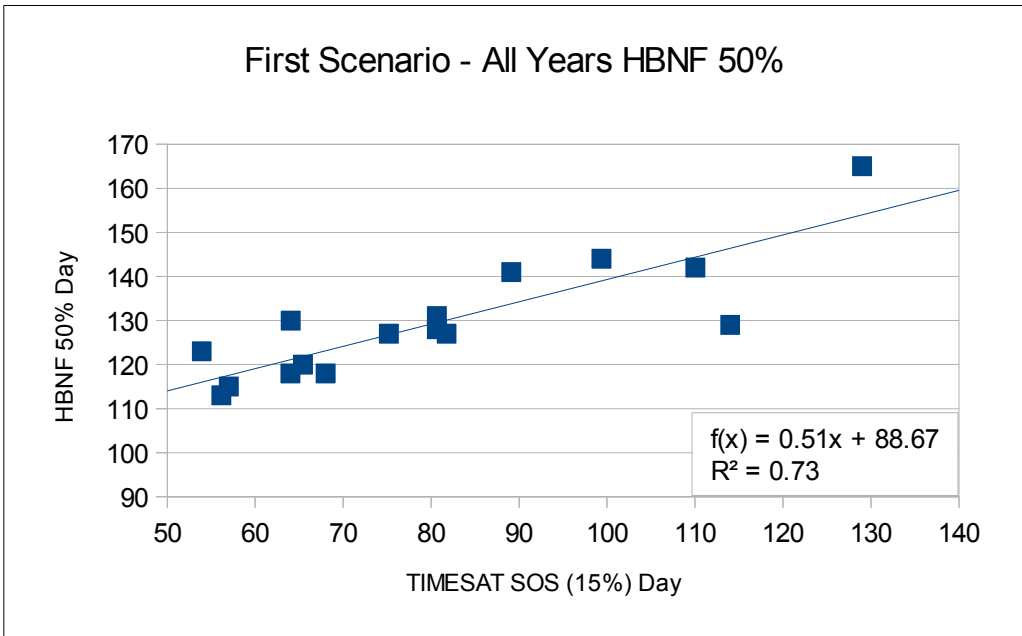


Figure 20: First Scenario – All Years HBNF 50%, n=16

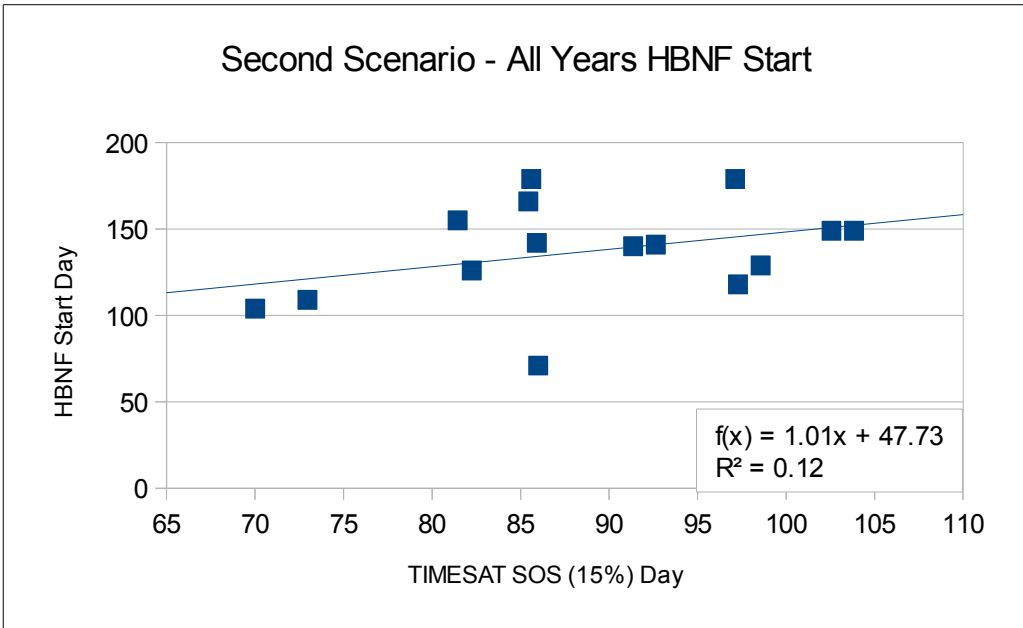


Figure 21: Second Scenario – All Years HBNF Start, n=15

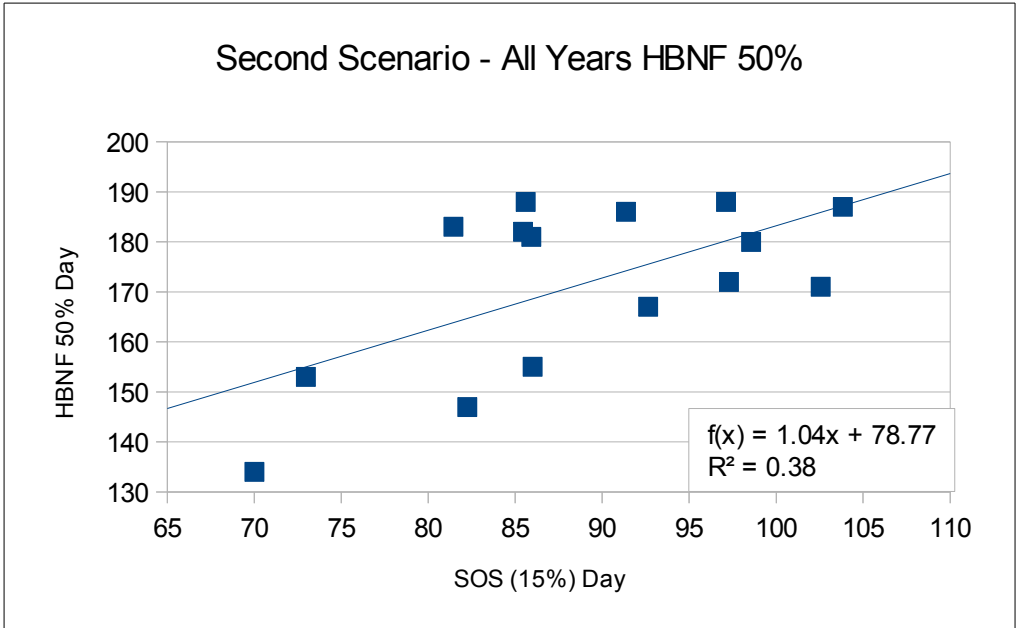


Figure 22: Second Scenario – All Years HBNF 50%

5. DISCUSSION

HBNFs are highly diverse and vary greatly between country, location and season. Nectar secretion rates relate to environmental factors and this can be partly seen in the continental geography. Belgium has early flows due to the temperate climate while Finland's occur much later.

But the microgeography is probably more effecting, as HBNFs can differ between years at the same location. For example, the 2011 NF start in Arlon began 50 days earlier than in 2010, but ended at a similar date, meaning the duration in 2011 was 40 days longer. For Vaz, 2009 and 2011 had similar NF durations, but in 2011 the NF shifted 3 weeks earlier.

When compared to NDVI SOS, the mid-point of the HBNF showed the strongest correlation. This affirms the research of Esaias (2011), who found a similar result in the tree-dominated Northeastern United States. The HBNF start day is a less consistent metric likely

because it is the edge of the distribution, which can be susceptible to compounding effects. HBNFs are variable in shape and timing (Figure 23) due to the complex underpinnings of nectar production in plants, the factors of which are many (Blomstedt, 2014: Section 2.5). However, the aggregate of flowers, which may be what the HBNF 50% days represents, appears to be a more stable measure of NFs, and therefore has a more consistent relationship with the NDVI SOS.

The spatially continuous area (scenario 1) in central Europe showed the strongest correlation between NDVI and HBNF. This area coincides with the DMEER WEB and ACMF, but this classification should not be used definitively. Zreško Pohorje did not fit the linear pattern of scenario 1 and lies in ACMF region. However it is near (15 km) from the border with Pannonian Mixed Forests (Figure 2). Similarly, Aubel is in Southern Temperate Atlantic and fits in scenario 1, but is only 15 km from WEB (Figure 3). Ath is also in Southern Temperate Atlantic, but further towards the sea, and did not belong in scenario 1. As there was no suitable resource mapping melliferous flowers in Europe (Blomstedt, 2014: Section 6.5), DMEER zones were used as a general guideline of vegetation homogeneity and the borders were considered fuzzy.

Scenario 2 included hives located in Finland, Slovenia and Belgium. These hives were

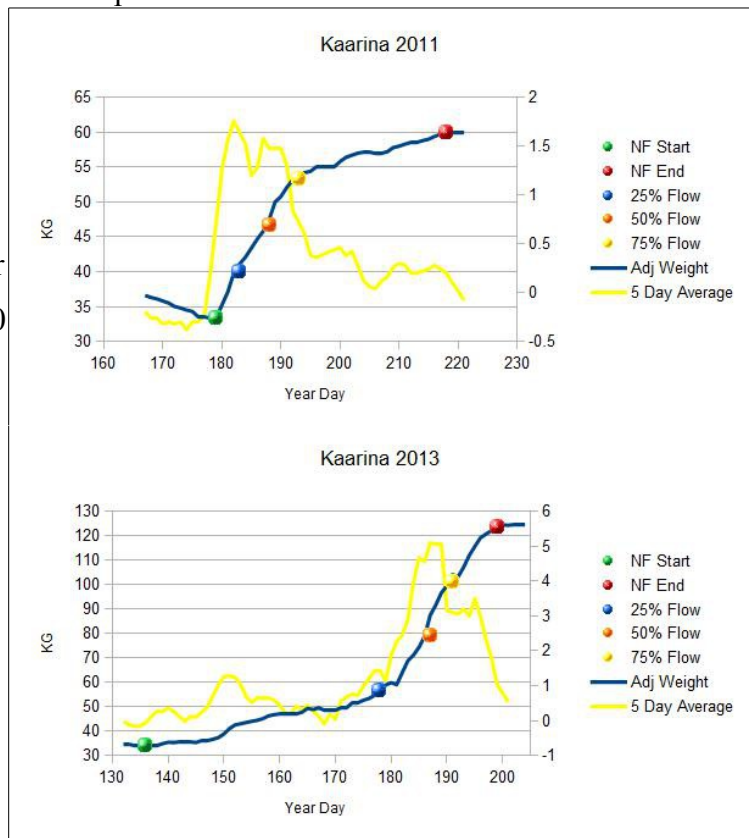


Figure 23: HBNF metrics of Kaarina 2011 and 2013, an example of two different HBNF curvatures from the same location

characterized by a later 50% HBNF day and had no notable correlation with SOS. One consideration is that in certain types of land cover the spring NDVI measurements may error due to the difference between understory and canopy greenness. However the hives in scenario 2 also generally had a much longer NF duration (Table 6), causing them to separate from the linear pattern in scenario 1. It is possible that the HBNFs in scenario 2 either have only a single, long NF or multiple flows combined, while scenario 1 had a spring HBNF separate from the summer/autumn flow.

Table 6: NF Duration

NF Duration (mean)	
Scenario 1	33
Scenario 2	53

The data was analysed annually to see if certain years had better correlation due to climatic factors. There does not seem to be the case, for 2011 showed a R² similar to the entire dataset. The data was also analysed by nation to account for disparate sources – each country may have different methods for managing the hives or collecting which could possibly effect the HBNF metrics. Belgium and Switzerland showed the strongest relationships for HBNF 50% day (Figures 13-14, R² = 0.62 and 0.70, respectively) while Finland and Slovenia had weak statistics. However, this is aligned with the scenarios, as the Swiss and Belgian hives are mainly within the same DMEER regions.

It's interesting to note the elevation of the hives when looking at Figure 17. The three points with later SOS days are from the town of Obervaz, 1162 m elevation. However Zresko Pohorje in Slovenia is equally high (1143m) but does not have nearly the same late SOS. The hives at lower elevation, which in this case are closest to the sea, do not follow the same pattern. Dekani is 8

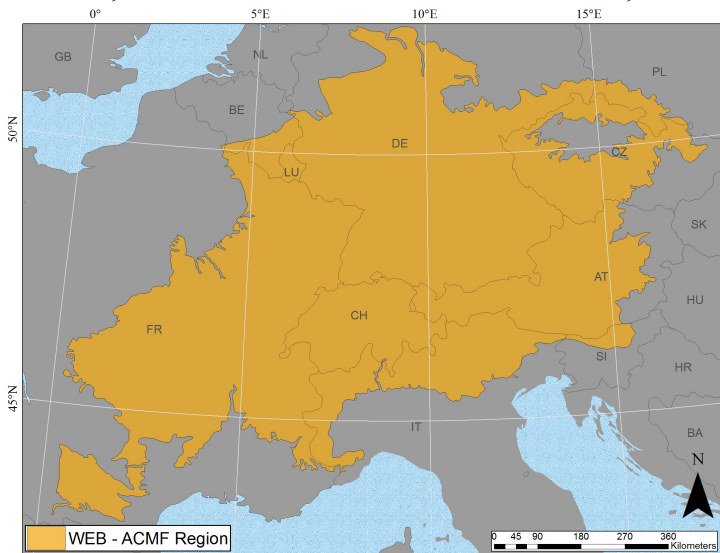


Figure 24: Combination of DMEER Western European Broadleaf and Alps Conifer and Mixed Forests

kilometres from the sea and only 65m in elevation. Though it is in the DMEER “Illyrian deciduous forests,” it still follows a linear pattern and lies within the spatially contiguous zone.

With HBNF correlated to the NDVI SOS in certain ecoregions, it can then be related to long-term climate models. A number of studies have investigated NDVI growing seasons in the Northern Hemisphere, with most purporting an

advancing spring and delayed end of season (as reviewed in Jeong et al., 2011). Stöckli and Vidale (2004) found that from 1982-2001 there has been a general shift to earlier phenological phases by -0.54 days per year, totalling -10.8 days over 20 years. Figure 25 shows the spatial pattern of NDVI change on the continent, and their research claimed an especially significant statistic for Central Europe. Though HBNF start dates are more variable, it is possible to infer that the mid-point of

HBNFs in this region are advancing at a similar rate of a half a day per annum.

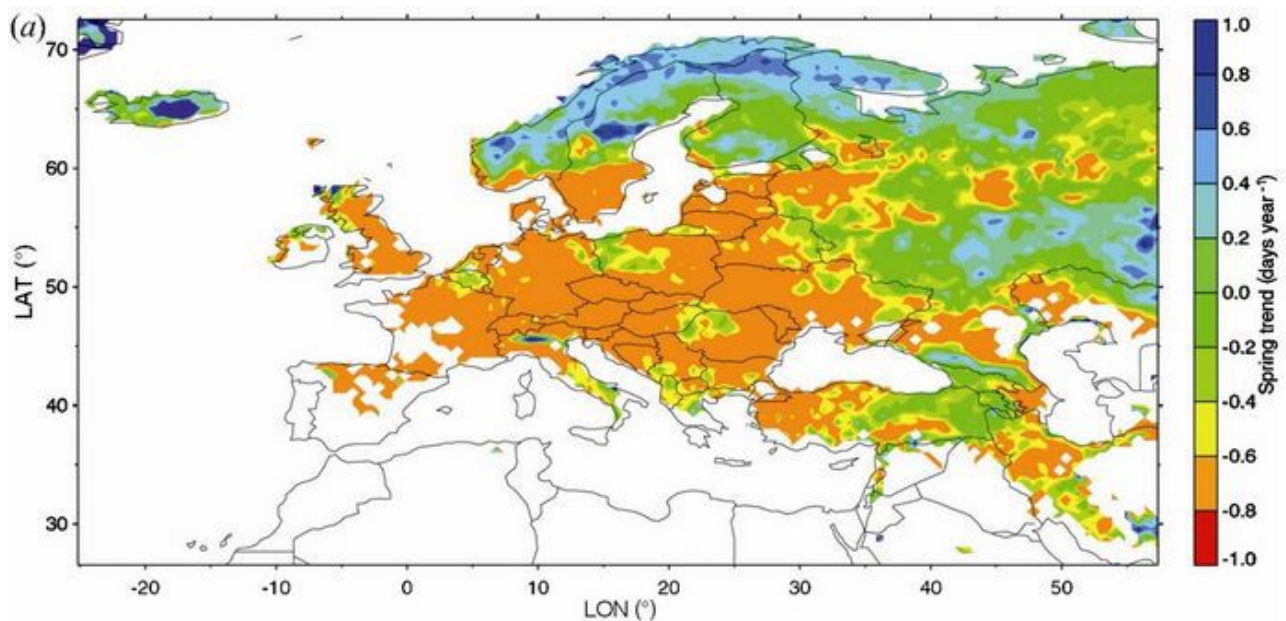


Figure 25: Advance in NDVI derived SOS from 1982-2001. From Stöckli and Vidale, (2004)

Several caveats must be taken into account for this research. First, this is a very general look at nectar flows, without taking into consideration plant types at each location. Nectar secretion is a very complex process, with each species, population and individual plant affected in different ways. As is well known to beekeepers, some years a nectar flow may fail completely, forcing them to feed their hives supplemental sugar. Several scale-hives considered for use in this research showed seasons where there was a small nectar flow, but overall a net loss. In other years these sites had large gains. Removing the sites with failed nectar flows distorted the data towards a stronger correlation. Further limitations include irregularity in scale-hive management, temporally coarse MODIS data and the weather (Blomstedt, 2014: Section 6).

6. CONCLUSION

This research has found a modest link between NDVI-derived SOS and the mid-point of the HBNF in a region of Central Europe. This is similar to what was found by Esaias (2011), both statistically and ecologically. The temperate Northeastern USA is connatural to Central Europe, and the rapid growth of NDVI can act as a provocation for nectar production for both regions. HBNF start was not influenced by the SOS date, likely due to the complexities of microclimates and temperature on nectar production in the early spring. The midpoint of the NF had the strongest correlation and this reflects the bulk of flowers. The relationship did not seem to vary by year or by country. However the countries which showed the strongest relationships also fell within the same DMEER zones.

This research only looks at a handful of scale-hive data points spread out over great distances. While the results are interesting, the small number of data points cannot be accepted as

conclusive and this research can be seen as a step towards further study. By looking at more seasons and locations of scale-hive data it will be possible to better understand European HBNFs.

Additionally, only the spring season was considered in this research. The summer and autumn flows are also of interest and can be studied further. Only recently, with the rise of electronic scales and data-loggers, has scale-hive data been collected at this precision and scope. Many other scale-hives are available for use, but require labour for their cleansing and homogenization. Only in the closing stages of this research project was it known that Germany, Denmark and Sweden also have scale networks. In theory, it is possible to create a continental scale-hive network and, using interpolation techniques (Blomstedt 2014: Section 5), the HBNF can be monitored in real-time. Establishing and maintaining scale-hives is an important step, as a record of HBNF is the best way to understand their change.

7. DATA CITATION

7.1 MODIS

NDVI – MOD13Q1

LST – MOD11A2

Oak Ridge National Laboratory Distributed Active Archive Center (ORNL DAAC). 2012. MODIS subsetted land products, Collection 5. Available on-line [<http://daac.ornl.gov/MODIS/modis.html>] from ORNL DAAC, Oak Ridge, Tennessee, U.S.A. Accessed March 1st, 2014.

7.2 SCALE-HIVE DATA

Finland

Ari Seppälä

Finnish Beekeepers Association

MTT Agrifood Research Finland

Seppo Korpela

Sakari Raiskio

<http://koti.tnnet.fi/web144/vaakapesa/selaa.php>

Accessed 19th March 2014

Slovenia

Jure Justinek

Čebelarske zveze Slovenije

<https://ecelebar.czs.si>

Accessed 30th January 2014

Switzerland

René Zumsteg

Verein Deutschschweizerischer Und Rätoromanischer Bienenfreunde

<http://www.vdrb.ch/service/waagvlker.html>

Accessed 15th March 2014

Belgium

Centre Apicole de Recherche et Information

<http://www.cari.be/balances/>

Accessed 3rd February 2014

7.3 DMEER

Digital Map of European Ecological Regions (DMEER), Version 2000/2005

http://www.eea.europa.eu/data-and-maps/figures/ds_resolveuid/D9AD8691-4E65-4596-8A02-454EFD46A197

Accessed 8th April 2014

8. BIBLIOGRAPHY

- Abu-Asab, M.S., Peterson, P.M., Shetler, S.G., Orli, S.S., 2001. Earlier plant flowering in spring as a response to global warming in the Washington, DC, area. *Biodiversity and Conservation* 10, 597–612.
- Baret, F., Guyot, G., 1991. Potentials and limits of vegetation indices for LAI and APAR assessment. *Remote Sensing of Environment* 35, 161–173.
- Bartomeus, I., Ascher, J.S., Wagner, D., Danforth, B.N., Colla, S., Kornbluth, S., Winfree, R., 2011. Climate-associated phenological advances in bee pollinators and bee-pollinated plants. *Proceedings of the National Academy of Sciences* 108, 20645–20649.
- Beaubien, E.G., Hall-Beyer, M., 2003. Plant phenology in western Canada: trends and links to the view from space. *Environmental Monitoring and Assessment* 88, 419–429.
- Biesmeijer, J.C., Roberts, S.P.M., Reemer, M., Ohlemüller, R., Edwards, M., Peeters, T., Schaffers, A.P., Potts, S.G., Kleukers, R., Thomas, C.D., Settele, J., Kunin, W.E., 2006. Parallel Declines in Pollinators and Insect-Pollinated Plants in Britain and the Netherlands. *Science* 313, 351–354.
- Blomstedt, W., 2014. Mapping Present and Historical European Honey Bee Nectar Flows with Scale Hives and Satellite-Derived Vegetation Indices: Part II Technical Report. University of Edinburgh.
- Bohn, U., 1994. International project for the construction of a map of the natural vegetation of Europe at a scale of 1: 2.5 million - its concept, problems of harmonization and application for nature protection, in: *Colloques Phytosociologiques*. pp. 23–45.
- Buchmann, S.L., Thoenes, S.C., 1990. The electronic scale honey bee colony as a management and research tool. *Bee Science* 1, 40–47.
- Bunce, R.G.H., 1995. A European land Classification. Institute of Terrestrial Ecology, Merlewood.
- Calderone, N.W., 2012. Insect Pollinated Crops, Insect Pollinators and US Agriculture: Trend Analysis of Aggregate Data for the Period 1992–2009. *PLoS ONE* 7.
- De Beurs, K.M., Henebry, G.M., 2010. Spatio-temporal statistical methods for modelling land surface phenology, in: Hudson, I.L., Keatley, M.R. (Eds.), *Phenological Research: Methods for Environmental and Climate Change Analysis*. Springer, Dordrecht, pp. 177–208.
- De Beurs, K.M., Henebry, G.M., 2004. Land surface phenology, climatic variation, and institutional change: analyzing agricultural land cover change in Kazakhstan. *Remote Sensing of Environment* 89, 497–509.
- Deering, D.W., Rouse, J.W., 1975. Measuring forage production of grazing units from Landsat MSS data, in: *International Symposium on Remote Sensing of Environment*, Ann Arbor, Mich. pp. 1169–1178.
- DMEER, 2000. DMEER: Digital Map of European Ecological Regions. <http://www.eea.europa.eu/data-and-maps/figures/dmeer-digital-map-of-european-ecological-regions> (accessed 05/05/14).

- Esaias, W.E., Nickeson, J.E., Tan, B., Nightingale, J.M., Wolfe, R.E., 2011. Mapping nectar flow phenology with satellites and Honey Bee hives to assess climate impacts. Presented at the Apimondia, Buenos Aires.
- Fisher, J.I., Mustard, J.F., Vadeboncoeur, M.A., 2006. Green leaf phenology at Landsat resolution: Scaling from the field to the satellite. *Remote Sensing of Environment* 100, 265–279.
- Fitter, A.H., Fitter, R.S.R., 2002. Rapid Changes in Flowering Time in British Plants. *Science* 296, 1689–1691.
- Gallai, N., Salles, J.M., Settele, J., Vaissière, B.E., 2009. Economic valuation of the vulnerability of world agriculture confronted with pollinator decline. *Ecological Economics* 68, 810–821.
- Gao, F., Morisette, J.T., Wolfe, R.E., Ederer, G., Pedelty, J., Masuoka, E., Myneni, R., Tan, B., Nightingale, J., 2008. An algorithm to produce temporally and spatially continuous MODIS-LAI time series. *Geoscience and Remote Sensing Letters, IEEE* 5, 60–64.
- Harbo, J.R., 1993. Worker-Bee Crowding Affects Brood Production, Honey Production, and Longevity of Honey Bees (Hymenoptera: Apidae). *Journal of Economic Entomology* 86, 1672–1678.
- Huete, A., Didan, K., Miura, T., Rodriguez, E.P., Gao, X., Ferreira, L.G., 2002. Overview of the radiometric and biophysical performance of the MODIS vegetation indices. *Remote Sensing of Environment* 83, 195–213.
- Huete, A., Justice, C., van Leeuwen, W., 1999. MODIS Vegetation Index (MOD 13) Algorithm Theoretical Basis Document Version 3. http://modis.gsfc.nasa.gov/data/atbd/atbd_mod13.pdf (accessed 05/05/14).
- Jensen, J.R., 2006. *Remote Sensing of the Environment: An Earth Resource Perspective*, 2nd Edition. ed. Prentice Hall, Upper Saddle River, NJ.
- Jeong, S.-J., Ho, C.-H., Gim, H.-J., Brown, M.E., 2011. Phenology shifts at start vs. end of growing season in temperate vegetation over the Northern Hemisphere for the period 1982–2008. *Global Change Biology* 17, 2385–2399.
- Jönsson, P., Eklundh, L., 2002. Seasonality extraction by function fitting to time-series of satellite sensor data. *IEEE Transactions on Geoscience and Remote Sensing*, 40, 1824–1832.
- Jönsson, P., Eklundh, L., 2004. TIMESAT—A program for analyzing time-series of satellite sensor data. *Computers & Geosciences* 30, 833–845.
- Jönsson, P., Eklundh, L., 2011. *TIMESAT 3.1 Software Manual*.
- Justice, C.O., Townshend, J.R.G., Vermote, E.F., Masuoka, E., Wolfe, R.E., Saleous, N., Roy, D.P., Morisette, J.T., 2002. An overview of MODIS Land data processing and product status. *Remote Sensing of Environment* 83, 3–15.
- Liang, L., Schwartz, M.D., Fei, S., 2011. Validating satellite phenology through intensive ground observation and landscape scaling in a mixed seasonal forest. *Remote Sensing of Environment* 115, 143–157.
- Los, S.O., Collatz, G.J., Bounoua, L., Sellers, P.J., Tucker, C.J., 2001. Global interannual variations in sea surface temperature and land surface vegetation, air temperature, and precipitation. *Journal of Climate* 14, 1535–1549.

- McGregor, S.E., 1976. Insect pollination of cultivated crop plants. Agricultural Research Service, US Department of Agriculture.
- McLellan, A.R., 1977. Honeybee colony weight as an index of honey production and nectar flow: a critical evaluation. *Journal of Applied Ecology* 14, 401–408.
- Meikle, W.G., Holst, N., Mercadier, G., Derouané, F., James, R.R., 2006. Using balances linked to dataloggers to monitor honeybee colonies. *Journal of Apicultural Research* 45, 39–41.
- Meikle, W.G., Rector, B.G., Mercadier, G., Holst, N., 2008. Within-day variation in continuous hive weight data as a measure of honey bee colony activity. *Apidologie* 39, 694–707.
- Menzel, A., Estrella, N., Fabian, P., 2001. Spatial and temporal variability of the phenological seasons in Germany from 1951 to 1996. *Global Change Biology* 7, 657–666.
- Menzel, A., Sparks, T.H., Estrella, N., Koch, E., Aasa, A., Ahas, R., Alm-Kübler, K., Bissolli, P., Braslavská, O., Briede, A., Chmielewski, F.M., Crepinsek, Z., Curnel, Y., Dahl, Å., Defila, C., Donnelly, A., Filella, Y., Jatczak, K., Måge, F., Mestre, A., Nordli, Ø., Peñuelas, J., Pirinen, P., Remišová, V., Scheifinger, H., Striz, M., Susnik, A., Van Vliet, A.J.H., Wielgolaski, F.-E., Zach, S., Züst, A., 2006. European phenological response to climate change matches the warming pattern. *Global Change Biology* 12, 1969–1976.
- Myneni, R.B., Keeling, C.D., Tucker, C.J., Asrar, G., Nemani, R.R., 1997. Increased plant growth in the northern high latitudes from 1981 to 1991. *Nature* 386, 698–702.
- National Research Council, 2007. Status of Pollinators in North America. The National Academies Press, Washington DC.
- Nightingale, J.M., Esaias, W.E., Wolfe, R.E., Nickeson, J.E., Ma, P.L.A., 2008. Assessing Honey Bee Equilibrium Range and Forage Supply using Satellite-Derived Phenology. Presented at the Geoscience and Remote Sensing Symposium, IGARSS 2008. IEEE International, pp. 763 – 766.
- Ollerton, J., Winfree, R., Tarrant, S., 2011. How many flowering plants are pollinated by animals? *Oikos* 120, 321–326.
- Painho, M., Farral, H., Barata, F., 1996. Digital map of European ecological regions (DMEER). Its concept and elaboration, in: Proceedings of the Second Joint European Conference & Exhibition on Geographical Information (Vol. 1): From Research to Application through Cooperation. IOS Press, pp. 437–446.
- Parmesan, C., 2006. Ecological and Evolutionary Responses to Recent Climate Change. *Annual Review of Ecology, Evolution, and Systematics* 37, 637–669.
- Pettorelli, N., Vik, J.O., Mysterud, A., Gaillard, J.-M., Tucker, C.J., Stenseth, N.C., 2005. Using the satellite-derived NDVI to assess ecological responses to environmental change. *Trends in Ecology & Evolution* 20, 503–510.
- Potts, S.G., Biesmeijer, J.C., Kremen, C., Neumann, P., Schweiger, O., Kunin, W.E., 2010. Global pollinator declines: trends, impacts and drivers. *Trends in Ecology & Evolution* 25, 345–353.
- Reed, B.C., Brown, J.F., VanderZee, D., Loveland, T.R., Merchant, J.W., Ohlen, D.O., 1994. Measuring phenological variability from satellite imagery. *Journal of Vegetation Science* 5,

703–714.

- Reed, B.C., Schwartz, M.D., Xiao, X., 2009. Remote sensing phenology, in: *Phenology of Ecosystem Processes*. Springer, pp. 231–246.
- Roy, D.P., Borak, J.S., Devadiga, S., Wolfe, R.E., Zheng, M., Descloitres, J., 2002. The MODIS land product quality assessment approach. *Remote Sensing of Environment* 83, 62–76.
- Running, S.W., Nemani, R.R., 1991. Regional hydrologic and carbon balance responses of forests resulting from potential climate change. *Climatic Change* 19, 349–368.
- Schmid-Hempel, P., 1987. Efficient nectar-collecting by honeybees: I. Economic models. *Journal of Animal Ecology* 56, 209–218.
- Schmid-Hempel, P., Schmid-Hempel, R., 1987. Efficient nectar-collecting by honeybees: II. Response to factors determining nectar availability. *The Journal of Animal Ecology* 56, 219–227.
- Schwartz, M.D., Crawford, T.M., 2001. Detecting energy-balance modifications at the onset of spring. *Physical Geography* 22, 394–409.
- Schwartz, M.D., Hanes, J.M., 2010. Intercomparing multiple measures of the onset of spring in eastern North America. *International Journal of Climatology* 30, 1614–1626.
- Schwartz, M.D., Reed, B.C., 1999. Surface phenology and satellite sensor-derived onset of greenness: An initial comparison. *International Journal of Remote Sensing* 20, 3451–3457.
- Schwartz, M.D., Reed, B.C., White, M.A., 2002. Assessing satellite-derived start-of-season measures in the conterminous USA. *International Journal of Climatology* 22, 1793–1805.
- Schwartz, M.D., Reiter, B.E., 2000. Changes in north American spring. *International Journal of Climatology* 20, 929–932.
- Seeley, T.D., 1985. *Honeybee ecology: a study of adaptation in social life*. Princeton University Press, Princeton, NJ.
- Seeley, T.D., 1987. The effectiveness of information collection about food sources by honey bee colonies. *Animal behaviour* 35, 1572–1575.
- Seeley, T.D., 1995. *The Wisdom of the Hive: The Social Physiology of Honey Bee Colonies*. Harvard University Press, Cambridge, MA.
- Sellers, P.J., 1985. Canopy reflectance, photosynthesis and transpiration. *International Journal of Remote Sensing* 6, 1335–1372.
- Solano, R., Didan, K., Jacobson, A., Huete, A., 2010. MODIS Vegetation Index User's Guide (MOD 13 Series)
http://vip.arizona.edu/documents/MODIS/MODIS_VI_UsersGuide_01_2012.pdf (accessed 03/03/14)
- Stenseth, N.C., Mysterud, A., 2002. Climate, changing phenology, and other life history traits: Nonlinearity and match–mismatch to the environment. *Proceedings of the National Academy of Sciences* 99, 13379–13381.
- Stocker, T.F., Qin, D., Plattner, G.-K., Tignor, M., Allen, S.K., Boschung, J., Nauels, A., Xia, Y.,

- Bex, V., Midgley, P.M., 2013. The Physical Science Basis. Working Group I Contribution to the Fifth Assessment Report of the Intergovernmental Panel on Climate Change. IPCC.
- Stöckli, R., Vidale, P.L., 2004. European plant phenology and climate as seen in a 20-year AVHRR land-surface parameter dataset. *International Journal of Remote Sensing* 25, 3303–3330.
- Studer, S., Stöckli, R., Appenzeller, C., Vidale, P.L., 2007. A comparative study of satellite and ground-based phenology. *International Journal of Biometeorology* 51, 405–414.
- Szabo, T.I., Lefkovitch, L.P., 1991. Effects of honey removal and supering on honey bee colony gain. *American Bee Journal* 130, 815–816.
- Tan, B., Morisette, J.T., Wolfe, R.E., Gao, F., Ederer, G.A., Nightingale, J., Pedelty, J.A., 2011. An enhanced TIMESAT algorithm for estimating vegetation phenology metrics from MODIS data. *IEEE Journal of Selected Topics in Applied Earth Observations and Remote Sensing* 4, 361–371.
- Thuiller, W., Lavorel, S., Araujo, M.B., Sykes, M.T., Prentice, I.C., 2005. Climate change threats to plant diversity in Europe. *Proceedings of the National Academy of Sciences of the United States of America* 102, 8245–8250.
- Tilman, D., Fargione, J., Wolff, B., D'Antonio, C., Dobson, A., Howarth, R., Schindler, D., Schlesinger, W.H., Simberloff, D., Swackhamer, D., 2001. Forecasting agriculturally driven global environmental change. *Science* 292, 281–284.
- Tucker, C.J., 1979. Red and photographic infrared linear combinations for monitoring vegetation. *Remote Sensing of Environment* 8, 127–150.
- Visscher, P.K., Seeley, T.D., 1982. Foraging Strategy of Honeybee Colonies in a Temperate Deciduous Forest. *Ecology* 63, 1790–1801.
- Visser, M.E., Both, C., 2005. Shifts in phenology due to global climate change: the need for a yardstick. *Proceedings of the Royal Society B: Biological Sciences* 272, 2561–2569.
- Von Frisch, K., 1967. *The Dance Language and Orientation of Bees*. Harvard University Press., Cambridge, MA.
- Walther, G.-R., Post, E., Convey, P., Menzel, A., Parmesan, C., Beebee, T.J., Fromentin, J.-M., Hoegh-Guldberg, O., Bairlein, F., 2002. Ecological responses to recent climate change. *Nature* 416, 389–395.
- White, M.A., de Beurs, K.M., Didan, K., Inouye, D.W., Richardson, A., Jensen, O.P., O'Keefe, J., Zhang, G., Nemani, R., 2009. Intercomparison, interpretation, and assessment of spring phenology in North America estimated from remote sensing for 1982–2006. *Global Change Biology* 15, 2335–2359.
- White, M.A., Hoffman, F., Hargrove, W.W., Nemani, R.R., 2005. A global framework for monitoring phenological responses to climate change. *Geophysical Research Letters* 32.
- White, M.A., Running, S.W., Thornton, P.E., 1999. The impact of growing-season length variability on carbon assimilation and evapotranspiration over 88 years in the eastern US deciduous forest. *International Journal of Biometeorology* 42, 139–145.
- Williams, I.H., 1994. The dependence of crop production within the European Union on pollination by honey bees. *Agricultural Zoology Reviews* 6, 229–257.

- Wilson, K.B., Baldocchi, D.D., 2000. Seasonal and interannual variability of energy fluxes over a broadleaved temperate deciduous forest in North America. *Agricultural and Forest Meteorology* 100, 1–18.
- Zhang, X., Friedl, M.A., Schaaf, C.B., 2009. Sensitivity of vegetation phenology detection to the temporal resolution of satellite data. *International Journal of Remote Sensing* 30, 2061–2074.
- Zhang, X., Friedl, M.A., Schaaf, C.B., Strahler, A.H., Hodges, J.C.F., Gao, F., Reed, B.C., Huete, A., 2003. Monitoring vegetation phenology using MODIS. *Remote Sensing of Environment* 84, 471–475.
- Zhang, X., Tarpley, D., Sullivan, J.T., 2007. Diverse responses of vegetation phenology to a warming climate. *Geophysical Research Letters* 34.
- Zhou, L., Tucker, C.J., Kaufmann, R.K., Slayback, D., Shabanov, N.V., Myneni, R.B., 2001. Variations in northern vegetation activity inferred from satellite data of vegetation index during 1981 to 1999. *Journal of Geophysical Research: Atmospheres* 106, 20069–20083.

Mapping The Phenology of European Honey Bee Nectar Flows

Part II-A: Technical Report

ii. TABLE OF CONTENTS

i. TITLE PAGE.....	1
ii. TABLE OF CONTENTS.....	2
iii. LIST OF ABBREVIATIONS AND ACRONYMS.....	4
iv. LIST OF FIGURES AND TABLES.....	5
1. INTRODUCTION.....	7
2. FURTHER LITERATURE REVIEW.....	7
2.1 BEEKEEPING.....	7
2.2 BEEKEEPING AND GIS.....	7
2.3 HONEY BEES.....	8
2.4 FORAGING.....	8
2.5 NECTAR PRODUCTION.....	9
2.6 PHENOLOGY.....	10
2.7 PHENOLOGY OF PLANTS.....	11
2.8 PHENOLOGY OF HONEY BEES.....	11
2.9 START OF SEASON.....	12
2.10 DIGITAL MAPS OF EUROPEAN ECOLOGICAL REGIONS (DMEER).....	14
2.10.1 ALPS CONIFER AND MIXED FORESTS.....	14
2.10.2 WESTERN EUROPEAN BROADLEAF FORESTS.....	15
3. TECHNICAL REPORT.....	16
3.1 MODIS METHODOLOGY.....	16
3.2 TIMESAT.....	17
3.3 NOISE.....	18
3.4 SMOOTHING.....	18
3.5 ASYMMETRIC GAUSSIAN METHOD.....	19
3.6 ADOPTION TO UPPER ENVELOPE.....	20
3.7 INTEGRATION OF TEMPERATURE DATA.....	20
4. ALTERNATIVE START OF SEASON MEASUREMENT.....	22
4.1 INTRODUCTION.....	22
4.2 DATA AND METHODS.....	24
4.2.1 MODIS.....	24
4.2.2 HBNF.....	24
4.3 RESULTS AND DISCUSSION.....	25
4.4 CONCLUSION.....	26
5. HBNF INTERPOLATION.....	27
5.1 INTRODUCTION.....	27
5.2 METHODOLOGY.....	27
5.3 RESULTS AND DISCUSSION.....	27
5.4 CONCLUSION.....	30

6. LIMITATIONS OF STUDY31

 6.1 MODIS.....31

 6.2 SCALE WEIGHT DATA.....31

 6.3 WEATHER.....32

 6.4 FORAGING.....33

 6.5 NECTAR SOURCES – FORAGE ZONES.....33

7. BIBLIOGRAPHY35

iii. LIST OF ABBREVIATIONS AND ACRONYMS

AVHRR – Advanced Very High Resolution Radiometer

BRDF – Bidirectional Reflectance Distribution Function

DMEER – Digital Maps of European Ecological Regions

EVI – Enhanced Vegetation Index

GIS – Geographical Information Science

HBNF – Honey Bee Nectar Flow

HDF – Hierarchical Data Format

LAI – Leaf Area Index

LSP – Land Surface Phenology

LST – Land Surface Temperature

MLDC – MODIS Land Cover Dynamics Algorithm

MODIS – Moderate Resolution Imaging Spectroradiometer

MVC – Maximum Value Composite

NASA – National Aeronautics and Space Administration

NBAR – Nadir BRDF-Adjusted Reflectance

NF – Nectar Flow

QA – Quality Assurance

SDS – Scientific Data Set

SOS – Start of Season

VI – Vegetation Index

iv. LIST OF FIGURES AND TABLES

Figure 1: Alps Conifer and Mixed Forests DMEER.....	14
Figure 2: Western European Broadleaf DMEER.....	15
Figure 3: Compositing method for MOD13 Q1/A1 products.....	16
Figure 4: Effect of parameter changes on local functions. In (a) parameter a2, which determines width of right function half, has been decreased (solid line) and increased (dashed line) compared to value of left half. In (b) parameter a3, which determines flatness of right function half, has been decreased (solid line) and increased (dashed line) compared to value of left half. From Jönsson and Eklundh (2004).....	19
Figure 5: Fitted functions around a maximum from the two-step procedure. The dashed line shows the fitted function from the first step, and the solid line the fit from the second step. The original NDVI time-series is shown by the noisy fine continuous line. From Jönsson and Eklundh (2004).....	20
Figure 6: An example of preprocessing NDVI data. During winter months, snow/cloud covered pixels are assigned a base NDVI value (yellow). Blue line is Gaussian curve derived by TIMESAT.....	21
Figure 7: The graphical interface of TIMESAT showing the parameters and settings used.....	21
Figure 8: TIMESAT SOS – HBNF 50%, n=7.....	25
Figure 9: Onset EVI Greenness (3km Mean), n=7.....	25
Figure 10: Onset EVI Greenness (Pixel), n=7.....	25
Figure 11: Belgium HBNF Start Day 2011.....	28
Figure 12: Belgium HBNF 50% Day 2011.....	28
Figure 13: Switzerland HBNF Start Day 2011.....	28
Figure 14: Switzerland HBNF 50% Day 2011.....	28
Figure 15: Slovenia HBNF Start Day 2011.....	28
Figure 16: Slovenia HBNF 50% Day 2011.....	28
Figure 17: Finland HBNF Start Day 2011.....	29
Figure 18: Finland HBNF 50% Day 2011.....	29
Figure 19: Bee Forage Regions of North America. From Ayers and Harman (1992).....	34

Table 1: A selection of SOS calculation methods: name and estimation category. From White (2009)..... 13

Table 2: MODIS Pixel Quality Assessment..... 17

Table 3: Onset EVI Greenness by year and location.....25

1. INTRODUCTION

This technical report supplements the Research Paper (Blomstedt, 2014) by offering a further literature review, describing the methods used in greater depth, detailing unsuccessful approaches, addressing other research questions, and discussing the study limitations.

2. FURTHER LITERATURE REVIEW

2.1 BEEKEEPING

European honey bees (*Apis mellifera*) have been managed by humans for several millennial, with the first evidence of beekeeping found in the Mediterranean area (Crane, 2013). Bees are generally kept in order to harvest hive products like honey, wax and propolis, but they are also known for pollinating crops. In the past decade both American and European countries have reported high rates of disorders affecting their honey bee colonies (Haubruge et al., 2006; vanEngelsdorp and Meixner, 2010). The most recent survey from 2012-13 showed that many Northern European countries suffered colony losses greater than 20% (Chauzat et al., 2014). Researchers have been unable to pin down a single cause for declining bee health and instead it is likely a combination of factors including poor management practices, parasites and diseases, pesticides, climate and nutrition (vanEngelsdorp and Meixner, 2010).

2.2 BEEKEEPING AND GIS

Although honey bees are influenced by their environment, few studies have incorporated honey bee data into GIS for the purposes of gauging these spatial relationships (Rogers and Staub, 2013). GIS has been utilized more extensively to study solitary bee populations in relation to changing land use and climate (e.g. Kremen et al., 2002; Watson et al., 2011; Giannini et al., 2012). For honey bees, GIS and remote sensing have been employed in the prediction of nests for the Asiatic giant honey bee (*Apis dorsata*) in Malaysia (Saberioon, 2010) as well as the spatial distribution of their forage (Ibrahim et al., 2012). GIS has also been used to predict forage suitability and prime beekeeping locations in the Philippines. (Estoque and Murayama, 2011), North Eastern Italy (Berardinelli and Vedova, 2004), Malaysia (Maris et al., 2008), Saudi Arabia (Abou-Shaara et al., 2013) and Belgium (Janssens, 2006). Finally, GIS has been incorporated by Naug (2009) to study the relationship between habitat loss and honeybee colony collapses, and by Henry et. al. (2012) to look at floral scheme efficiency.

2.3 HONEY BEES

The European bee is one of seven bee species in the *Apis* genus and the only native to Europe. Regional climates have caused the evolution of several subspecies of *Apis mellifera* on the continent, including *Apis mellifera mellifera* (German dark bees), *Apis mellifera ligustica* (Italian bees), *Apis mellifera carnica* (Carniolian bees) and *Apis mellifera caucasica* (Caucasian bees) (Ruttner, 1975). It is a eusocial insect, living in large colonies with a complex social system consisting of three castes: queen, worker and drone. Each colony normally has a single queen who is the mother of all the inhabitants. After hatching and a brief mating flight, the queen spends the remainder of her life laying eggs inside the hive. Workers are unfertilized females and make up the majority (~90%) of the population. As their name suggests, they perform virtually all the tasks required by the colony, including cleaning, rearing larvae, defending from attackers and foraging. Drones are the male and do little else besides congregate outside the hive and attempt to mate with virgin queens on summer afternoons.

Hive population varies by season, with growth is usually at or near the maximum in the spring (Winston, 1991). In an annual period a colony will rear some 150,000 bees, but will overwinter with only a few thousand. Colonies need to collect 120 kg of nectar and 20 kg of pollen annually to survive (Seeley, 1985). Nectar is processed and ripened into honey; a hygroscopic, antibacterial liquid that, with a water content of 18%, is resistant to yeasts and fermentation. Bees also consume honey to secrete wax, with approximately 8 kg of honey needed to make 1 kg of wax (Whitcomb Jr, 1946). The wax is used to build the comb structure on which all in-nest activities occur. With the average load of nectar around 10 mg, a hive will make almost 4 million trips for nectar and one million for pollen per annum (Winston, 1991). In strong colonies and under ideal conditions, workers can make up to 163,000 trips daily (Gary, 1967). Yet many feral colonies barely collect enough resources and many starve to death every winter (Seeley, 1985).

2.4 FORAGING

To gather food, honey bees must leave their hive and enter the surrounding environment. Bees have been reported to forage at temperatures between 5° and 45° C (Heinrich, 1979; Cooper et al., 1985; Spangler, 1992) but foraging generally does not begin until temperatures reach 12°-14° C (Winston, 1991). Relationships between wind, rain and foraging show decreasing foraging intensity resulting from higher winds and heavier rainfall (Ribbands, 1953). Furthermore, light intensity and global solar radiation values are positively correlated with flight departures (Burrill and Dietz, 1981).

The foraging range of a honey bee colony depends on the availability of resources. Flying for nectar or pollen requires energy expenditure and foragers will not travel long distances if unnecessary. In agricultural areas, the median foraging radius of honey bee colonies is only a few hundred meters (Ribbands, 1953; Michener, 1974) but in a deciduous forest in New York State, colonies foraged over a large radius, from 0.5 to 10 km, with a mean of 2.3km (Visscher and Seeley, 1982). In central Germany, Steffan-Dewenter and Kuhn (2003) found a mean of 1.5 km with a range of up to 10 km. Karl von Frisch, the original reporter of the bee dance language, discovered a scout bee could report sources up to 13.5 km away (Von Frisch, 1967). The foraging distance varies greatly on the time of year, with bees often forced to fly much greater distances in the summer due to the scarcity of nectar (Beekman and Ratnieks, 2000; Beekman et al., 2004; Couvillon et al., 2014). The range is also influenced by the particular hive, as foraging distances have been shown to differ significantly between matched colonies (Waddington et al., 1994). Visscher and Seeley (1982) found the 95th percentile of foragers was at 6km, a radius encircling more than 100 km². Except in extreme cases, such as large-scale monocrop agriculture, there will be an array of floral sources within this area.

2.5 NECTAR PRODUCTION

Nectar is a sugar-rich liquid produced by flowers as a part of plant-animal mutualism. It is the food for an enormous variety of insects, a tenth of all bird species and also can act as an energy drink for some larger animals. Nectar composition varies widely, quantitatively more than qualitatively, presumably because it is produced to reward different kinds of animals (Faegri and Van der Pijl, 1966). Its basic constituents are water, ions, carbohydrates, amino acids, low molecular weight proteins, enzymes and antioxidants to maintain homeostasis (Carter and Thornburg, 2004).

Nectar secretion is a complex process based on the genetics of the plant as well as many facets of the environment. This means nectar secretion may vary not only between species, but between population, individual or even flower. Temperature is the environmental variable most often cited as related to nectar secretion rate (Nicolson et al., 2007). Secretion does not start below a certain temperature, the critical threshold according to the species, and then tends to increase alongside temperature (Fahn, 1949; Shuel, 1952; Corbet, 1990; Jakobsen and Kritjansson, 1994). However it also reported to slow with increasing temperature in certain plants (Freeman and Head, 1990; Jakobsen and Kritjansson, 1994). The optimum range of temperature for nectar secretion is known for only a few species (Jakobsen and Kritjansson, 1994 and references therein). Water availability is also considered a factor in the regulation of nectar secretion rate (Wyatt et al., 1992)

as are soil nutrients (Shuel, 1957), ambient humidity (Corbet et al., 1979) and the use of fertilizers (Fahn, 1949; Shuel, 1992). Visits by insects or artificial withdrawal of nectar are also thought to stimulate secretion (Heinrich, 1975; Real and Rathcke, 1991).

Nectar is not secreted at a constant rate. For most plants there is not only a difference between night and day, but a characteristic rhythm of secretion throughout the 24 hours (Cruden et al., 1983). Due to higher humidity, nectar secretion during the night usually contains more water than in the day; for certain plants (*Borago*, *Teucrium*) the diurnal rate of nectar secretion may remain constant while the sugar content varies, while for others (*Lythrum*, *Salvia*) the quantity may fluctuate while the sugar concentration remains the same (Crane, 1975). For many plants the optimal time for nectar secretion (maximum quantity and sugar content) is during the morning, and the foraging bees will adjust to the daily plant rhythm. Their visits to a certain species of flowers reach a maximum in the peak period of nectar secretion – i.e. when the flowers offer the greatest quantity of the most highly concentrate nectar (Michener, 1974). When a plant has two separate peaks periods, the curve plotted for bee visits will also show two peaks.

2.6 PHENOLOGY

Phenology, which is derived from the Greek word *phaino* meaning to show or to appear, is the study of recurring plant and animal life cycle stages, especially their timing and relationships with weather and climate (Schwartz, 2003). Sprouting and flowering of plants in the spring, bud burst, colour changes of leaves in the fall, bird migration and nesting, insect hatching and animal hibernation are all examples of phenological events (Dube et al., 1984). These events are genetically predetermined but also strongly modulated by climatic conditions, particularly temperature, day length and water availability (Schaber and Badeck, 2003; Zhang et al., 2005). Currently there is great concern over the Earth's changing climate (Walther et al., 2002; IPCC, 2007). With the past century warming 0.85° C and predicted to continue (Stocker et al., 2013), phenology is seen as an efficient method to compare records of the past to the current biotic response.

Phenological records go back to the 1730s in the UK (Sparks and Carey, 1995) and even longer in China (Hameed and Gong, 1994) and Japan (Aono and Kazui, 2008). Many European countries have records for a variety of phenological events for decades or even longer (Chmielewski, 1996). The second half of the 20th century showed an assortment of shifting spring phenologies, with Western and Central Europe advancing four weeks and Eastern Europe delaying by up to two weeks (Ahas et al., 2002). Spring advances have been reported for a variety of living

organisms including vertebrates (Lehikoinen et al., 2004; Thackeray et al., 2010) invertebrates (Roy and Sparks, 2000) and terrestrial plants (Menzel et al., 2006)

2.7 PHENOLOGY OF PLANTS

Flowering in angiosperms is an important phenological measure. Plants in temperate areas are adapted to an annual seasonal cycle with a winter dormancy period that is sensitive to temperature and light. In many cases flowering time is directly related to temperature (Sparks et al., 2000), but some species may not flower earlier as a response to increased temperatures (22% of species included by (Menzel et al., 2006)). Other potential cues for flowering initiation include photoperiodicity, precipitation, soil humidity and snow melt (Price and Waser, 1998; Inouye et al., 2003) as well as other, more peculiar stimulus (Lambrecht et al., 2007).

Plants are frequently shown to be flowering earlier compared to the past (Root et al., 2003; Parmesan, 2007) but most studies use first flowering dates describe changes in phenology (Sparks and Carey, 1995; Inouye et al., 2003; Miller-Rushing and Primack, 2008). This is often because only first flowering dates are available; it's much easier for an observer to note the date that a species first flowers rather than monitoring the progression of flowering from an entire population, which could last for weeks or even months. But first flowering lies at the edge of the flowering distribution and can be susceptible to compounding effects. Those observations may be affected by population size and sampling effort (Miller-Rushing et al., 2008).

2.8 PHENOLOGY OF HONEY BEES

The importance of temperature on insect phenology has been extensively demonstrated (Zhou et al., 1995; Sparks and Yates, 1997; Forister and Shapiro, 2003; Stefanescu et al., 2003). Invertebrates are perhaps the most sensitive branches of organisms to climate change (Gordo and Sanz, 2006). Insects are small and poikilothermic, therefore their thermoregulation and activity are strongly affected by weather variability. In species with a wintering larval stage, warmer years will cause adults will emerge earlier.

While not as prevalent as some other phenological databases (Sparks and Carey, 1995), beekeepers and researchers have recorded honey bee phenology. In certain areas (e.g. Slovenia) scale-hive records have been kept for over 100 years. Another phenological event is the honey bee “cleansing flight,” when bees first leave the hive to excrete the faeces stored in their gut. These flights are related to ambient temperatures (Scheifinger et al., 2005), specifically a strong negative relationship with temperature in February to April (Gordo and Sanz, 2006). Sparks (2010) reported

an advance in these cleansing flights in Poznań, Poland by over a month during the period 1985-2009. Gordo and Sanz (2006) also reported an advance of cleansing flights in Spain during 1952-2004.

Honey bees are one of the few insects that do not take an obligate diapause, meaning they spend the winter as adults in an active state. Consequently they are able to react much more quickly to the changing conditions outside the hive. This appears to make them less of a concern to the concept of a trophic collapse, however the colony may suffer from rapidly changing phenologies. Because honey bee nectar flows (HBNF) can be short and intense, the hive must be prepared with an adequate foraging force when the flowers are secreting nectar. If this comes early, when only a minimal number of foragers are available, the colony will not be able to take full advantage of the flow and subsequently not have enough food for the coming dearth.

While honey bees only have to wake from their lethargy, other species of bees spend the cold period inactive in larval form, meaning they must complete their development in response to environmental factors in the spring. The few species which have been studied show more complex responses in their spring emergence (Bosch and Kemp, 2003; Sgolastra et al., 2010). These species are more susceptible to the threat of trophic decoupling, as they are often specialist pollinators with a smaller number of plant species to forage on. These under-appreciated pollinators are often more effective than honey bees are contribute greatly to agricultural production (Garibaldi et al., 2013).

2.9 START OF SEASON

Remote sensing integrates signals from land surface processes as well as reflectance from plants, so satellite-based phenology is often called land surface phenology (LSP). One sought after measure of LSP is the start of season (SOS) which is defined as the rapid sustained increase in remotely sensed greenness after the longest annual period of photosynthetic senescence (White et al., 2009). With remote sensing's ability to detect LSP at large scales, it is possible to model phenological patterns at a regional continental or global scale.

There have been many attempts to calculate SOS and other phenological metrics (Lloyd, 1990; Reed et al., 1994; Myneni et al., 1997; White et al., 1997, 2002; Zhang et al., 2003; Jönsson and Eklundh, 2004; Fisher et al., 2007; Tan et al., 2008; de Beurs and Henebry, 2010). One problem facing these methods is that an accepted definition of spring arrival does not exist. Frequently SOS, “green-up,” leaf-out and “green wave” are used interchangeably, but in reality may refer to different biological processes. White and Nemani (2003) point out a potential confusion and bias on how to

calculate phenological transition times due to the mix of methods and definitions being used.

Table 1: A selection of SOS calculation methods: name and estimation category. From White (2009)

Full name	Algorithm: SOS estimate
Quadratic	Conceptual-mathematical: first composite period of growing degree accumulation best fitting the observed NDVI time series
NDVI 0.2	Global threshold: NDVI exceeds 0.2
NDVI 0.3	Global threshold: NDVI exceeds 0.3
Delayed Moving Average	Conceptual-mathematical: smoothed NDVI exceeds expected value of near-term historical NDVI
Harmonic Analyses of NDVI Time-Series – Fast Fourier Transform	Conceptual-mathematical: maximum increase on Fourier approximation of NDVI
TIMESAT	Conceptual-mathematical: high amplitude divergence from a multiple-model NDVI fit
Midpointpixel	Local threshold: NDVI exceeds locally tuned threshold; run for every pixel
Percent-Above-Threshold	Local threshold: NDVI exceeds locally tuned threshold; run for the group behavior of all pixels within an ecoregion
Gaussian	Hybrid: average date when Gaussian fit of NDVI exceeds three global thresholds
Midpointcluster	Local threshold: NDVI exceeds locally tuned threshold; run for time series aggregated to a cluster level

LSP and SOS calculations have often compared poorly with field-based phenology. Schwartz and Hanes (2010) found few significant correlations between five SOS calculations at three observed sites in the eastern United States, concluding that collecting ground data at an areal scale similar to satellite data was needed. White et al. (2009) performed a comprehensive intercomparison of Advanced Very High Resolution Radiometer (AVHRR)-based SOS methods over broad regions of North America, relating them to ground phenology data, bioclimatic model predictions and cryospheric/hydrologic seasonality metrics (Table 1). Tested SOS measures found that individual methods differed from each other by ± 60 days with a standard deviation of ± 20 . The estimates were most accurate in northern latitudes and least in arid, tropic and Mediterranean ecoregions. In a comparison with an ensemble of SOS models averaged by ecoregion from 1982–2006, TIMESAT had the least SOS day of year variability anomalies.

2.10 DIGITAL MAPS OF EUROPEAN ECOLOGICAL REGIONS (DMEER)

2.10.1 ALPS CONIFER AND MIXED FORESTS

Situated in Central Europe, the Alps conifer and mixed forests stretch 1200 kilometres across France, Italy, Germany, Austria, Slovenia and Switzerland and Liechtenstein (Figure 1). The Alps are ecologically significant region similar to the original forest cover of central and southern Europe. Some of these forests can be considered almost in a natural state. Over 4500 species of plants are found this region, 400 which are endemic.

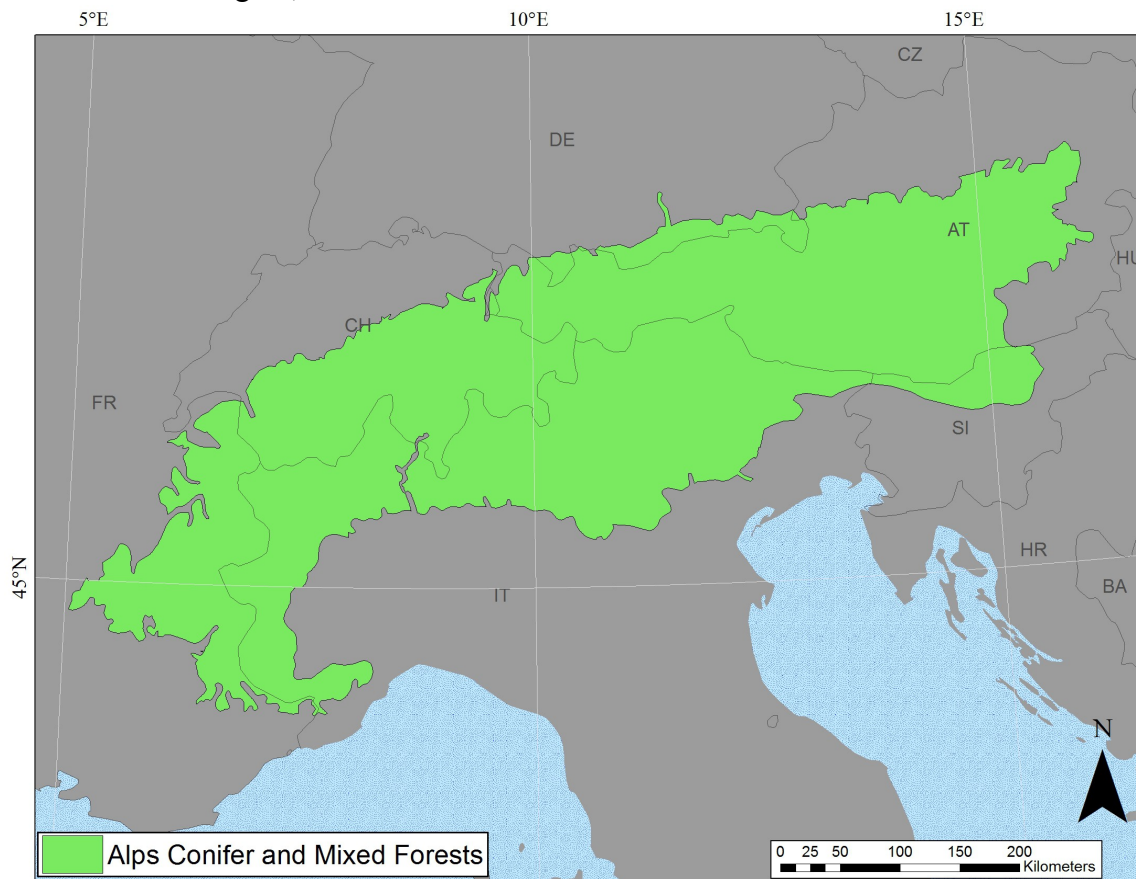


Figure 1: Alps Conifer and Mixed Forests DMEER

The Alps are a temperate, cool transitional zone between central and Mediterranean Europe. They can be divided into three major sections; the western is influenced by the mild and humid Atlantic air streams, the central has continental climate and the eastern region exhibits a Mediterranean climate. Three relevant ecological patterns can be identified within this mountain system – deep valleys with broad-leaved trees, evergreen trees in Mediterranean areas and mountain forests composed of mixed European Beech (*Fagus sylvatica*), Silver Fir (*Abies alba*), Norway Spruce (*Picea abies*) and others (Bohn et al., 2000). However these can be split up even further, with 200 habitat types classified throughout the mountain range (Fund and Hogan, 2014). Wildflowers present in the ecoregion are the endemic Alpine Columbine (*Aquilegia alpina*) and the

near endemic Jeweled Rocket (*Sisymbrium austriacum*); other non-endemics include Snow in Summer (*Cerastium tomentosum*) and Candle Larkspur (*Delphinium elatum*).

2.10.2 WESTERN EUROPEAN BROADLEAF FORESTS

Western European Broadleaf Forests are a palearctic ecoregion of approximately 492,360 km² across eastern France, southern Germany, northern Switzerland, northern Austria, part of the Czech Republic and a small area of western Poland (Figure 2). This region covers extensive lowlands, but also higher elevation such as the Alps and Ardennes. Generally these contain lowland

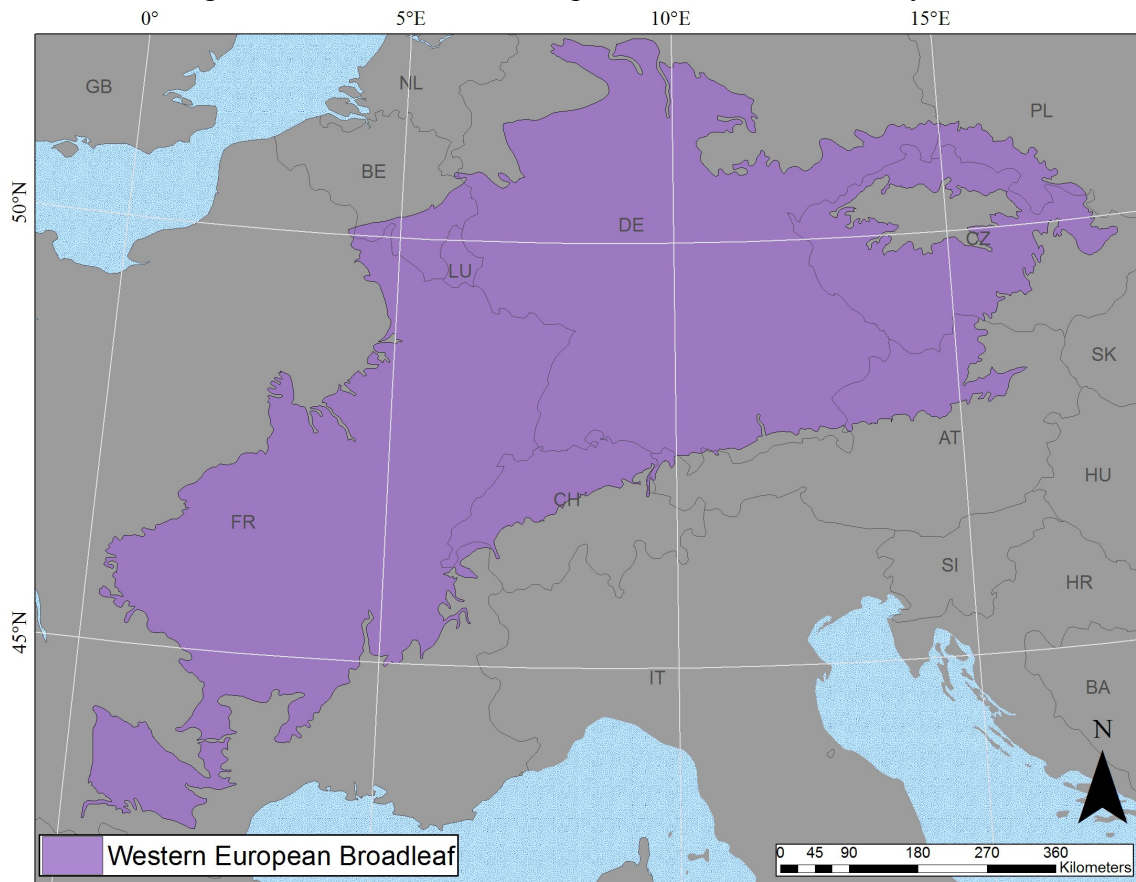


Figure 2: Western European Broadleaf DMEER

to altimontane beech and mixed beech forests of Western Europe, small areas of sub-Mediterranean and meso-supra-Mediterranean downy oak forests and mixed oak hornbeam forests (Bohn et al., 2000). It is classified within the biome of temperate Broadleaf and Mixed forests

This ecoregion has variety of plant assemblies, ranging from true broadleaf forests, to raised bogs and moorlands, although most of the land area has been converted to agriculture (Fund and Hogan, 2013). The main cultivated crops are corn, wheat and oats. This ecoregion holds large cities like Lyon, Nancy and Munich, and it suffers from heavy degradation due to millennia of expanding human populations.

3. TECHNICAL REPORT

3.1 MODIS METHODOLOGY

The Moderate Resolution Imaging Spectroradiometer (MODIS) is an instrument aboard NASA scientific research satellites Terra (EOS AM-1) and Aqua (EOS PM-1) designed for the long-term global remote sensing of the earth's surface and biosphere. Both satellites are at an altitude of 705 km in a near polar orbit with an inclination of 98.2 and a mean period of 98.9 minutes (Salomonson et al., 1989). They are sun-synchronous, with Terra crossing the equator at 10:30 AM, and Aqua at 1:30 PM (Barnes et al., 2002) and together cover the entire Earth's surface every 1 to 2 days. MODIS acquires data in 6 spectral bands spaced between 0.4 μm to 14.4 μm at varying spatial resolutions (2 bands at 250m, 5 bands at 500 m and 29 bands at 1km). It employs a whiskbroom scanning radiometer at a scan rate of 20.3 rpm, with a cross track swath size of 2330 km by 10 km (at nadir) (Nishihama et al., 1997). A global network of ground control points has improved the geolocation accuracy of Terra to better than 45 m and Aqua better than 60 m (Wolfe, 2006). The MODIS project offers a number of processed datasets related to the earth's surface, such as vegetation indices (VI).

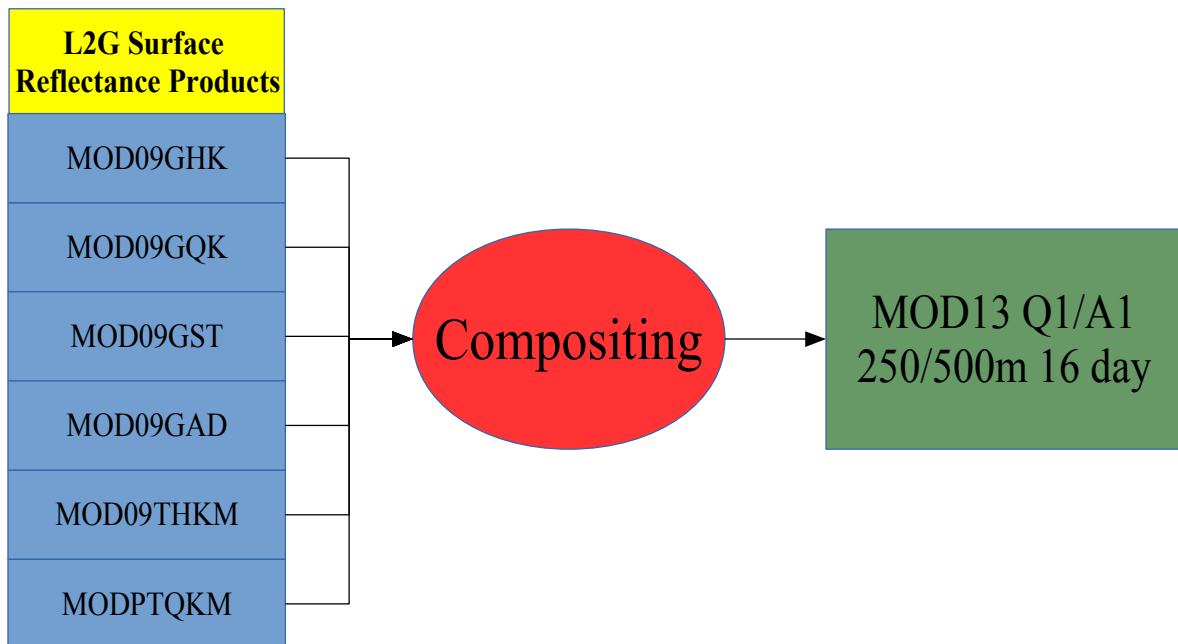


Figure 3: Compositing method for MOD13 Q1/A1 products

MOD13Q1 is a land product derived from data captured by the MODIS Terra satellite. The dataset began production in February 2000 and provides a tile raster VI with a resolution of 250 meters at a 16 day temporal granularity. The MOD13A1 algorithm separates all observations by their orbits and applies a filter to the data based on quality, cloud, and viewing geometry (Solano et

al., 2010). The VI algorithm operates on a per-pixel basis and requires multiple observations to generate a composited index (Figure 3). The pixels are sorted by quality; cloud contaminated and extreme off-nadir sensor views are considered low quality while cloud-free, nadir view with no residual atmospheric contamination are considered high quality. Only the high-quality cloud-free pixels are retained for compositing. Due to orbit overlap, multiple observations may exist for one day and a possible of 64 may occur in a cycle. But because of clouds and sensor spatial coverage, the number is frequently less, with decreasing observations from polar to equatorial latitudes. The number of acceptable pixels over a 16-day compositing period is often fewer than 10, usually varying between 1-5 (Solano et al., 2010). The objective of the compositing methodology is to determine a single value per pixel from all the data retained by the filter, which is assumed to be representative for the pixel over the 16 day period.

This VI compositing algorithm includes (i) the maximum value composite (MVC), meaning each pixel is assigned the maximum value across all observations for that pixel acquired during the compositing period, and (ii) a constraint of view angle–MVC (Holben, 1986). As a result the quality of MODIS NDVI data is significantly enhanced (Huete et al., 2002). Each MODIS land surface dataset contains, along with the science and metadata, one or more quality assurance (QA) layers. These provide pixel level QA (Table 2) as well as summary statistics of certain attributes.

Table 2: MODIS Pixel Quality Assessment

Rank Key	Summary QA	Description
-1	Fill/No Data	Not Processed
0	Good Data	Use with confidence
1	Marginal data	Useful, but look at other QA information
2	Snow/Ice	Target covered with snow/ice
3	Cloudy	Target not visible, covered with cloud

3.2 TIMESAT

A time series is a sequence of observations where adjacent measurements are dependant on time (Box et al., 2013). The value of coarse-resolution time-series NDVI data has been firmly established for monitoring vegetation (Malingreau, 1986; Reed et al., 1996; Tucker et al., 1986) and major phenological events (Reed et al., 1994; Zhang et al., 2003). TIMESAT is a program developed by Per Jönsson and Lars Eklundh for the analysis of time series of satellite sensor data (Jönsson and Eklundh, 2002, 2004). TIMESAT was originally intended for extracting seasonality information from noisy AVHRR NDVI data, but the current version is able to accept different types

of remotely sensed time-series (e.g. data from MODIS Terra/Aqua). The advantages of TIMESAT are (i) it is freely available open source software, (ii) it provides three different smoothing functions to fit time series data, (iii) a user-defined weighting scheme is applicable in the smoothing process, and (iv) a comprehensive set of phenology metrics is generated from the smoothed time series satellite data. The creators of TIMESAT found the program to be generally successful except when the noise level was high and growing season short. A disadvantage is that TIMESAT requires the estimation of up to 8 parameters (de Beurs and Henebry, 2010).

3.3 NOISE

Forest canopy NDVI derived from satellite data can be affected by factors not related to the vegetation. The constituents of a cloudless atmosphere, such as Rayleigh scattering, oxygen, ozone, water vapour and aerosols, may affect the signal by scattering or absorption (Holben, 1986; Goward et al., 1991). Also, depending on the illumination and observed geometry, the spectral bidirectional reflectance of forests may decrease or increase without any change in the forest characteristics due to bidirectional reflectance distribution function (BRDF) effects (Gutman, 1991; Deering et al., 1999). This scattering may cause the NDVI to be lower than the canopy.

The noise is partially accounted for in the MODIS algorithm (Huete et al., 1999) and much of it can be removed by eliminating the values for which the quality assessment indicate poor pixel quality. But TIMESAT is not able to calculate the temporal curve with excessive missing or poor quality data. For a time-series with one growing season per year the threshold of the retrievable data gap within TIMESAT is four months. With a larger data gap green-up information could be missing from the series and the fitted curve would not be accurate.

3.4 SMOOTHING

The short-frequency variation caused by noise in time-series data can be suppressed by means of running averages, running medians or compound smoothers (Van Dijk et al., 1987). There are three smoothing functions available in TIMESAT software: adaptive Savitzky-Golay filtering, asymmetric Gaussian and double logistic. The adaptive Savitzky-Golay method captures rapid changes in the time-series but it is sensitive to noise due to its use of local polynomial functions. Both asymmetric Gaussian and double logistic use semi-local methods and are less sensitive to noise. These tend to provide a better description of the beginning and end of the growing season (Tan et al., 2008). Gao et. al. (2008) found that both asymmetric Gaussian and logistic algorithms in TIMESAT produce similar results, but asymmetric Gaussian is better able to handle incomplete

time-series data. Because the hive sites are in areas where winters frequently caused landscape to be covered in snow, and the metric of concern is the SOS, the asymmetric Gaussian method was selected.

3.5 ASYMMETRIC GAUSSIAN METHOD

The adopted local model functions have the general form:

$$f(t) = f(t; c_1, c_2, a_1, \dots, a_5) = c_1 + c_2 g(t; a_1, \dots, a_5) \tag{Equation 1}$$

where

$$g(t; a_1, \dots, a_5) = \begin{cases} \exp\left[-\left(\frac{t-a_1}{a_2}\right)^{a_3}\right], & \text{if } t > a_1 \\ \exp\left[-\left(\frac{a_1-t}{a_4}\right)^{a_5}\right], & \text{if } t < a_1 \end{cases} \tag{Equation 2}$$

is a Gaussian-type function. In equation 1, parameters c_1 and c_2 determine the base level and the amplitude. In equation 2, the parameter a_1 determines the time of the maximum NDVI (measured in time units). The upper part of equation 2 is fitted to the right half of the time series (time after the peak a_1 is reached) while the lower part of the equation fits to the left. The parameters a_2 and a_4 determine the width of the curves on the right and left side, respectively. The parameters a_3 and a_5 determine the flatness (or kurtosis) of the curves on the right and left side, respectively. The effects of varying the parameters $a_2 \dots a_5$ are shown in figure 4.

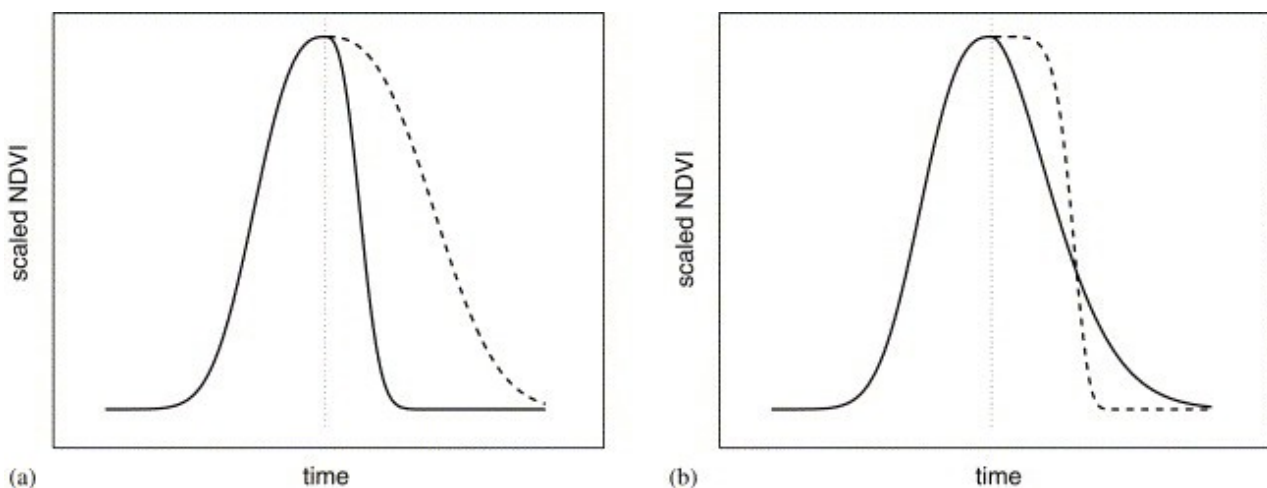


Figure 4: Effect of parameter changes on local functions. In (a) parameter a_2 , which determines width of right function half, has been decreased (solid line) and increased (dashed line) compared to value of left half. In (b) parameter a_3 , which determines flatness of right function half, has been decreased (solid line) and increased (dashed line) compared to value of left half. From Jönsson and Eklundh (2004)

The local model functions are well suited for describing the shape of NDVI time-series in overlapping intervals around maxima and minima. If a set of data points is selected (t_i, I_i), $I = n_1, \dots, n_2$ in an interval around a maximum or minimum, the parameters c_1, c_2 and a_1, \dots, a_5 are obtained by minimizing the merit function:

$$x^2 = \sum_{i=n_1}^{n_2} \left[\frac{f(t_i; c_1, c_2, a_1, \dots, a_5) - I_i}{\sigma_i} \right]^2 \quad \text{Equation 3}$$

where σ_i is the measurement uncertainty of the i th data point, presumed to be known. If the measurement uncertainties are not known, they may all be set to the constant value $\sigma = 1$.

3.6 ADOPTION TO UPPER ENVELOPE

Most noise in NDVI data, even for data classified as clear by the cloud mask, is considered to be negatively biased. The determination of the parameters of the model function is done in two steps: the first parameters are obtained by minimizing the merit function with σ_i as obtained from ancillary data. Data points below the model function of the first fit are thought of as being less important, and in the second step the minimization is redone with the σ_i of the low data points increased by a factor of two. This two step procedure leads to a model function that is adopted to the upper envelope of the NDVI data.

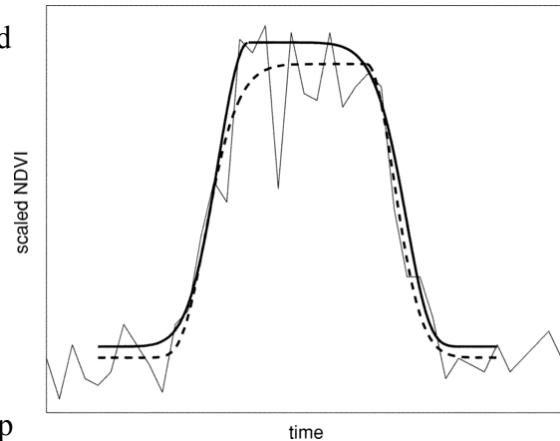


Figure 5: Fitted functions around a maximum from the two-step procedure. The dashed line shows the fitted function from the first step, and the solid line the fit from the second step. The original NDVI time-series is shown by the noisy fine continuous line. From Jönsson and Eklundh (2004)

3.7 INTEGRATION OF TEMPERATURE DATA

During the winter months, snow frequently covers the landscape of northern latitudes and high altitudes, preventing NDVI measurements. But because the biochemical processes of vegetation are sensitive to colder temperatures (Levitt, 1980), during times of dormancy reflective characteristics should remain constant. The photosynthesis of vegetation will increase after the temperature reaches a certain minimum threshold. Following the methodology of Tan et. al. (2008), a winter season was defined as a period longer than half a month when an area is snow-covered or the night land surface temperature is equal to or below 0°C . Using the MODIS Terra product 1km

Land Surface Temperature/Emissivity (MOD11A2: (Wan et al., 2002)) and the snow flag in the MOD13Q1 QA data, a winter season was marked for each hive location. During this time a minimum NDVI was assigned. This minimum NDVI was approximated by a clear capture at the end of the previous season's “brown down” or during a snow-free clear capture during the winter season when the night land surface temperature (LST) was below 0° C. Thus, it was possible to replace the winter season with a smooth, gap-filled curve (Figure 6).

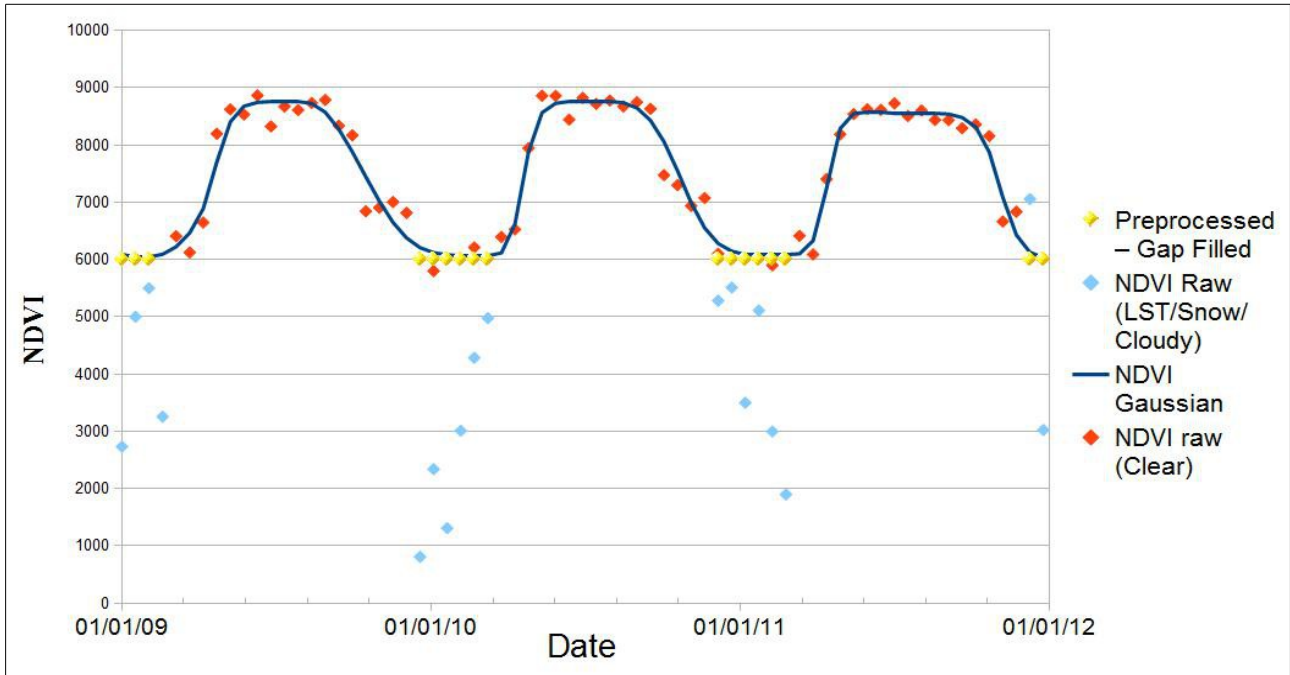


Figure 6: An example of preprocessing NDVI data. During winter months, snow/cloud covered pixels are assigned a base NDVI value (yellow). Blue line is Gaussian curve derived by TIMESAT

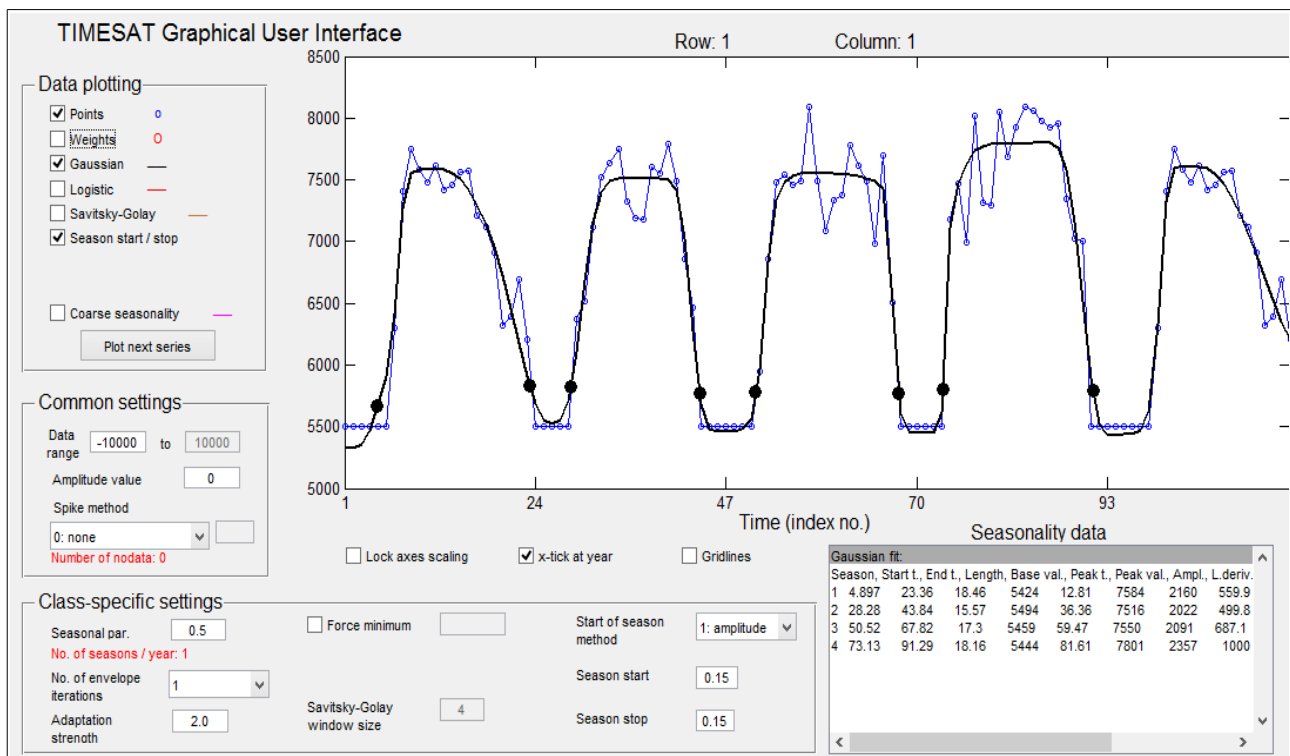


Figure 7: The graphical interface of TIMESAT showing the parameters and settings used

4. ALTERNATIVE START OF SEASON MEASUREMENT

4.1 INTRODUCTION

With a modest correlation found between satellite-derived SOS and HBNF, it is tempting to extrapolate these findings across the continent using a similar VI MODIS dataset. The Land Cover Dynamics Product (MCD12Q2:(Zhang et al., 2006)), consists of preprocessed yearly phenophase changes based on the Enhanced Vegetation Index (EVI). In previous research, Nightingale et al. (2008) found that EVI did not have as strong a relationship to any HBNF metrics. However, if a relationship could be found between MCD12Q2's "Onset of Greenness Increase" scientific data set (SDS) layer and the metrics of the HBNF, it would be simple to map the HBNF of Europe during the time period 2001-2010.

Starting with the launch of Terra and Aqua satellites in 2000, EVI has been adopted as a standard product by NASA and enthusiastically accepted in the research community (e.g. Huete et al., 2002). Like NDVI, it is produced at varying spatial (250m, 1km, 0.05 degree) and temporal (16-day, monthly) resolutions across the entire globe. Where the NDVI is chlorophyll sensitive, the EVI is more responsive to canopy structural variations, including leaf area index (LAI), canopy type, plant physiognomy and canopy architecture (Gao et al., 2000). EVI has improved sensitivity over high biomass regions and improved vegetation monitoring capability through a de-coupling of the canopy background signal. It minimizes canopy background variations to maintain sensitivity over dense vegetation and uses the blue band to remove residual atmosphere contamination caused by smoke and sub-pixel thin clouds (Huete et al., 1999). EVI is calculated:

$$EVI = G \frac{\rho_{NIR} - \rho_{red}}{\rho_{NIR} + C_1 * \rho_{red} - C_2 * \rho_{blue} + L} \quad \text{Equation 4}$$

where ρ are atmospherically corrected or partially atmospherically corrected (Rayleigh and ozone absorption) surface reflectances, L is the canopy background adjustment that addresses non-linear, differential NIR and red radiant transfer through the canopy, and C_1 and C_2 are the coefficients of the aerosol resistance terms which use the blue band to correct for aerosol influences in the red band (Huete et al., 2002). The coefficients adopted in the EVI algorithm are $L=1$, $C_1=6$, $C_2=7.5$, and G (gain factor) = 2.5 (Huete et al., 1994, 1997).

MCD12Q2 was designed to provide information related to phenology in support of ecological and global change science (Friedl, 2012). It was calculated at 500 m spatial resolution

yearly for the entire globe using the MODIS Land Cover Dynamics algorithm (MLCD) to identify phenophase transition dates based on logistic functions fit to time series of EVI. For each pixel a times series of EVI is assembled, the data undergo a gap-filling and smoothing process, periods of sustained EVI increase or decrease are identified, logistic models are fit to the time series and transition dates are identified as local maxima and minima in the rate of change of curvature of the fitted logistic function (Zhang et al., 2003, 2006; Ganguly et al., 2010). Four dates are calculated for two full vegetation cycles of each pixel. These dates correspond to the onset of EVI increase (green up), the onset of EVI maximum (maturity), the onset of EVI decrease (senescence) and the onset of EVI minimum (dormancy).

MLCD product uses EVI calculated from composited 8-day normalized BRDF-adjusted reflectance data (MCD43A4: (Schaaf et al., 2002)) with two full years of Nadir BRDF-Adjusted Reflectance (NBAR)-EVI observations assembled using a window that includes six months of data before and after the 12-month period of interest. MCD43A4 data are produced every 8-days using overlapping 16-day compositing windows, creating a possibility of 46 EVI values for a year and as many as 92 EVI observations for the entire MLCD time series. However in practice the number of observations available in any MLCD two-year window is much less due to cloud cover, aerosols and snow/ice cover. The MLCD algorithm removes snow and ice with a flag from the MCD43A2 BRDF-Albedo Quality product and replaces it with the most recent snow/ice free value. The collection 5 MODIS LST product (MOD11A2: (Wan et al., 2002)) is used to further filter the EVI time-series by replacing those observations where LST is lower than 5° C with background, snow-free values. This step accounts for cases where the NBAR product fails to accurately identify snow or ice and where vegetation is otherwise assumed to be biologically inactive. Remaining gaps in the time series are removed using a three-date moving window average, and the series are smoothed using a three-point median-value moving-window technique as described in Zhang et. al. (2006).

Sustained periods of EVI increase are determined from the filtered, gap-filled and smoothed EVI time series using moving windows composed of 5 consecutive observations. Transient variations in EVI, which may cause spurious detection of transitions, are excluded by requiring that the local maximum EVI value be at least 70% of the annual maximum and that the change in EVI must exceed 35% of the annual amplitude. For each identified period of sustained EVI increase or decrease, sigmoid curves are fit to the corresponding EVI time series using non-linear least squares. Phenophase transition dates are then estimated by identifying local maxima and minima in the rate of change in curvature of the fitted logistic function (Zhang et al., 2003).

MCD12Q2 has some known issues that may hinder it's use. It is designed for the northern

hemisphere, is less accurate at high latitudes during the winter and does not detect subtle change (e.g., some areas with evergreen vegetation). The algorithm has more difficulty in the tropics where vegetation follows a more complex cycle pattern. The product allows a pixel to display two phenological cycles, but because vegetation phenology does not follow a uniform annual cycle everywhere, pixels can contain incomplete cycles in any 12 month period and incomplete cycles are not marked. Also, a major problem for MCD12Q2 is that the quality control SDS in Collection 5 of this product was discovered to be corrupted due to a bug in the source code and it has not been produced since 2010.

4.2 DATA AND METHODS

4.2.1 MODIS

MODIS Land Cover product (MCD12Q2) was acquired from NASA's Earth Observing System Data and Information System's Reverb ECHO website (<http://reverb.echo.nasa.gov/reverb/>). Data was acquired from 2009 and 2010 for the extent of Europe. Each dataset came compressed as Hierarchical Data Format (HDF) containing 7 SDS. The first SDS (Onset_Greenness_Increase) contained two bands, each representing a separate phenological cycle. Only the first cycle was selected and mosaicked using QGIS. From each mosaic, raster calculator was used to replace fill (=32767) with null values and the ordinal day was calculated from its given format (# of days from January 2000). Available scale-hive data points were overlain and buffered to 3 kilometres. The zonal statistics tool was used to calculate the mean onset greenness increase within 3 kilometres of each hive.

4.2.2 HBNF

HBNF metrics and TIMESAT NDVI SOS were calculated as described in Blomstedt (2014). Due to the available time frame of MCD12Q2, only hive locations with data from 2009 and 2010 were used in this analysis.

4.3 RESULTS AND DISCUSSION

Table 3: Onset EVI Greenness by year and location

Location	Year	TIMESAT	Onset EVI Greenness	Onset EVI Greenness	HBNF 50%
		NDVI SOS	(3km Mean)	(centre pixel)	
Ordinal Day					
Vaz	2009	110	117	118	142
Grangeneuve	2009	64	79	75	130
Grangeneuve	2010	68	129	79	118
Ath	2010	70	73	69	134
Aubel	2010	64	89	71	118
Arlon	2010	99	84	91	144
Dekani	2010	89	83	89	141

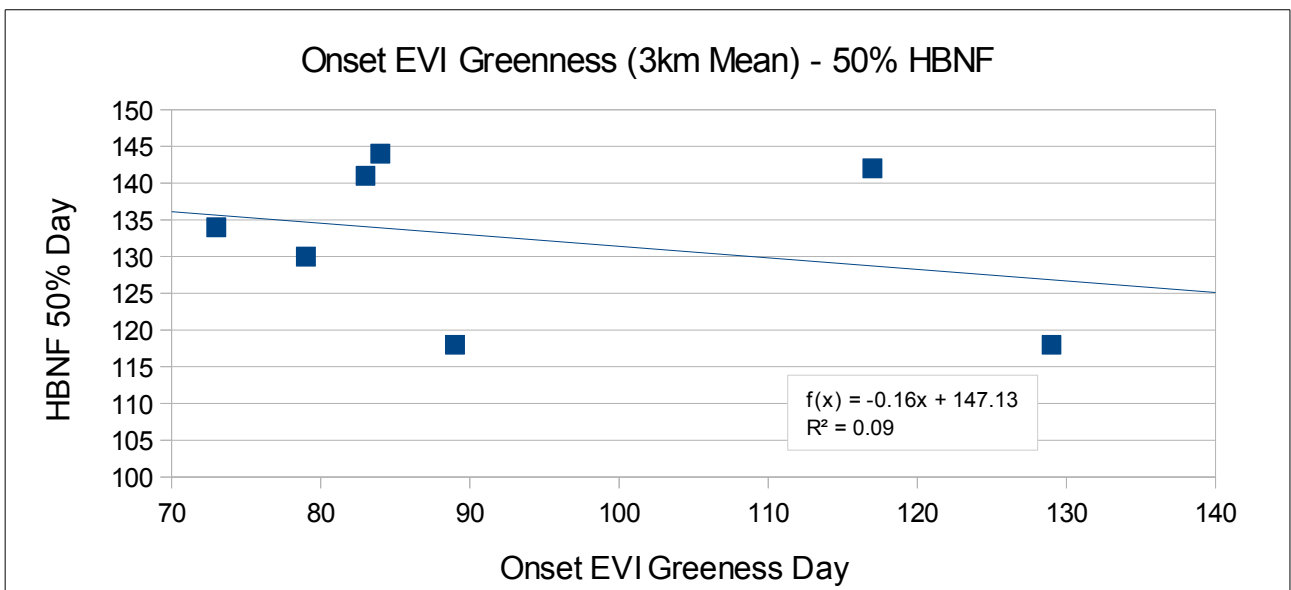


Figure 8: Onset EVI Greenness (3km Mean), n=7

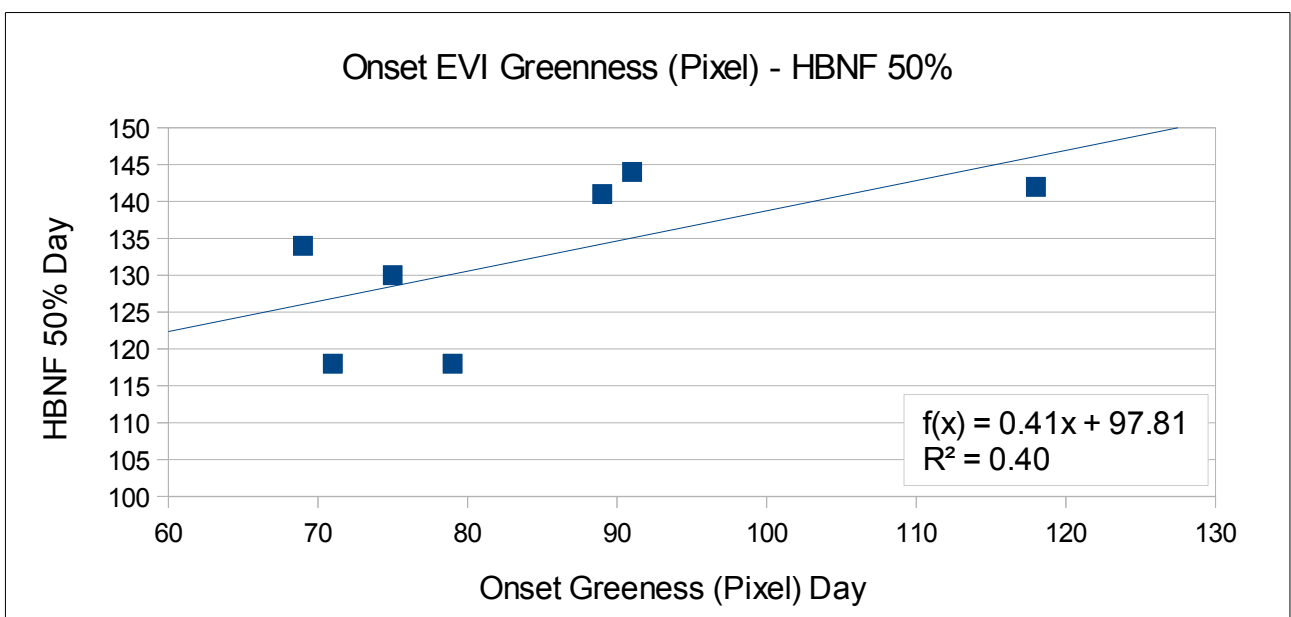


Figure 9: Onset EVI Greenness (Pixel), n=7

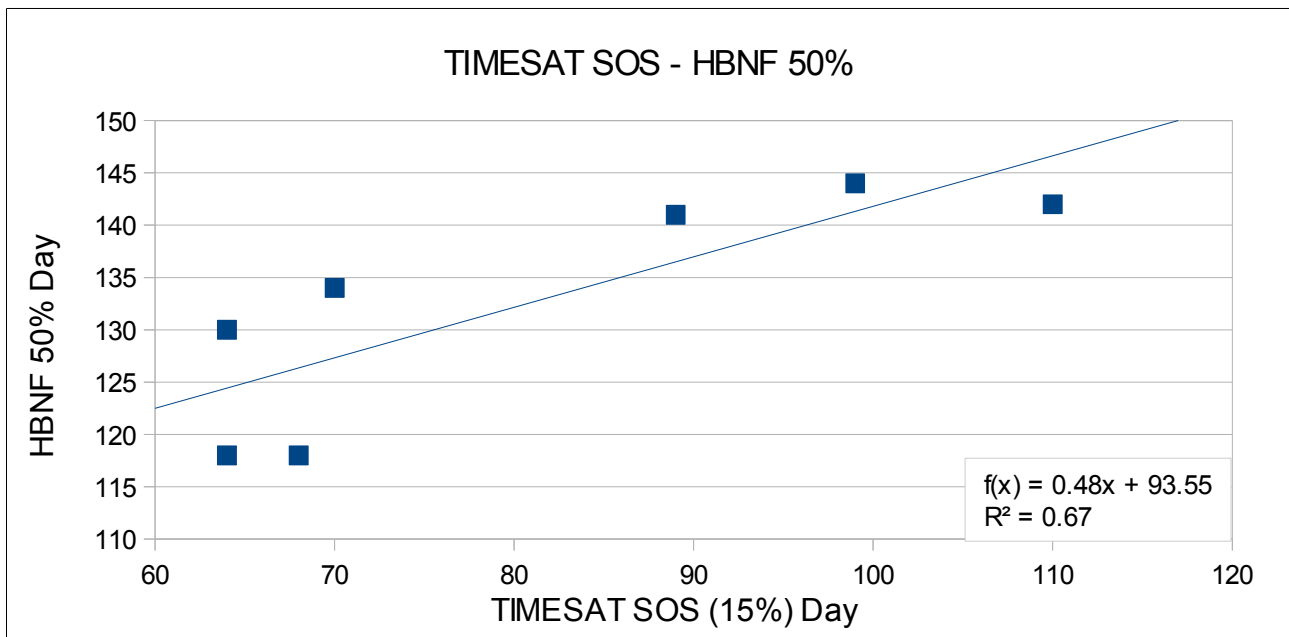


Figure 10: TIMESAT SOS – HBNF 50%, $n=7$

Comparison of the EVI onset of greenness 3km mean and HBNF 50% shows no relationship (Figure 8, $R^2=0.09$). This is likely due to the high variation in onset date within a 3 kilometre radius of each hive. For example, the 2010 Grangeneuve hive is within a pixel that has an onset date of 79, but is surrounded by pixels with dates 145, 146, Null, 204, 127, 127, 155 and 84. It is difficult to believe that a location less than a kilometre away would have an SOS 125 days (4 months) difference. Also, these values differ greatly from the surrounding pixels in 2009, and it is uncertain if the bug discovered in QA control is the reason for this. These high numbers lead to an elevated mean and a weak relationship.

In an attempt to remove these higher values, the centre 500 x 500 metre pixel in which the hive was located was used as the SOS day. This analysis brought a stronger relationship (Figure 9, $R^2=0.40$) but it still is not as strong as TIMESAT NDVI of the same locations and years (Figure 10, $R^2=0.67$). This may be due to the higher resolution of NDVI (MOD13Q1, 250 meters) used to derive SOS with TIMESAT, HBNF's weaker relationship found with EVI (Nightingale et al., 2008), the MCLD algorithm or the product's malfunctioning quality assessment.

4.4 CONCLUSION

These results suggest that the MCD13Q2 product does not relate well the HBNF metrics. Though it is a ready-made MODIS product for use in phenological studies, it cannot be used in mapping nectar flows.

5. HBNF INTERPOLATION

5.1 INTRODUCTION

Interpolation is the process of using point-field data to predict values in unsampled locations and generate continuous maps. Interpolation is based on the first rule of geography defined by Tobler (1970) as “Everything is related to everything else, but near things are more related than distant things.” Inverse Distance Weighting (IDW) is a local deterministic technique where a surface is created based on a model, algorithm and user defined parameters (De Smith et al., 2007). It is exact, meaning it must honour the measured point values, and uses a weighted moving average with a specified number of neighbouring points. IDW implements a distance-weight function so that at a greater distance, the cell has less influence on the output.

Like elevation, rainfall or temperature, HBNF metrics are spatially dependant and have the potential to be mapped as a spectrum across the landscape. Interpolation maps offer a way to make data more accessible. This portion of research aims to visualize the HBNF data and answer the following questions.

1. What are the spatial patterns of HBNF for each country?
 - 1.1. Do HBNF occur later at a higher elevation?
 - 1.2. Do HBNF occur earlier with proximity to the coast?

5.2 METHODOLOGY

HBNF metrics were used from the same locations as Blomstedt (2014). Two to four other sites per country were used as additional data to aid in interpolation. The data collection of these sites was often not as precise or regular as the original locations. The year 2011 was used due to it having a complete set of data points from every country and interpolation was performed on HBNF start day and 50% day.

5.3 RESULTS AND DISCUSSION

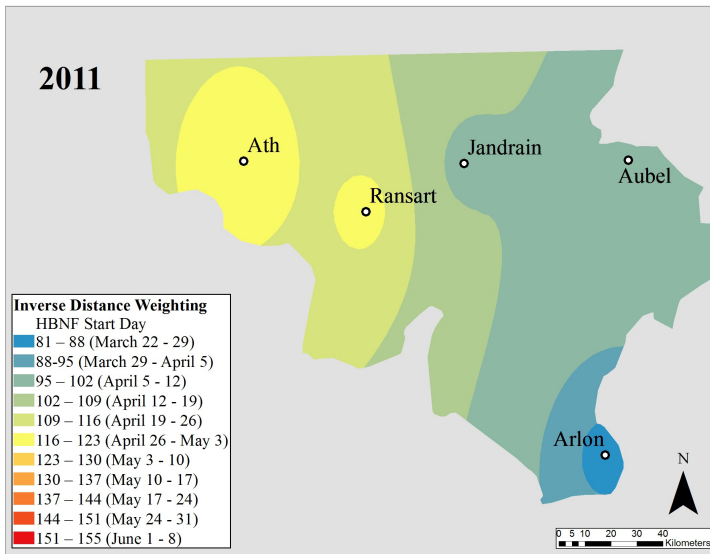


Figure 11: Belgium HBNF Start Day 2011

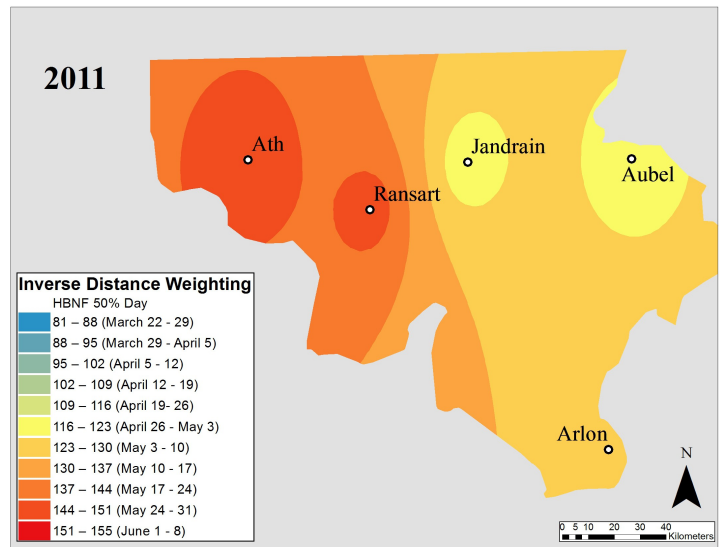


Figure 12: Belgium HBNF 50% Day 2011

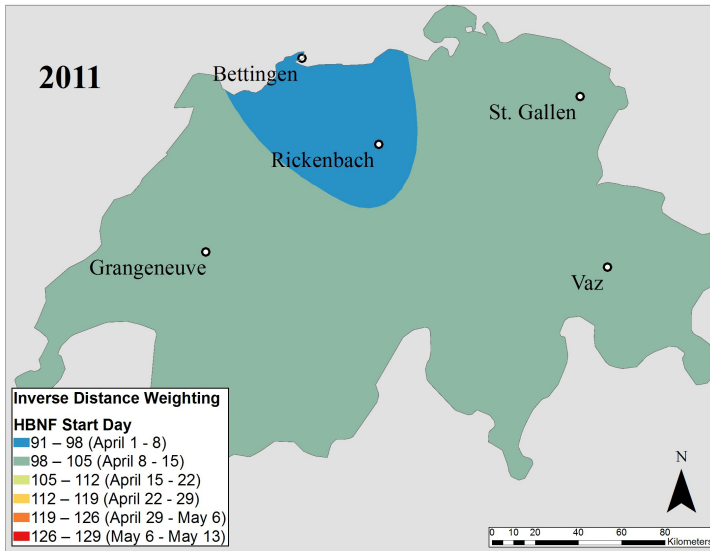


Figure 13: Switzerland HBNF Start Day 2011

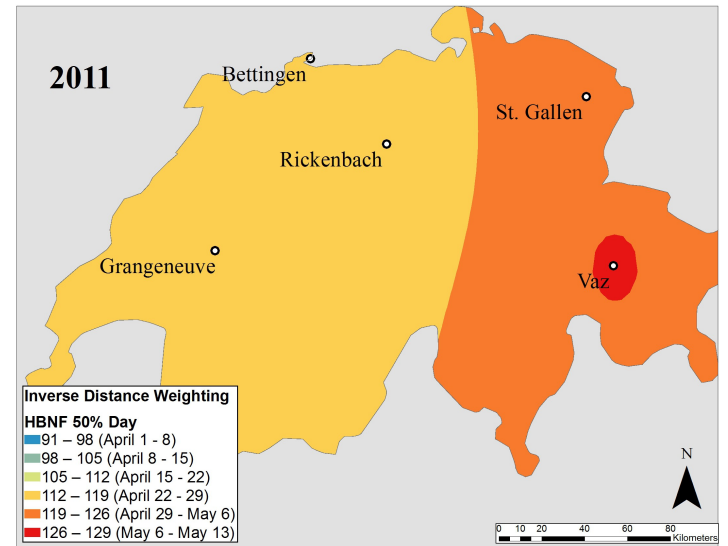


Figure 14: Switzerland HBNF 50% Day 2011

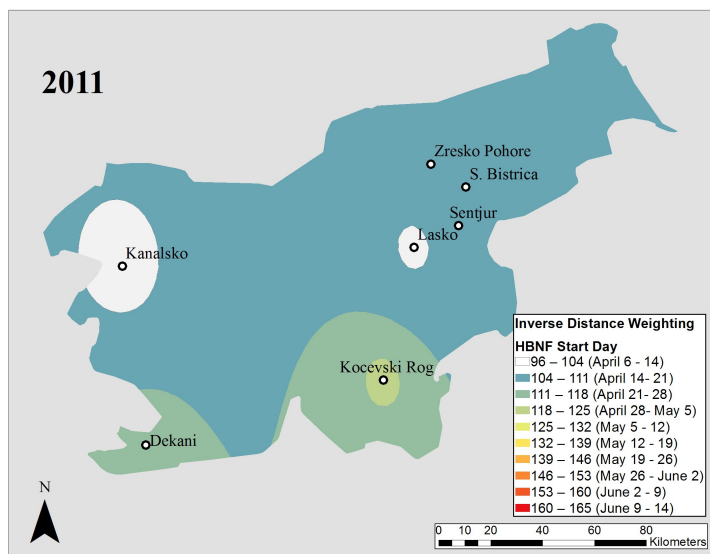


Figure 15: Slovenia HBNF Start Day 2011

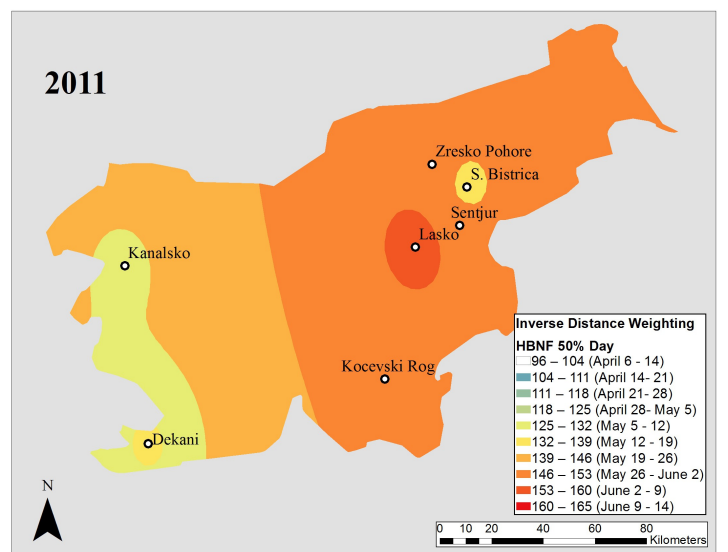


Figure 16: Slovenia HBNF 50% Day 2011

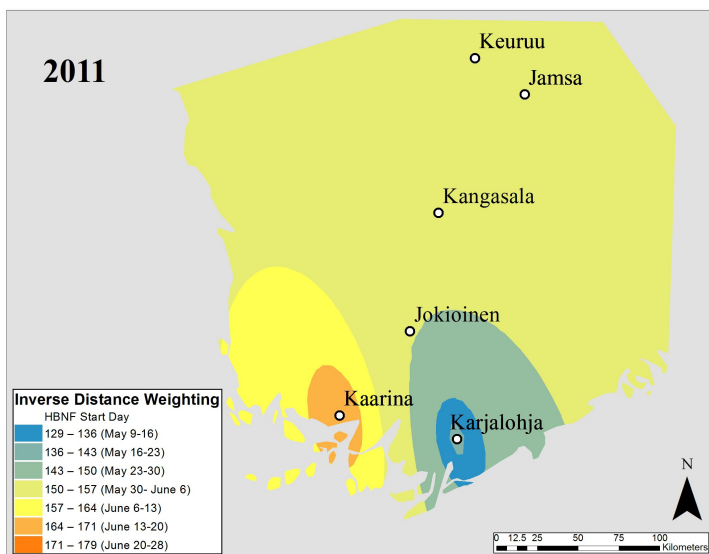


Figure 17: Finland HBNF Start Day 2011

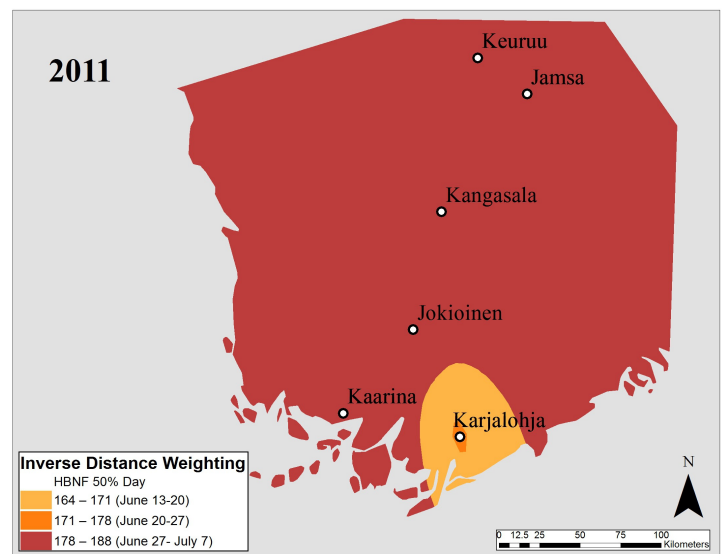


Figure 18: Finland HBNF 50% Day 2011

The interpolated surfaces show a rough estimate (one week) of the HBNFs by country during 2011. Belgium's HBNFs occurred earlier inland, in the eastern part of the country (Figure 11-12). In Switzerland, the flow in the lower north began a week earlier than in the higher elevations (Figure 13). The Swiss 50% day map shows Vaz, which is at an elevation of 1162 metres, had a much later flow (Figure 14). Slovenian flows occurred later in the southern part of the country, with Kočevski Rog and Laško having long flows and later 50% days (Figure 15-16). In Finland, both Karjalohja and Kaarina are located near the coast, but the former had an early NF start while the latter was later than the rest of the country by two weeks (Figure 17). However the 50% day occurred in the same week for nearly all Finnish locations (Figure 18).

Spring HBNFs are highly heterogeneous and vary greatly by location and year. A variety of environmental and geographical factors influence the HBNF. Elevation, in particular, will determine local flora species and will cause later bloom-time. This can be generally seen in the Swiss map (Figure 13), with the lower north valley having an earlier NF start than the rest of the alpine country. This appeared to even out by HBNF 50% day, and Vaz in the eastern part of the country had a longer, later flow (Figure 14). However the HBNF did not follow other assumed patterns. In Belgium the two hives closest to the coast (Ath, Ranset), which were also lower in elevation, had later HBNF start and 50% days (Figures 11-12). Finland's two coastal hives NF start differed by a month (Karjalohja = May 9, Kaarina = June 9) while the inland hives all began in the same week (Figure 17). Animations were created with ArcGIS for the 2011 Slovenia and Switzerland seasons to show the weekly progression of the HBNFs through the spring. These can be found on the

research website (<http://www/geos.ed.ac.uk/~mscgis/13-14/s1356375/>).

5.4 CONCLUSION

In actuality, maps of HBNF are likely to be much more detailed and nuanced. Nectar secretion is often related to temperature (Jakobsen and Kritjánsson, 1994) and microclimates created by natural formations or urban settings will influence the local HBNF. Phenology is shown to be more advanced in urban settings (Roetzer et al., 2000), and hive locations Ath, Arlon and St. Gallen are within urban influence. The four adjacent hives in eastern Slovenia (Figure 15) illustrate a pattern that is more likely than the broad, interpolated sweep across dozens of kilometres (e.g. Switzerland, figures 12-13). However this exercise gives an interesting baseline for interpolating scale-hive point data into a continuous surface. To the author's knowledge, no research of this kind has been published. With additional scale-hive data points, continuous years of data, as well as geostatistical techniques which incorporate elevation, honey flows could be more precisely quantified and mapped at a landscape level.

6. LIMITATIONS OF STUDY

6.1 MODIS

Investigations of seasonal changes and interannual variability of global vegetation activity using satellite-derived NDVI must assume that changes in NDVI are based on vegetation response to climate. Interannual signal is subtle and subject to non-vegetated effects. Satellite drift, calibration uncertainties, inter-satellite sensor differences, bidirectional and atmospheric effects, can introduce variability and be misidentified as NDVI changes.

What is actually measured in remote sensing SOS is poorly understood and likely varies depending on the land cover. For example, the initial greening LSP may be the measurement of the understory rather than the canopy. This may lead to some error, but as seen in figure 15 of Blomstedt (2014), it is not likely the NDVI, but the duration of the HBNF which is shifting the points away from the linear trend.

MODIS data used in this project (MOD13Q1) is produced at 16 day intervals and may be too temporally coarse for studying a phenological metric which may only be changing at a fraction of day per year. The MOD13Q1 algorithm reviews the captures from the 16 day period and selects maximum value across all observations for that pixel. This value is assigned to the date of production, though it may come from a capture over two weeks prior. For the next date of production, 16 days later, the clearest NDVI value may fall at the end of that interval, making the actual capture dates four weeks apart. This study attempts to remedy this potential error by averaging the pixel values for one production period and applying a Gaussian smoothing to the time-series.

6.2 SCALE WEIGHT DATA

One source of uncertainty arrives from methods and equipment used to collect scale-hive data. Not only does each country in Europe have their separate scale-hive network, with their own type of scale and beehive, but each scale-hive is tended by an individual beekeeper. The practices of a beekeeper has a strong influence on the hive's productivity and health. For example, removing honey combs from a hive causes stress in the colony, causing a smaller harvest (Szabo and Lefkovitch, 1991). Szabo and Mueller (1996) describe colony management practices that promote accurate measurement of weight, but it is not known what beekeeping methods were used for the scale-hives in this research. The scale-hive network in the US has an extensive protocol on how to make scale-hive measurements that provide insight across the regions (Esaias, 2007). The important points include

- **Exposure to the elements** – If a hive is not sheltered the scale may register weight gain from precipitation. It's possible for a rainfall-induced weight gain last up to 36 hours (Meikle et al., 2006).
- **Storage space** – If the colony runs out of empty comb they will not be able to store additional nectar and they will cease foraging even if there is still a flow. A lack of space also encourages swarming.
- **Swarming** – If the hive is not carefully and frequently inspected in the spring, the bees may swarm causing both a change in weight as well as a weakened colony for the remainder of the spring.
- **Size, strength and health of colony** – These three traits depend on the environment, genetics of the bees and management the beekeeper. While colonies should gather nectar relative to their size and strength, all colonies cannot be considered the same. If a colony is weakened from illness, pests or pesticides, it may not be able to forage properly. There are as many ways to remedy the above maladies as there are beekeepers.
- **Recording of weight changes** – feeding a colony syrup, pollen patties, adding supers, empty comb, harvesting honey all effect the weight of a hive. A fastidious beekeeper will note each change and adjust the weight, but at times these notes are forgotten. Of concern are the Swiss hives used in this study, which stated the data-user must make these judgements from looking at the numbers.

Also, of note, scale weight does not truly distinguish between collection of nectar, pollen, water or propolis, production of brood or wax, and bees themselves (McLellan, 1977). The number of bees may triple or quadruple during the spring season, accounting for a few kilograms. Stored honey always represents more than half the colony weight, pollen does not comprise more than 10% and wax less than 1%. However, changes in hive weight do correlate closely ($r=0.95$ on average) with honey production (McLellan, 1977).

6.3 WEATHER

Weather and other environmental factors influence bees ability to forage for pollen and nectar. During a rainy spring, bees may not be able leave their hive to forage for food. Heavy or prolonged rains also may cause damage to blossoms, causing the nectar flow to slow or cease. Data on rainfall was not offered for most of the scale-hive locations and was not taken in account for this research.

6.4 FORAGING

One of the important choices of a foraging bee is what to collect. This is partly determined by the availability of flowers in the field, but there is always a consistent proportion of foragers for nectar and pollen (Seeley, 1995). Workers tend to visit only one species of flower on a trip, aligning with the pollination requirements of the plant. They continue to visit that flower for prolonged periods until it ceases to produce nectar or pollen or until a superior source becomes available (Winston, 1991). Hence, a colony may not give a true picture of the flowers in the landscape

It is not uncommon to find two beehives in the same location with one hive gathering fresh nectar and the other unsuccessfully scouting. This can be seen in Waddington (1994), where two matched colonies found different sources of nectar. As with any individual animal, searching ability, environment and luck are factors in foraging.

6.5 NECTAR SOURCES – FORAGE ZONES

The floral sources for the HBNFs used in this research were not identified. The scale-hives were spread over thousands of kilometres and 15° latitude, with the species of melliferous flowers likely differing greatly. Some scale-hive data identified forage from surrounding area (See table 1 in Blomstedt (2014)). Other scale-hive data contained notes by beekeepers who knew the floral source of the NF. However these notes were not provided with enough regularity to incorporate, and this analysis did not consider the particular nectar sources. HBNFs from agricultural sources (e.g. a field of *Brassica napus*) could have a very different effect than a HBNF from wildflowers or urban gardens. Instead this study aspired in simplicity and considered the local HBNF as a whole. Further research could look at scale-hives in a more narrow geographical range while considering NF sources.

There have been attempts to divide Europe into similar ecological regions (Mücher et al., 2003; Metzger et al., 2005; Council Directive, 1992) but there is not one specifically made for honey bee forage. For North American beekeepers, Ayers and Harman (1992) created a honey bee forage classification with 14 regions based on natural patterns of land use and flora (Figure 19). This is an avenue for further research, though at a European scale it may be more difficult due to the continent's complex geology and land-form patterns (Jay Harman, personal communication).

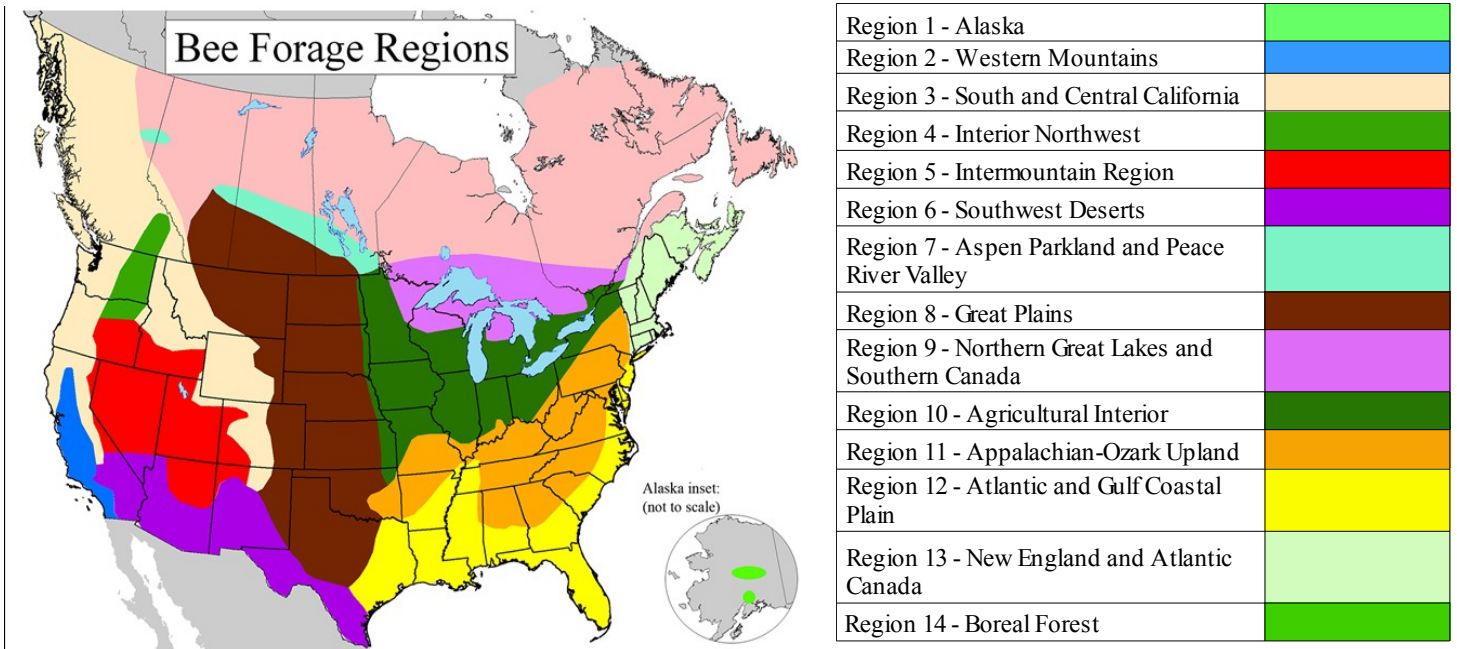


Figure 15: Bee Forage Regions of North America. From Ayers and Harman (1992)

7. BIBLIOGRAPHY

- Abou-Shaara, H.F., Al-Ghamdi, A.A., Mohamed, A.A., 2013. A Suitability Map for Keeping Honey Bees Under Harsh Environmental Conditions Using Geographical Information System. *World Applied Sciences Journal* 22, 1099–1105.
- Ahas, R., Aasa, A., Menzel, A., Fedotova, V.G., Scheifinger, H., 2002. Changes in European spring phenology. *International Journal of Climatology* 22, 1727–1738.
- Aono, Y., Kazui, K., 2008. Phenological data series of cherry tree flowering in Kyoto, Japan, and its application to reconstruction of springtime temperatures since the 9th century. *International Journal of Climatology* 28, 905–914.
- Ayers, G.S., Harman, J.R., 1992. Bee forage of North America and the potential for planting for bees, in: Graham, J. (Ed.), *The Hive and the Honey Bee*. Dadant & Sons, Hamilton, Il, pp. 437–533.
- Barnes, W.L., Xiong, X., Salomonson, V.V., 2002. Status of Terra MODIS and Aqua MODIS. Presented at the Geoscience and Remote Sensing Symposium, IEEE International, pp. 970–972.
- Beekman, M., Ratnieks, F.L.W., 2000. Long-range foraging by the honey-bee, *Apis mellifera* L. *Functional Ecology* 14, 490–496.
- Beekman, M., Sumpter, D.J.T., Seraphides, N., Ratnieks, F.L.W., 2004. Comparing foraging behaviour of small and large honey-bee colonies by decoding waggle dances made by foragers. *Functional Ecology* 18, 829–835.
- Berardinelli, I., Vedova, G.D., 2004. Use of GIS in the management of apiculture: preliminary note. *APOidea* 1, 31–36.
- Blomstedt, W., 2014. Mapping Present and Historical European Honey Bee Nectar Flows with Scale Hives and Satellite-Derived Vegetation Indices: Part I Research Paper. University of Edinburgh.
- Bohn, U., Gollub, G., Hettwer, C., 2000. Reduced general map of the natural vegetation of Europe. 1: 10 million. Bonn-Bad Godesberg.
- Bosch, J., Kemp, W.P., 2003. Effect of wintering duration and temperature on survival and emergence time in males of the orchard pollinator *Osmia lignaria* (Hymenoptera: Megachilidae). *Environmental Entomology* 32, 711–716.
- Box, G.E.P., Jenkins, G.M., Reinsel, G.C., 2013. *Time Series Analysis: Forecasting and Control*. John Wiley & Sons.
- Burrill, R.M., Dietz, A., 1981. The response of honey bees to variations in solar radiation and temperature. *Apidologie* 12, 319–328.
- Carter, C., Thornburg, R.W., 2004. Is the nectar redox cycle a floral defense against microbial attack? *Trends in Plant Science* 9, 320–324.

- Chauzat, M.-P., Laurent, M., Riviere, M.-P., Saugeon, C., Hendrikx, P., Ribiere-Chabert, M., pathology Unit, H., 2014. A pan-European epidemiological study on honeybee colony losses 2012-2013. European Union Reference Laboratory for Honey Bee Health (EURL), EPILOBEE.
- Chmielewski, F.M., 1996. The international phenological gardens across Europe. Present state and perspectives. *Phenology and Seasonality* 1, 19–23.
- Cooper, P.D., Schaffer, W.M., Buchmann, S.L., 1985. Temperature regulation of honey bees (*Apis mellifera*) foraging in the Sonoran desert. *Journal of Experimental Biology* 114, 1–15.
- Corbet, S.A., 1990. Pollination and the Weather. *Israel Journal of Botany* 39, 13–30.
- Corbet, S.A., Willmer, P.G., Beament, J.W.L., Unwin, D.M., Prys-Jones, O., 1979. Post-secretory determinants of sugar concentration in nectar. *Plant, Cell & Environment* 2, 293–308.
- Council Directive, 1992. Council Directive 1992 92/43/EEC of 21 May on the conservation of natural habitats and of wild fauna and flora. *International Journal of the European Communities* L206, 7–49.
- Couvillon, M.J., Schürch, R., Ratnieks, F.L.W., 2014. Waggle Dance Distances as Integrative Indicators of Seasonal Foraging Challenges. *PLoS ONE* 9.
- Crane, E., 1975. *Honey: a comprehensive survey*. Heinemann, London.
- Crane, E., 2013. *The World History of Beekeeping and Honey Hunting*. Routledge, London.
- Cruden, R.W., Hermann, S.M., Peterson, S., 1983. *Patterns of nectar production and plant-pollinator coevolution*. Columbia University Press, New York.
- De Beurs, K.M., Henebry, G.M., 2010. Spatio-temporal statistical methods for modelling land surface phenology, in: Hudson, I.L., Keatley, M.R. (Eds.), *Phenological Research: Methods for Environmental and Climate Change Analysis*. Springer, Dordrecht, pp. 177–208.
- De Smith, M.J., Goodchild, M.F., Longley, P., 2007. *Geospatial analysis: a comprehensive guide to principles, techniques and software tools*. Matador, Leicester UK.
- Deering, D.W., Eck, T.F., Banerjee, B., 1999. Characterization of the Reflectance Anisotropy of Three Boreal Forest Canopies in Spring–Summer. *Remote Sensing of Environment* 67, 205–229.
- Dube, P.A., Perry, L.P., Vittum, M.T., 1984. *Instructions for phenological observations: lilac and honeysuckle*, Vermont Agricultural Experiment Station Bulletin. University of Vermont, Burlington.
- Esaias, W.E., 2007. Protocol for Scale Hive Measurements of the Honey Bee Nectar Flow. <http://honeybeenet.gsfc.nasa.gov/About/SHprotocol.htm> (accessed 04/06/14).
- Estoque, R.C., Murayama, Y., 2011. Suitability Analysis for Beekeeping Sites Integrating GIS & MCE Techniques, in: Murayama, Y., Thapa, R.B. (Eds.), *Spatial Analysis and Modeling in Geographical Transformation Process: Gis-Based Applications*. Springer, Dordrecht, pp. 215–233.

- Faegri, K., Van der Pijl, L., 1966. The principles of pollination ecology. Pergamon Press, Oxford.
- Fahn, A., 1949. Studies in the ecology of nectar secretion. *Palestine Journal of Botany* 4, 207–24.
- Fisher, J.I., Richardson, A.D., Mustard, J.F., 2007. Phenology model from surface meteorology does not capture satellite-based greenup estimations. *Global Change Biology* 13, 707–721.
- Forister, M.L., Shapiro, A.M., 2003. Climatic trends and advancing spring flight of butterflies in lowland California. *Global Change Biology* 9, 1130–1135.
- Freeman, C.E., Head, K.C., 1990. Temperature and sucrose composition of floral nectars in *Ipomopsis longiflora* under field conditions. *The Southwestern Naturalist* 35, 423–426.
- Friedl, M., 2012. User Guide for the MODIS Land Cover Dynamics Product (MCD12Q2) http://www.bu.edu/lcsc/files/2012/08/MCD12Q2_UserGuide.pdf (accessed 30/06/14).
- Fund, W.W., Hogan, C.M., 2013. Western European broadleaf forests. <http://www.eoearth.org/view/article/177334> (accessed 30/06/14).
- Fund, W.W., Hogan, C.M., 2014. Alps conifer and mixed forests. <http://www.eoearth.org/view/article/150000> (accessed 04/07/14).
- Ganguly, S., Friedl, M.A., Tan, B., Zhang, X., Verma, M., 2010. Land surface phenology from MODIS: Characterization of the Collection 5 global land cover dynamics product. *Remote Sensing of Environment* 114, 1805–1816.
- Gao, F., Morisette, J.T., Wolfe, R.E., Ederer, G., Pedelty, J., Masuoka, E., Myneni, R., Tan, B., Nightingale, J., 2008. An algorithm to produce temporally and spatially continuous MODIS-LAI time series. *Geoscience and Remote Sensing Letters, IEEE* 5, 60–64.
- Gao, X., Huete, A.R., Ni, W., Miura, T., 2000. Optical–Biophysical Relationships of Vegetation Spectra without Background Contamination. *Remote Sensing of Environment* 74, 609–620.
- Garibaldi, L.A., Steffan-Dewenter, I., Winfree, R., Aizen, M.A., Bommarco, R., Cunningham, S.A., Kremen, C., Carvalheiro, L.G., Harder, L.D., Afik, O., 2013. Wild pollinators enhance fruit set of crops regardless of honey bee abundance. *Science* 339, 1608–1611.
- Gary, N.E., 1967. Diurnal variations in the intensity of flight activity from honeybee colonies. *Journal of Apicultural Research* 6, 65–68.
- Giannini, T.C., Acosta, A.L., Garófalo, C.A., Saraiva, A.M., Alves-dos-Santos, I., Imperatriz-Fonseca, V.L., 2012. Pollination services at risk: Bee habitats will decrease owing to climate change in Brazil. *Ecological Modelling* 244, 127–131.
- Gordo, O., Sanz, J.J., 2006. Temporal trends in phenology of the honey bee *Apis mellifera* (L.) and the small white *Pieris rapae* (L.) in the Iberian Peninsula (1952–2004). *Ecological Entomology* 31, 261–268.
- Goward, S.N., Markham, B., Dye, D.G., Dulaney, W., Yang, J., 1991. Normalized difference vegetation index measurements from the Advanced Very High Resolution Radiometer. *Remote Sensing of Environment* 35, 257–277.

- Gutman, G.G., 1991. Vegetation indices from AVHRR: An update and future prospects. *Remote Sensing of Environment* 35, 121–136.
- Hameed, S., Gong, G., 1994. Variation of spring climate in lower-middle Yangtse River Valley and its relation with solar-cycle length. *Geophysical Research Letters* 21, 2693–2696.
- Haubruge, E., Nguyen, B.K., Widart, J., Thomé, J.-P., Fickers, P., Depauw, E., 2006. Le dépérissement de l'abeille domestique, *Apis mellifera* L., 1758 (Hymenoptera: Apidae): faits et causes probables. *Notes fauniques de Gembloux* 59, 3–21.
- Heinrich, B., 1975. Energetics of pollination. *Annual Review of Ecology and Systematics* 6, 139–170.
- Heinrich, B., 1979. Thermoregulation of African and European honeybees during foraging, attack, and hive exits and returns. *Journal of Experimental Biology* 80, 217–229.
- Henry, M., Fröchen, M., Maillet-Mezeray, J., Breyne, E., Allier, F., Odoux, J.-F., Decourtye, A., 2012. Spatial autocorrelation in honeybee foraging activity reveals optimal focus scale for predicting agro-environmental scheme efficiency. *Ecological Modelling* 225, 103–114.
- Holben, B.N., 1986. Characteristics of maximum-value composite images from temporal AVHRR data. *International Journal of Remote Sensing* 7, 1417–1434.
- Huete, A., Didan, K., Miura, T., Rodriguez, E.P., Gao, X., Ferreira, L.G., 2002. Overview of the radiometric and biophysical performance of the MODIS vegetation indices. *Remote Sensing of Environment* 83, 195–213.
- Huete, A., Justice, C., Liu, H., 1994. Development of vegetation and soil indices for MODIS-EOS. *Remote Sensing of Environment* 49, 224–234.
- Huete, A., Justice, C., van Leeuwen, W., 1999. MODIS Vegetation Index (MOD 13) Algorithm Theoretical Basis Document Version 3. http://modis.gsfc.nasa.gov/data/atbd/atbd_mod13.pdf (accessed 05/05/14).
- Huete, A.R., Liu, H.Q., Batchily, K., van Leeuwen, W., 1997. A comparison of vegetation indices over a global set of TM images for EOS-MODIS. *Remote Sensing of Environment* 59, 440–451.
- Ibrahim, I.F., Balasundram, S.K., Abdullah, N.-A.P., Sood, A.M., Mardan, M., Saberioon, M.M., 2012. The spatial distribution of *Apis dorsata* host plants using an integrated geographical information system-remote sensing approach. *American Journal of Agricultural & Biological Science* 7, 396–406.
- Inouye, D.W., Saavedra, F., Lee-Yang, W., 2003. Environmental influences on the phenology and abundance of flowering by *Androsace septentrionalis* (Primulaceae). *American Journal of Botany* 90, 905–910.
- IPCC, 2007. Climate change 2007: Mitigation. Contribution of Working Group II to the Fourth Assessment Report of the Intergovernmental Panel on Climate Change. Cambridge University Press, Cambridge, UK.
- Jakobsen, H.B., Krittjánsson, K., 1994. Influence of temperature and floret age on nectar secretion in

Trifolium repens L. *Annals of Botany* 74, 327–334.

- Janssens, X., 2006. Pr evision des potentialit es de production de miel   l' chelle d'un rucher au moyen d'un syst me d'information g ographique. *Apidologie* 37, 351–365.
doi:10.1051/apido:2006006
- J nsson, P., Eklundh, L., 2002. Seasonality extraction by function fitting to time-series of satellite sensor data. *IEEE Transactions on Geoscience and Remote Sensing*, 40, 1824–1832.
- J nsson, P., Eklundh, L., 2004. TIMESAT—A program for analyzing time-series of satellite sensor data. *Computers & Geosciences* 30, 833–845.
- Kremen, C., Williams, N.M., Thorp, R.W., 2002. Crop pollination from native bees at risk from agricultural intensification. *Proceedings of the National Academy of Sciences* 99, 16812–16816.
- Lambrecht, S.C., Loik, M.E., Inouye, D.W., Harte, J., 2007. Reproductive and physiological responses to simulated climate warming for four subalpine species. *New Phytologist* 173, 121–134.
- Lehikoinen, E.S.A., Sparks, T.H., Zalakevicius, M., 2004. Arrival and departure dates. *Advances in Ecological Research* 35, 1–31.
- Levitt, J., 1980. Responses of plants to environmental stresses. Volume II. Water, radiation, salt, and other stresses., 2nd ed. Academic Press, New York.
- Lloyd, D., 1990. A phenological classification of terrestrial vegetation cover using shortwave vegetation index imagery. *International Journal of Remote Sensing* 11, 2269–2279.
- Malingreau, J.-P., 1986. Global vegetation dynamics: satellite observations over Asia. *International Journal of Remote Sensing* 7, 1121–1146.
- Maris, N.M.N., Mansor, S., Shafri, H.Z.M., 2008. Apicultural Site Zonation Using GIS and Multi-Criteria Decision Analysis. *Pertanika Journal of Tropical Agricultural Science* 31, 147–162.
- McLellan, A.R., 1977. Honeybee colony weight as an index of honey production and nectar flow: a critical evaluation. *Journal of Applied Ecology* 14, 401–408.
- Meikle, W.G., Holst, N., Mercadier, G., Derouan , F., James, R.R., 2006. Using balances linked to dataloggers to monitor honeybee colonies. *Journal of Apicultural Research* 45, 39–41.
- Menzel, A., Sparks, T.H., Estrella, N., Koch, E., Aasa, A., Ahas, R., Alm-K bler, K., Bissolli, P., Braslavsk , O., Briede, A., Chmielewski, F.M., Crepinsek, Z., Curnel, Y., Dahl,  ., Defila, C., Donnelly, A., Filella, Y., Jatczak, K., M ge, F., Mestre, A., Nordli,  ., Pe uelas, J., Pirinen, P., Remi ov , V., Scheifinger, H., Striz, M., Susnik, A., Van Vliet, A.J.H., Wielgolaski, F.-E., Zach, S., Zust, A., 2006. European phenological response to climate change matches the warming pattern. *Global Change Biology* 12, 1969–1976.
- Metzger, M.J., Bunce, R.G.H., Jongman, R.H.G., M cher, C.A., Watkins, J.W., 2005. A climatic stratification of the environment of Europe. *Global Ecology and Biogeography* 14, 549–563.
- Michener, C.D., 1974. The social behavior of the bees: a comparative study. Harvard University

Press, Cambridge, MA.

- Miller-Rushing, A.J., Inouye, D.W., Primack, R.B., 2008. How well do first flowering dates measure plant responses to climate change? The effects of population size and sampling frequency. *Journal of Ecology* 96, 1289–1296.
- Miller-Rushing, A.J., Primack, R.B., 2008. Global Warming and flowering times in Thoreau's Concord: a community perspective. *Ecology* 89, 332–341.
- Mücher, C.A., Bunce, R.G.H., Jongman, R.H.G., Klijn, J.A., Koomen, A., Metzger, M.J., Wascher, D.M., 2003. Identification and characterisation of environments and landscapes in Europe. Alterra Wageningen, Netherlands.
- Myneni, R.B., Keeling, C.D., Tucker, C.J., Asrar, G., Nemani, R.R., 1997. Increased plant growth in the northern high latitudes from 1981 to 1991. *Nature* 386, 698–702.
- Naug, D., 2009. Nutritional stress due to habitat loss may explain recent honeybee colony collapses. *Biological Conservation* 142, 2369–2372.
- Nicolson, S.W., Nepi, M., Pacini, E., 2007. Nectaries and nectar. Springer, Dordrecht.
- Nightingale, J.M., Esaias, W.E., Wolfe, R.E., Nickeson, J.E., Ma, P.L.A., 2008. Assessing Honey Bee Equilibrium Range and Forage Supply using Satellite-Derived Phenology. Presented at the Geoscience and Remote Sensing Symposium, IGARSS 2008. IEEE International, pp. 763 – 766.
- Nishihama, M., Wolfe, R., Solomon, D., Patt, F., Blanchette, J., Fleig, A., Masuoka, E., 1997. MODIS level 1A Earth location: Algorithm theoretical basis document version 3.0. SDST-092, MODIS Science Data Support Team.
- Parmesan, C., 2007. Influences of species, latitudes and methodologies on estimates of phenological response to global warming. *Global Change Biology* 13, 1860–1872.
- Price, M.V., Waser, N.M., 1998. Effects of Experimental Warming on Plant Reproductive Phenology in a Subalpine Meadow. *Ecology* 79, 1261–1271.
- Real, L.A., Rathcke, B.J., 1991. Individual Variation in Nectar Production and Its Effect on Fitness in *Kalmia latifolia*. *Ecology* 72, 149.
- Reed, B.C., Brown, J.F., VanderZee, D., Loveland, T.R., Merchant, J.W., Ohlen, D.O., 1994. Measuring phenological variability from satellite imagery. *Journal of Vegetation Science* 5, 703–714.
- Reed, B.C., Loveland, T.R., Tieszen, L.L., 1996. An approach for using AVHRR data to monitor US Great Plains grasslands. *Geocarto International* 11, 13–22.
- Ribbands, C.R., 1953. The behaviour and social life of honeybees. Bee Research Association, London.
- Roetzer, T., Wittenzeller, M., Haeckel, H., Nekovar, J., 2000. Phenology in central Europe—differences and trends of spring phenophases in urban and rural areas. *International Journal of Biometeorology* 44, 60–66.

- Rogers, S., Staub, B., 2013. Standard use of Geographic Information System (GIS) techniques in honey bee research, in: Dietemann, V., Ellis, J.D., Neumann, P. (Eds.), *The COLOSS BEEBOOK, Volume I: Standard Methods for Apis Mellifera Research*. Journal of Apicultural Research 52.
- Root, T.L., Price, J.T., Hall, K.R., Schneider, S.H., Rosenzweig, C., Pounds, J.A., 2003. Fingerprints of global warming on wild animals and plants. *Nature* 421, 57–60.
- Roy, D.B., Sparks, T.H., 2000. Phenology of British butterflies and climate change. *Global Change Biology* 6, 407–416.
- Ruttner, F., 1975. Races of bees, in: *The Hive and the Honey Bee*. Dadant, Hamilton, IL, pp. 19–38.
- Saberioon, 2010. Predict Location(s) of *Apis dorsata* Nesting Sites Using Remote Sensing and Geographic Information System in Melaleuca Foresti. *American Journal of Applied Sciences* 7, 252–259.
- Salomonson, V.V., Barnes, W., Maymon, P.W., Montgomery, H.E., Ostrow, H., 1989. MODIS: Advanced facility instrument for studies of the Earth as a system. *IEEE Transactions on Geoscience and Remote Sensing*, 27, 145–153.
- Schaaf, C.B., Gao, F., Strahler, A.H., Lucht, W., Li, X., Tsang, T., Strugnell, N.C., Zhang, X., Jin, Y., Muller, J.-P., Lewis, P., Barnsley, M., Hobson, P., Disney, M., Roberts, G., Dunderdale, M., Doll, C., d'Entremont, R., Hu, B., Liang, S., Privette, J., Roy, D., 2002. First operational BRDF, albedo nadir reflectance products from MODIS. *Remote sensing of Environment* 83, 135–148.
- Schaber, J., Badeck, F.-W., 2003. Physiology-based phenology models for forest tree species in Germany. *International Journal of Biometeorology* 47, 193–201.
- Scheifinger, H., Koch, E., Winkler, H., 2005. Results of a first look into the Austrian animal phenological records. *Meteorologische Zeitschrift* 14, 203–209.
- Schwartz, M.D., 2003. *Phenology: an integrative environmental science*. Springer.
- Schwartz, M.D., Hanes, J.M., 2010. Intercomparing multiple measures of the onset of spring in eastern North America. *International Journal of Climatology* 30, 1614–1626.
- Seeley, T.D., 1985. *Honeybee ecology: a study of adaptation in social life*. Princeton University Press, Princeton, NJ.
- Seeley, T.D., 1995. *The Wisdom of the Hive: The Social Physiology of Honey Bee Colonies*. Harvard University Press, Cambridge, MA.
- Sgolastra, F., Bosch, J., Molowny-Horas, R., Maini, S., Kemp, W.P., 2010. Effect of temperature regime on diapause intensity in an adult-wintering Hymenopteran with obligate diapause. *Journal of insect physiology* 56, 185–194.
- Shuel, R.W., 1952. Some factors affecting nectar secretion in red clover. *Plant physiology* 27, 95–110.
- Shuel, R.W., 1957. Some aspects of the relation between nectar secretion and nitrogen, phosphorus,

- and potassium nutrition. *Canadian Journal of Plant Science* 37, 220–236.
- Shuel, R.W., 1992. The Production of Nectar, in: Graham, J. (Ed.), *The Hive and the Honey Bee*. Dadant and Sons, Hamilton, Illinois, pp. 401–436.
- Solano, R., Didan, K., Jacobson, A., Huete, A., 2010. MODIS Vegetation Index User's Guide (MOD 13 Series)
http://vip.arizona.edu/documents/MODIS/MODIS_VI_UsersGuide_01_2012.pdf (accessed 03/04/14).
- Spangler, H.G., 1992. The influence of temperature on the wingbeat frequencies of free-flying honey bees, *Apis mellifera* L.(Hymenoptera: Apidae). *Bee Science* 2, 181–186.
- Sparks, T., Langowska, A., Głazaczow, A., Wilkaniec, Z., Bieńkowska, M., Tryjanowski, P., 2010. Advances in the timing of spring cleaning by the honeybee *Apis mellifera* in Poland. *Ecological Entomology* 35, 788–791.
- Sparks, T.H., Carey, P.D., 1995. The responses of species to climate over two centuries: an analysis of the Marsham phenological record, 1736-1947. *Journal of Ecology* 83, 321–329.
- Sparks, T.H., Jeffree, E.P., Jeffree, C.E., 2000. An examination of the relationship between flowering times and temperature at the national scale using long-term phenological records from the UK. *International Journal of Biometeorology* 44, 82–87.
- Sparks, T.H., Yates, T.J., 1997. The effect of spring temperature on the appearance dates of British butterflies 1883-1993. *Ecography* 20, 368–374.
- Stefanescu, C., Peñuelas, J., Filella, I., 2003. Effects of climatic change on the phenology of butterflies in the northwest Mediterranean Basin. *Global Change Biology* 9, 1494–1506.
- Steffan-Dewenter, I., Kuhn, A., 2003. Honeybee foraging in differentially structured landscapes. *Proceedings of the Royal Society of London* 270, 569–575.
- Stocker, T.F., Qin, D., Plattner, G.-K., Tignor, M., Allen, S.K., Boschung, J., Nauels, A., Xia, Y., Bex, V., Midgley, P.M., 2013. The Physical Science Basis. Working Group I Contribution to the Fifth Assessment Report of the Intergovernmental Panel on Climate Change. IPCC.
- Szabo, T., Lefkovitch, L., 1991. Effects of honey removal and supering on honey bee colony gain,. *American Bee Journal* 131, 120–122.
- Szabo, T.I., Mueller, A.E., 1996. Factors affecting the weight changes of honey bee colonies. *American Bee Journal* 136, 417–419.
- Tan, B., Morisette, J.T., Wolfe, R.E., Gao, F., Ederer, G.A., Nightingale, J., Pedelty, J.A., 2008. Vegetation phenology metrics derived from temporally smoothed and gap-filled MODIS data, in: *Geoscience and Remote Sensing Symposium*. IEEE, p. 593.
- Thackeray, S.J., Sparks, T.H., Frederiksen, M., Burthe, S., Bacon, P.J., Bell, J.R., Botham, M.S., Brereton, T.M., Bright, P.W., Carvalho, L., Clutton-Brock, T., Dawson, A., Edwards, M., Elliott, J.M., Harrington, R., Johns, D., Jones, I.D., Jones, J.T., Leech, D., Roy, D.B., Scott, W.A., Smith, M., Smithers, R.J., Winfield, I.J., Wanless, S., 2010. Trophic level asynchrony in rates of phenological change for marine, freshwater and terrestrial environments. *Global*

Change Biology 16, 3304–3313.

Tobler, W.R., 1970. A computer movie simulating urban growth in the Detroit region. *Economic geography* 46, 234–240.

Tucker, C.J., Justice, C.O., Prince, S.D., 1986. Monitoring the grasslands of the Sahel 1984-1985. *International Journal of Remote Sensing* 7, 1571–1581.

Van Dijk, A., Callis, S.L., Sakamoto, C.M., Decker, W.L., 1987. Smoothing vegetation index profiles: An alternative method for reducing radiometric disturbance in NOAA/AVHRR data. *Photogrammetric Engineering and Remote Sensing* 53, 1059–1067.

vanEngelsdorp, D., Meixner, M.D., 2010. A historical review of managed honey bee populations in Europe and the United States and the factors that may affect them. *Journal of Invertebrate Pathology* 103, 80–95.

Visscher, P.K., Seeley, T.D., 1982. Foraging Strategy of Honeybee Colonies in a Temperate Deciduous Forest. *Ecology* 63, 1790–1801.

Von Frisch, K., 1967. *The Dance Language and Orientation of Bees*. Harvard University Press., Cambridge, MA.

Waddington, K.D., Herbert, T.J., Visscher, P.K., Richter, M.R., 1994. Comparisons of forager distributions from matched honey bee colonies in suburban environments. *Behavioral Ecology and Sociobiology* 35, 423–429.

Walther, G.-R., Post, E., Convey, P., Menzel, A., Parmesan, C., Beebee, T.J., Fromentin, J.-M., Hoegh-Guldberg, O., Bairlein, F., 2002. Ecological responses to recent climate change. *Nature* 416, 389–395.

Wan, Z., Zhang, Y., Zhang, Q., Li, Z., 2002. Validation of the land-surface temperature products retrieved from Terra Moderate Resolution Imaging Spectroradiometer data. *Remote Sensing of Environment* 83, 163–180.

Watson, J.C., Wolf, A.T., Ascher, J.S., 2011. Forested landscapes promote richness and abundance of native bees (Hymenoptera: Apoidea: Anthophila) in Wisconsin apple orchards. *Environmental Entomology* 40, 621–632.

Whitcomb Jr, W., 1946. Feeding bees for comb production. *Gleanings in Bee Culture* 74, 198–292.

White, M.A., de Beurs, K.M., Didan, K., Inouye, D.W., Richardson, A., Jensen, O.P., O’Keefe, J., Zhang, G., Nemani, R., 2009. Intercomparison, interpretation, and assessment of spring phenology in North America estimated from remote sensing for 1982–2006. *Global Change Biology* 15, 2335–2359.

White, M.A., Hoffman, F., Hargrove, W.W., Nemani, R.R., 2005. A global framework for monitoring phenological responses to climate change. *Geophysical Research Letters* 32.

White, M.A., Nemani, R.R., 2003. Canopy duration has little influence on annual carbon storage in the deciduous broad leaf forest. *Global Change Biology* 9, 967–972.

White, M.A., Nemani, R.R., Thornton, P.E., Running, S.W., 2002. Satellite evidence of

phenological differences between urbanized and rural areas of the eastern United States deciduous broadleaf forest. *Ecosystems* 5, 260–273.

- White, M.A., Thornton, P.E., Running, S.W., 1997. A continental phenology model for monitoring vegetation responses to interannual climatic variability. *Global Biogeochemical Cycles* 11, 217–234.
- Winston, M.L., 1991. *The Biology of the Honey Bee*. Harvard University Press, Cambridge, MA.
- Wolfe, M.R.E., 2006. MODIS geolocation, in: *Earth Science Satellite Remote Sensing*. Springer, pp. 50–73.
- Wyatt, R., Broyles, S.B., Derda, G.S., 1992. Environmental influences on nectar production in milkweeds (*Asclepias syriaca* and *A. exaltata*). *American Journal of Botany* 79, 636–642.
- Zhang, X., Friedl, M.A., Schaaf, C.B., 2006. Global vegetation phenology from Moderate Resolution Imaging Spectroradiometer (MODIS): Evaluation of global patterns and comparison with in situ measurements. *Journal of Geophysical Research: Biogeosciences* 111.
- Zhang, X., Friedl, M.A., Schaaf, C.B., Strahler, A.H., Hodges, J.C.F., Gao, F., Reed, B.C., Huete, A., 2003. Monitoring vegetation phenology using MODIS. *Remote Sensing of Environment* 84, 471–475.
- Zhang, X., Friedl, M.A., Schaaf, C.B., Strahler, A.H., Liu, Z., 2005. Monitoring the response of vegetation phenology to precipitation in Africa by coupling MODIS and TRMM instruments. *Journal of Geophysical Research: Atmospheres* 110.
- Zhou, X., Harrington, R., Woiwod, I.P., Perry, J.N., Bale, J.S., Clark, S.J., 1995. Effects of temperature on aphid phenology. *Global Change Biology* 1, 303–313.

Mapping the Phenology of European Honey Bee Nectar Flows

Part II-B: Appendices

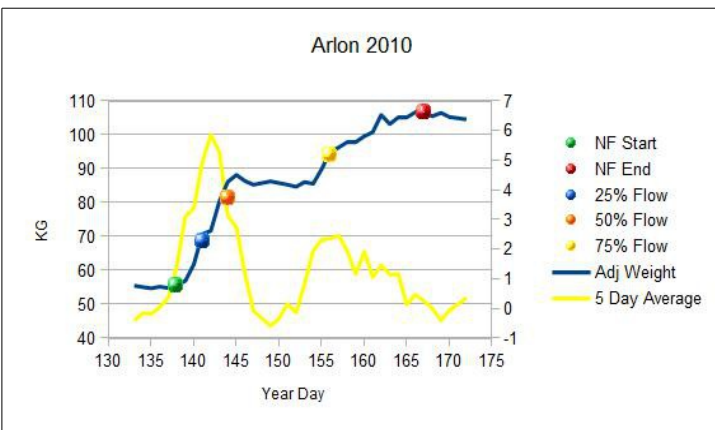
Appendix A: Scale-Hive Data p. 2-32

Appendix B: Additional Scatterplots p. 33-34

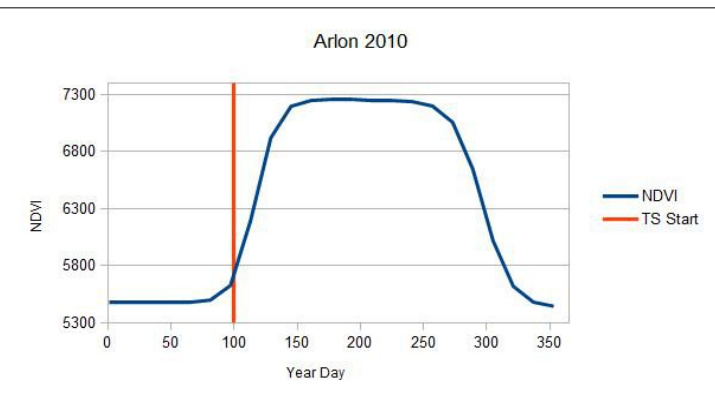
Appendix C: Data Index p. 35

Name	X	Y	Ele. (m)	DMEER
Arlon	49.6833	5.7999	376	Western European Broadleaf forests

2010 HBNF	Day	Weight (KG)
NF Start	138	55.7
NF End	167	106.6
NF Duration	29	50.9
Quarter		12.725
25% Flow	141	68.425
50% Flow	144	81.15
75% Flow	156	93.875



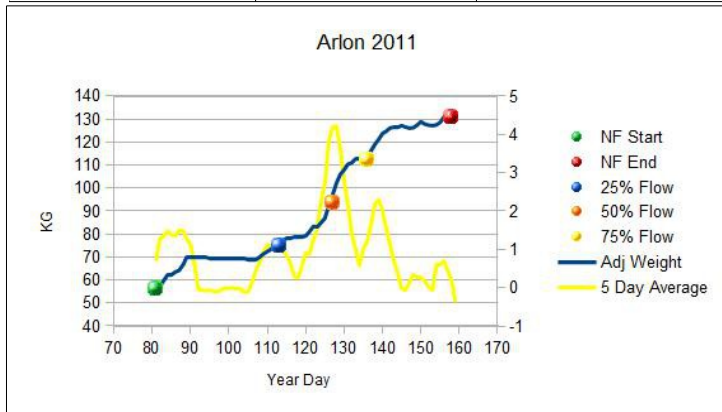
2010 NDVI	Day	Value
SOS	99.36	Base val 5429
End	332.32	Peak val 7252
Length	15.59	Ampl. 1794
Peak t	219.04	L.deriv. 662.4
		R.deriv. 507.7
		L.integral 101900
		S.integral 20090



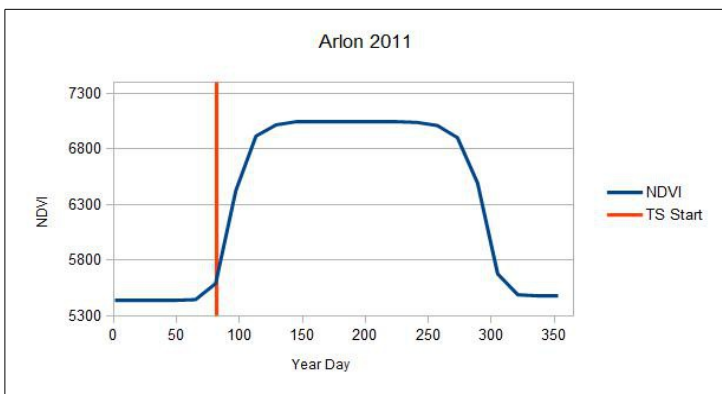
2010			
Day	Adj KG	Adj Day	5 Day Avg
131	56	-0.7	-0.14
132	55.7	-0.3	-0.18
133	55.5	-0.2	-0.4
134	55.1	-0.4	-0.16
135	54.7	-0.4	-0.18
136	55.2	0.5	0.04
137	54.8	-0.4	0.36
138	55.7	0.9	1.42
139	56.9	1.2	3.1
140	61.8	4.9	3.38
141	70.7	8.9	4.94
142	71.7	1	5.86
143	80.4	8.7	5.28
144	86.2	5.8	3.14
145	88.2	2	2.72
146	86.4	-1.8	1.18
147	85.3	-1.1	-0.08
149	86.3	1	-0.58
150	85.8	-0.5	-0.34
151	85.3	-0.5	0.16
152	84.7	-0.6	-0.14
153	86.1	1.4	0.82
154	85.6	-0.5	1.94
155	89.9	4.3	2.32
156	95	5.1	2.36
157	96.3	1.3	2.46
158	97.9	1.6	1.94
159	97.9	0	1.16
160	99.6	1.7	1.92
161	100.8	1.2	1.06
162	105.9	5.1	1.46
163	103.2	-2.7	1.14
164	105.2	2	1.16
165	105.3	0.1	0.14
166	106.6	1.3	0.46
167	106.6	0	0.26
168	105.5	-1.1	0
169	106.5	1	-0.4
170	105.3	-1.2	-0.06
172	104.6	-0.7	0.36

Name	X	Y	Ele. (m)	DMEER
Arlon	49.6833	5.7999	376	Western European Broadleaf forests

2011 HBNF	Day	Weight (KG)
NF Start	81	56.1
NF End	158	130.7
NF Duration	77	74.6
Quarter		18.65
25% Flow	112	74.75
50% Flow	127	93.4
75% Flow	133	112.05



2011 NDVI	Day	Value
SOS	81.76	Base val 5429
End	319.2	Peak val 7043
Length	15.59	Ampl. 1584
Peak t	208.16	L.deriv. 685.6
		R.deriv. 650.8
		L.integral 101300
		S.integral 19430

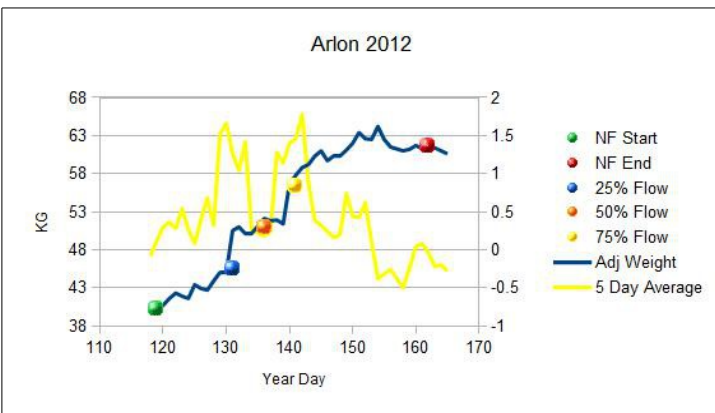


2011			
Day	Adj KG	Adj Day	5 Day Avg
79	56	-0.2	-0.02
80	55.8	-0.2	0.24
81	56.1	0.3	0.7
82	57.3	1.2	1.28
83	59.7	2.4	1.34
84	62.4	2.7	1.48
85	62.5	0.1	1.38
86	63.5	1	1.36
87	64.2	0.7	1.5
88	66.5	2.3	1.48
89	69.9	3.4	1.28
90	69.9	0	1.12
91	69.9	0	0.64
92	69.8	-0.1	-0.04
93	69.7	-0.1	-0.06

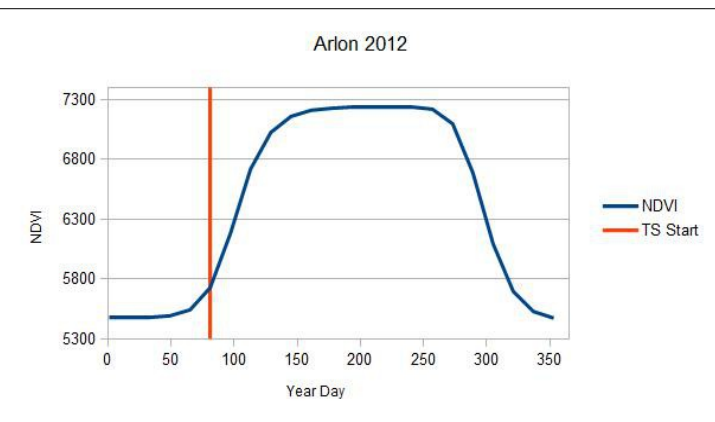
94	69.7	0	-0.08
95	69.6	-0.1	-0.06
96	69.5	-0.1	-0.08
97	69.5	0	-0.08
98	69.3	-0.2	-0.06
99	69.3	0	0
100	69.3	0	-0.02
101	69.5	0.2	0
102	69.4	-0.1	-0.02
103	69.3	-0.1	-0.04
104	69.2	-0.1	-0.12
105	69.1	-0.1	-0.1
106	68.9	-0.2	0.14
107	68.9	0	0.44
108	70	1.1	0.66
109	71.4	1.4	0.92
110	72.4	1	1.12
111	73.5	1.1	1.1
112	74.5	1	1.16
113	75.5	1	1.1
114	77.2	1.7	0.96
115	77.9	0.7	0.86
116	78.3	0.4	0.64
117	78.8	0.5	0.3
118	78.7	-0.1	0.26
119	78.7	0	0.56
120	79.2	0.5	0.92
121	81.1	1.9	0.88
122	83.4	2.3	1.26
123	83.1	-0.3	1.54
124	85	1.9	2.26
125	86.9	1.9	2.74
126	92.4	5.5	3.82
127	97.1	4.7	4.2
128	102.2	5.1	4.22
129	106	3.8	3.6
130	108	2	2.8
131	110.4	2.4	2.16
132	111.1	0.7	1.4
133	113	1.9	0.98
134	113	0	0.58
135	112.9	-0.1	1.02
136	113.3	0.4	1.2
137	116.2	2.9	1.64
138	119	2.8	2.18
139	121.2	2.2	2.3
140	123.8	2.6	2
141	124.8	1	1.52
142	126.2	1.4	1.1
143	126.6	0.4	0.68
144	126.7	0.1	0.36
145	127.2	0.5	-0.02
146	126.6	-0.6	-0.06
147	126.1	-0.5	0.14
148	126.3	0.2	0.34
149	127.4	1.1	0.26
150	128.9	1.5	0.26
151	127.9	-1	0.18
152	127.4	-0.5	0.02
153	127.2	-0.2	-0.06
154	127.5	0.3	0.6
155	128.6	1.1	0.6
156	130.9	2.3	0.7
157	130.4	-0.5	0.44
158	130.7	0.3	0.18
159	129.7	-1	-0.38

Name	X	Y	Ele. (m)	DMEER
Arlon	49.6833	5.7999	376	Western European Broadleaf forests

2012 HBNF	Day	Weight (KG)
NF Start	119	40.2
NF End	162	61.7
NF Duration	43	21.5
Quarter		5.375
25% Flow	131	45.575
50% Flow	136	50.95
75% Flow	141	56.325



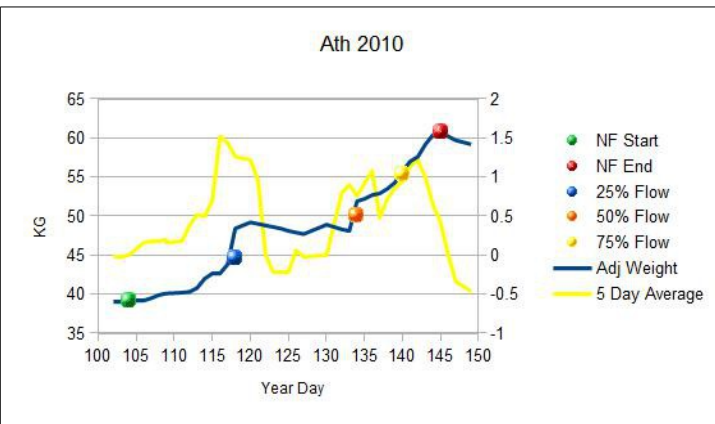
2012 NDVI	Day	Value
SOS	80.64	Base val 5429
End	334.88	Peak val 7231
Length	15.59	Ampl. 1763
Peak t	216.48	L.deriv. 455.8
		R.deriv. 490
		L.integral 109000
		S.integral 21460



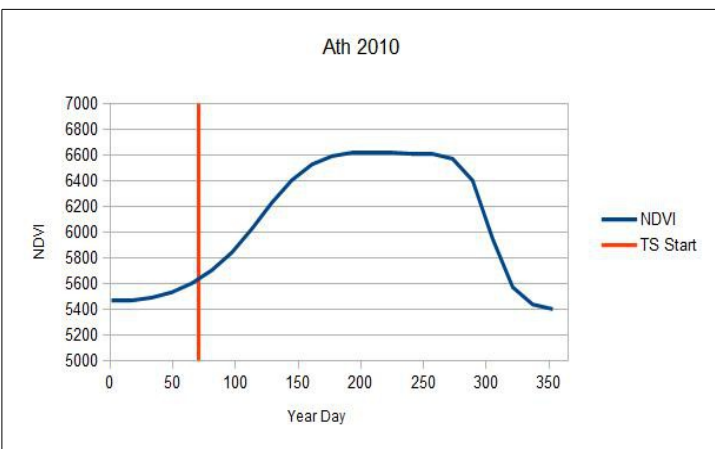
2012			
Day	Adj KG	Adj Day	5 Day Avg
116	41	-0.1	-0.26
117	40.8	-0.2	-0.2
118	40.1	-0.7	-0.08
119	40.2	0.1	0.12
120	40.7	0.5	0.3
121	41.6	0.9	0.36
122	42.3	0.7	0.28
123	41.9	-0.4	0.54
124	41.6	-0.3	0.26
125	43.4	1.8	0.08
126	42.9	-0.5	0.4
127	42.7	-0.2	0.68
128	43.9	1.2	0.32
129	45	1.1	1.52
130	45	0	1.66
131	50.5	5.5	1.26
132	51	0.5	1.04
133	50.2	-0.8	1.42
134	50.2	0	0.26
136	52.1	1.9	0.18
137	51.8	-0.3	0.24
138	51.9	0.1	1.28
139	51.4	-0.5	1.14
140	56.6	5.2	1.4
141	57.8	1.2	1.46
142	58.8	1	1.78
143	59.2	0.4	0.88
144	60.3	1.1	0.38
145	61	0.7	0.32
146	59.7	-1.3	0.24
147	60.4	0.7	0.16
148	60.4	0	0.2
149	61.1	0.7	0.74
150	62	0.9	0.44
151	63.4	1.4	0.42
152	62.6	-0.8	0.62
153	62.5	-0.1	0.1
154	64.2	1.7	-0.38
155	62.5	-1.7	-0.32
156	61.5	-1	-0.26
158	61	-0.5	-0.5
159	61.2	0.2	-0.24
160	61.7	0.5	0.04
161	61.3	-0.4	0.08
162	61.7	0.4	-0.04
163	61.4	-0.3	-0.22
164	61	-0.4	-0.2
165	60.6	-0.4	-0.28

Name	X	Y	Ele. (m)	DMEER
Ath	50.6289	3.7614	38	Southern Temperate Atlantic

2010 HBNF	Day	Weight (KG)
NF Start	104	39.2
NF End	145	60.8
NF Duration	41	21.6
Quarter		5.4
25% Flow	118	44.6
50% Flow	134	50
75% Flow	140	55.4



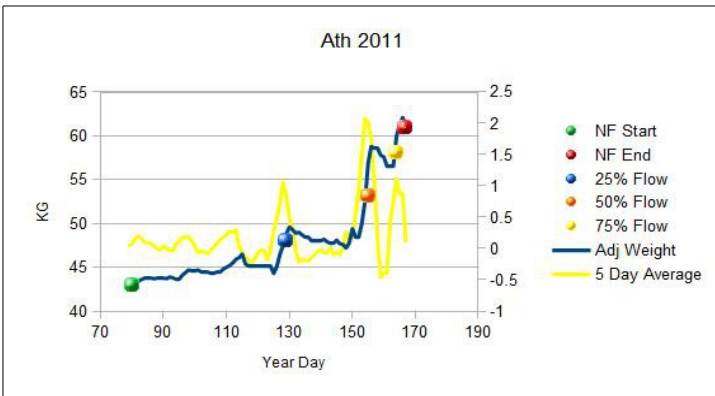
2010 NDVI	Day	Value
SOS	70.56	Base val 5429
End	335.84	Peak val 6618
Length	15.59	Ampl. 1189
Peak t	231.84	L.deriv. 175.1
		R.deriv. 417.7
		L.integral 106500
		S.integral 14180



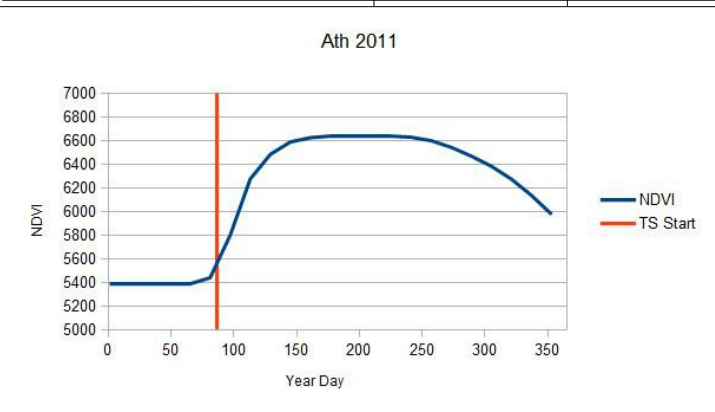
2010			
Day	Adj KG	Adj Day	5 Day Avg
100	39.3	0	-0.06
101	39.2	-0.1	-0.04
102	39.1	-0.1	-0.02
103	39.1	0	-0.02
104	39.2	0.1	0
105	39.2	0	0.08
106	39.2	0	0.16
107	39.5	0.3	0.18
108	39.9	0.4	0.18
109	40.1	0.2	0.2
109	40.1	0	0.16
111	40.2	0.1	0.18
112	40.3	0.1	0.38
113	40.8	0.5	0.52
114	42	1.2	0.5
115	42.7	0.7	0.7
116	42.7	0	1.52
117	43.8	1.1	1.44
118	48.4	4.6	1.26
120	49.2	0.8	1.22
121	49	-0.2	0.96
122	48.8	-0.2	0
123	48.6	-0.2	-0.22
124	48.4	-0.2	-0.22
125	48.1	-0.3	-0.22
126	47.9	-0.2	0.06
127	47.7	-0.2	-0.02
130	48.9	1.2	0
132	48.3	-0.6	0.8
133	48.1	-0.2	0.9
134	51.9	3.8	0.76
135	52.2	0.3	0.92
136	52.7	0.5	1.08
137	52.9	0.2	0.48
138	53.5	0.6	0.72
139	54.3	0.8	0.86
140	55.8	1.5	0.94
141	57	1.2	1.14
142	57.6	0.6	1.22
143	59.2	1.6	1
144	60.4	1.2	0.64
145	60.8	0.4	0.42
146	60.2	-0.6	0
147	59.7	-0.5	-0.34

Name	X	Y	Ele. (m)	DMEER
Ath	50.6289	3.7614	38	Southern Temperate Atlantic

2011 HBNF	Day	Weight (KG)
NF Start	80	43
NF End	167	61
NF Duration	96	20.1
Quarter		5.025
25% Flow	129	48.025
50% Flow	155	53.05
75% Flow	164	58.075



2011 NDVI	Day	Value
SOS	86.08	Base val 5429
End	404.16	Peak val 6634
Length	15.59	Ampl. 1217
Peak t	226.88	L.deriv. 378.1

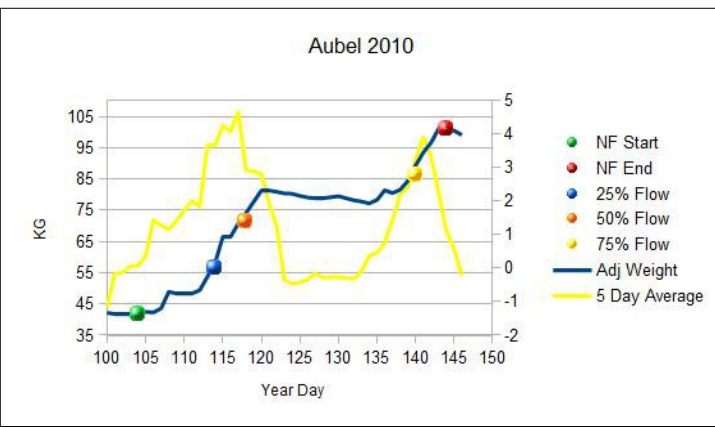


2011			
Day	Adj KG	Adj Day	5 Day Avg
77	43	0	-0.06
78	42.8	-0.2	-0.02
79	42.8	0	0.04
80	43	0.2	0.08
81	43.2	0.2	0.16
82	43.4	0.2	0.2
83	43.6	0.2	0.16
84	43.8	0.2	0.1
86	43.8	0	0.08
87	43.7	-0.1	0.04
88	43.8	0.1	0
89	43.8	0	-0.02
90	43.8	0	0.04
91	43.7	-0.1	0
92	43.9	0.2	-0.02

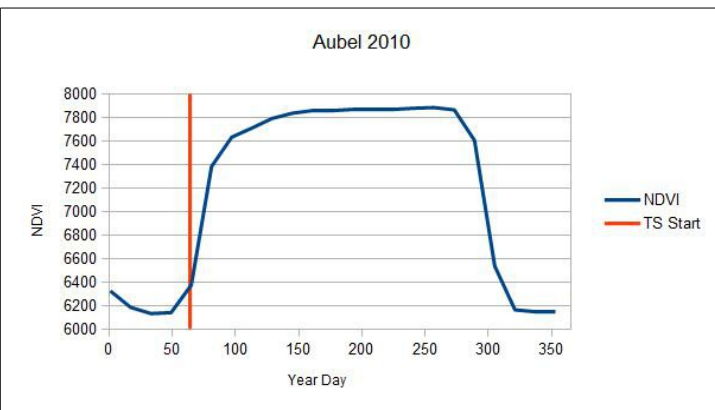
93	43.8	-0.1	-0.02
94	43.7	-0.1	0.08
95	43.7	0	0.1
96	44.1	0.4	0.18
97	44.4	0.3	0.18
98	44.7	0.3	0.18
99	44.6	-0.1	0.12
100	44.6	0	0.02
101	44.7	0.1	-0.06
102	44.5	-0.2	-0.04
103	44.4	-0.1	-0.06
104	44.4	0	-0.08
105	44.3	-0.1	-0.02
106	44.3	0	0.02
107	44.4	0.1	0.08
108	44.5	0.1	0.14
109	44.8	0.3	0.18
110	45	0.2	0.22
111	45.2	0.2	0.28
112	45.5	0.3	0.26
113	45.9	0.4	0.3
114	46.1	0.2	0.04
115	46.5	0.4	-0.06
116	45.4	-1.1	-0.14
117	45.2	-0.2	-0.18
118	45.2	0	-0.26
120	45.2	0	-0.06
121	45.2	0	-0.02
122	45.1	-0.1	-0.02
123	45.1	0	-0.18
124	45.1	0	-0.02
125	44.3	-0.8	0.28
126	45.1	0.8	0.48
127	46.5	1.4	0.74
128	47.5	1	1.06
129	48.8	1.3	0.84
130	49.6	0.8	0.48
131	49.3	-0.3	0.3
132	48.9	-0.4	-0.02
133	49	0.1	-0.22
134	48.7	-0.3	-0.18
135	48.5	-0.2	-0.18
136	48.4	-0.1	-0.2
137	48	-0.4	-0.14
138	48	0	-0.1
139	48	0	-0.04
140	48	0	-0.02
141	48.2	0.2	-0.06
142	47.9	-0.3	-0.06
143	47.7	-0.2	0.02
144	47.7	0	-0.1
145	48.1	0.4	-0.06
146	47.7	-0.4	-0.1
147	47.6	-0.1	0.02
148	47.2	-0.4	0.26
149	47.8	0.6	0.14
150	49.4	1.6	0.18
151	48.4	-1	0.56
152	48.5	0.1	0.94
153	50	1.5	1.5
154	52.5	2.5	2.08
155	56.9	4.4	2.02
156	58.8	1.9	1.72
157	58.6	-0.2	1.06
158	58.6	0	0.14
159	57.8	-0.8	-0.46
160	57.6	-0.2	-0.4
161	56.5	-1.1	-0.4
162	56.6	0.1	0.42

Name	X	Y	Ele. (m)	DMEER
Aubel	50.7048	5.8577	225	Southern Temperate Atlantic

2010 HBNF	Day	Weight (KG)
NF Start	104	41.9
NF End	144	101.2
NF Duration	40	59.3
Quarter		14.825
25% Flow	114	56.725
50% Flow	118	71.55
75% Flow	140	86.375



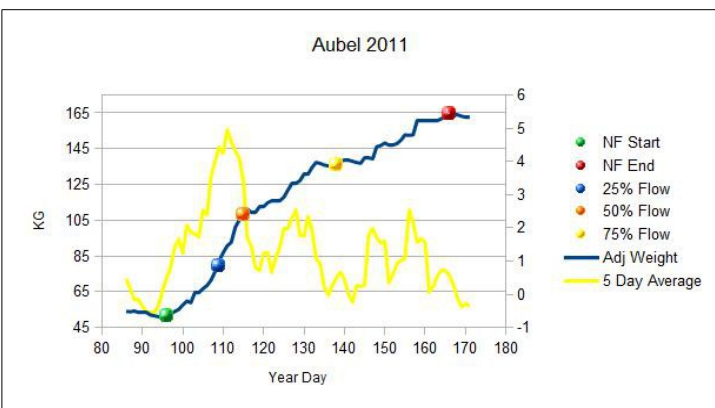
2010	Day	Value
SOS	64.32	Base val 5442
End	309.6	Peak val 7883
Length	245.28	Ampl. 1744
Peak t	189.28	L.deriv. 701.9
		R.deriv. 993.8
		L.integral 128000
		S.integral 23620



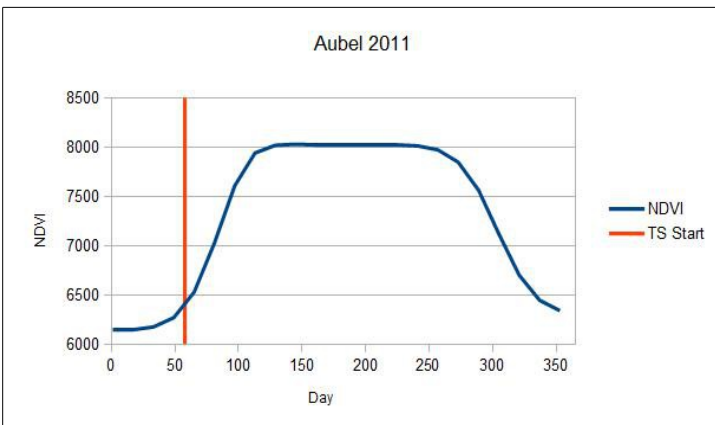
2010			
Day	Adj KG	Adj Day	5 Day Avg
97	47.6	-0.6	-0.84
98	42.5	-5.1	-1.06
99	42.5	0	-1.26
100	42.2	-0.3	-1.16
101	41.9	-0.3	-0.16
102	41.8	-0.1	-0.12
103	41.7	-0.1	0.06
104	41.9	0.2	0.08
105	42.5	0.6	0.36
106	42.3	-0.2	1.44
107	43.6	1.3	1.28
108	48.9	5.3	1.16
109	48.3	-0.6	1.42
111	48.3	0	2.02
112	49.4	1.1	1.84
113	53.7	4.3	3.68
114	58.1	4.4	3.68
115	66.7	8.6	4.26
116	66.7	0	4.08
117	70.7	4	4.66
118	74.1	3.4	2.94
120	81.4	7.3	2.84
121	81.4	0	1.94
122	80.9	-0.5	1.24
123	80.4	-0.5	-0.36
124	80.3	-0.1	-0.46
125	79.6	-0.7	-0.42
126	79.1	-0.5	-0.34
127	78.8	-0.3	-0.16
128	78.7	-0.1	-0.28
130	79.5	0.8	-0.26
132	78.2	-1.3	-0.32
133	77.8	-0.4	-0.08
134	77.2	-0.6	0.38
135	78.3	1.1	0.46
136	81.4	3.1	0.76
137	80.5	-0.9	1.44
138	81.6	1.1	2.2
139	84.4	2.8	2.42
140	89.3	4.9	3.22
141	93.5	4.2	3.92
142	96.6	3.1	3.36
143	101.2	4.6	2.24
144	101.2	0	1.12
145	100.5	-0.7	0.58
146	99.1	-1.4	-0.22

Name	X	Y	Ele. (m)	DMEER
Aubel	50.7048	5.8577	225	Southern Temperate Atlantic

2011 HBNF	Day	Weight (KG)
NF Start	96	51.5
NF End	166	164.5
NF Duration	70	113
Quarter		28.25
25% Flow	109	79.75
50% Flow	115	108
75% Flow	138	136.25



2011 NDVI	Day	Value
SOS	57.92	Base val 6228
End	328.32	Peak val 8029
Length	270.4	Ampl. 1801
Peak t	189.6	L.deriv. 525.2
		R.deriv. 394.6
		L.integral 143200
		S.integral 24850

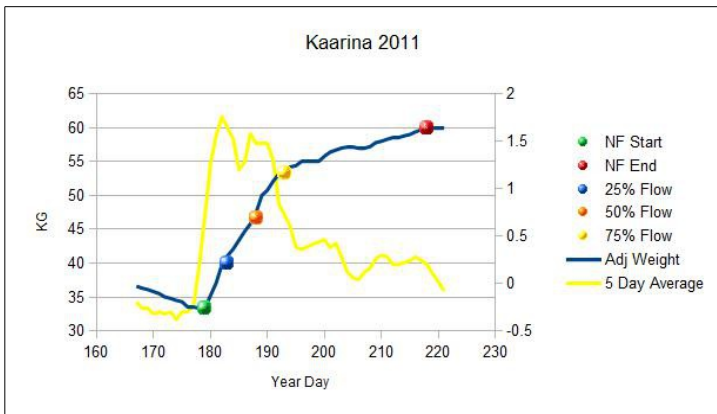


2011			
Day	Adj KG	Adj Day	5 Day Avg
86	54	-0.1	0.46
87	53.8	-0.2	0.16
88	54.2	0.4	-0.16
89	53.7	-0.5	-0.16
90	53.3	-0.4	-0.36
91	53.2	-0.1	-0.54
92	52	-1.2	-0.54
93	51.5	-0.5	-0.56
94	51	-0.5	-0.34
95	50.5	-0.5	0.12

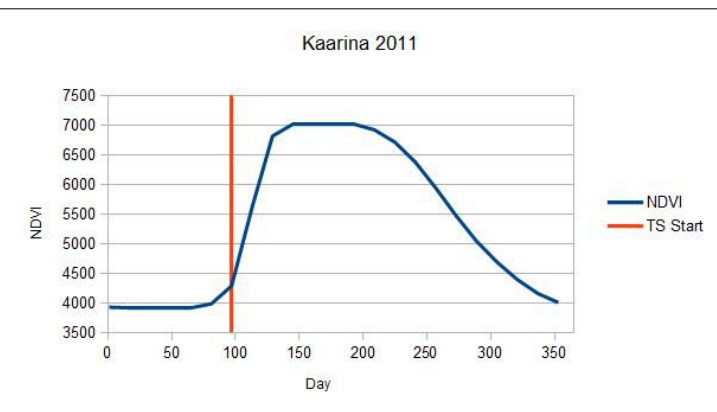
96	51.5	1	0.48
97	52.6	1.1	0.82
98	53.9	1.3	1.42
99	55.1	1.2	1.66
100	57.6	2.5	1.24
101	59.8	2.2	2.08
102	58.8	-1	1.86
103	64.3	5.5	1.82
104	64.4	0.1	1.74
105	66.7	2.3	2.54
106	68.5	1.8	2.4
107	71.5	3	3.56
108	76.3	4.8	4.02
109	82.2	5.9	4.44
110	86.8	4.6	4.24
111	90.7	3.9	4.96
112	92.7	2	4.6
113	101.1	8.4	4.32
114	105.2	4.1	4.1
115	108.4	3.2	3.38
116	111.2	2.8	1.68
117	109.6	-1.6	1.44
118	109.5	-0.1	0.8
119	112.4	2.9	0.72
120	112.4	0	1.24
121	114.8	2.4	1.26
122	115.8	1	0.66
123	115.8	0	1.1
124	115.7	-0.1	1.4
125	117.9	2.2	1.98
126	121.8	3.9	1.98
127	125.7	3.9	2.3
128	125.7	0	2.54
129	127.2	1.5	1.76
130	130.6	3.4	1.78
131	130.6	0	2.34
132	134.6	4	1.92
133	137.4	2.8	1.06
134	136.8	-0.6	0.92
135	135.9	-0.9	0.22
136	135.2	-0.7	-0.02
137	135.7	0.5	0.26
138	137.3	1.6	0.5
139	138.1	0.8	0.66
140	138.4	0.3	0.46
141	138.5	0.1	0
142	138	-0.5	-0.24
143	137.3	-0.7	0.26
144	136.9	-0.4	0.24
145	139.7	2.8	0.28
146	139.7	0	1.78
147	139.4	-0.3	1.98
148	146.2	6.8	1.7
149	146.8	0.6	1.54
150	148.2	1.4	1.6
151	147.4	-0.8	0.34
152	147.4	0	0.6
153	147.9	0.5	0.92
154	149.8	1.9	1.02
155	152.8	3	1.08
156	152.5	-0.3	2.54
157	152.8	0.3	2.16
158	160.6	7.8	1.56
159	160.6	0	1.68
160	160.6	0	1.54
161	160.9	0.3	0.06
162	160.5	-0.4	0.24
163	160.9	0.4	0.56
164	161.8	0.9	0.72
165	163.4	1.6	0.7
166	164.5	1.1	0.56
167	164	-0.5	0.28
168	163.7	-0.3	-0.12
169	163.2	-0.5	-0.38
170	162.8	-0.4	-0.28

Name	X	Y	Ele. (m)	DMEER
Kaarina	60.4360	22.4323	38	Samatic mixed forests

2011 HBNF	Day	Weight (KG)
NF Start	179	33.3
NF End	218	60
NF Duration	39	26.7
Quarter		6.675
25% Flow	183	39.975
50% Flow	188	46.65
75% Flow	193	53.325



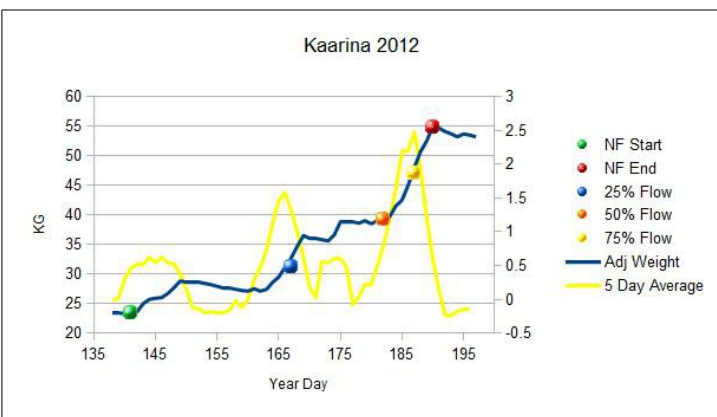
2011 NDVI	Day	Value
SOS	97.12	Base val 3928
End	319.2	Peak val 7021
Length	222.08	Ampl. 3093
Peak t	180.48	L.deriv. 1269
		R.deriv. 408.1
		L.integral 90300
		S.integral 31380



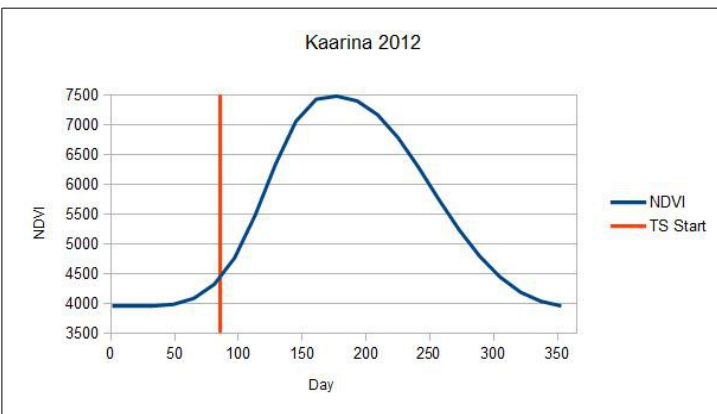
2011			
Day	Adj KG	Adj Day	5 Day Avg
167	36.6	-0.2	-0.2
168	36.3	-0.3	-0.26
169	36.1	-0.2	-0.26
170	35.8	-0.3	-0.32
171	35.5	-0.3	-0.3
172	35	-0.5	-0.32
173	34.8	-0.2	-0.3
174	34.5	-0.3	-0.38
175	34.3	-0.2	-0.3
176	33.6	-0.7	-0.3
177	33.5	-0.1	-0.24
178	33.3	-0.2	0.18
179	33.3	0	0.7
180	35.2	1.9	1.26
181	37.1	1.9	1.56
182	39.8	2.7	1.76
183	41.1	1.3	1.64
184	42.1	1	1.52
185	43.4	1.3	1.2
186	44.7	1.3	1.28
187	45.8	1.1	1.58
188	47.5	1.7	1.48
189	50	2.5	1.48
190	50.8	0.8	1.48
191	52.1	1.3	1.3
192	53.2	1.1	0.84
193	54	0.8	0.72
194	54.2	0.2	0.6
195	54.4	0.2	0.38
196	55.1	0.7	0.36
199	55.1	0	0.44
200	55.8	0.7	0.46
201	56.4	0.6	0.38
202	56.7	0.3	0.42
203	57	0.3	0.28
204	57.2	0.2	0.12
205	57.2	0	0.06
206	57	-0.2	0.04
207	57	0	0.12
208	57.2	0.2	0.16
209	57.8	0.6	0.26
210	58	0.2	0.3
211	58.3	0.3	0.28
212	58.5	0.2	0.2
213	58.6	0.1	0.2
214	58.8	0.2	0.22
215	59	0.2	0.24
216	59.4	0.4	0.28
217	59.7	0.3	0.24
218	60	0.3	0.2
219	60	0	0.1
220	60	0	0.02

Name	X	Y	Ele. (m)	DMEER
Kaarina	60.4360	22.4323	38	Samatic mixed forests

2012		Day	Weight (KG)
NF Start		141	23.4
NF End		190	54.9
NF Duration		49	31.5
Quarter			7.875
25% Flow		167	31.275
50% Flow		182	39.15
75% Flow		187	47.025



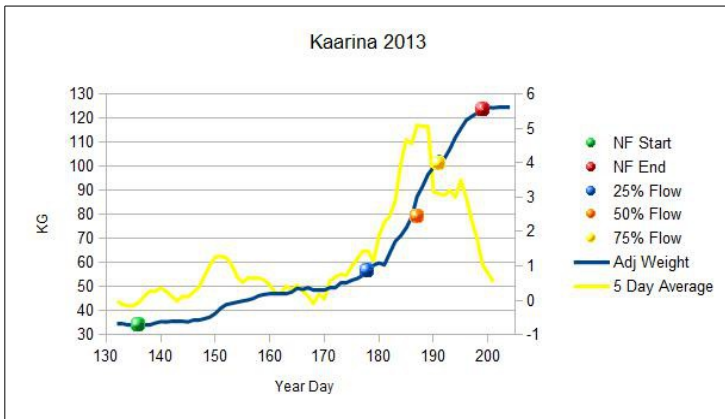
2012 NDVI		Day	Value
SOS	85.6	Base val	3937
End	303.04	Peak val	7478
Length	217.44	Ampl.	3541
Peak t	181.12	L.deriv.	741.7
		R.deriv.	483
		L.integral	90700
		S.integral	31640



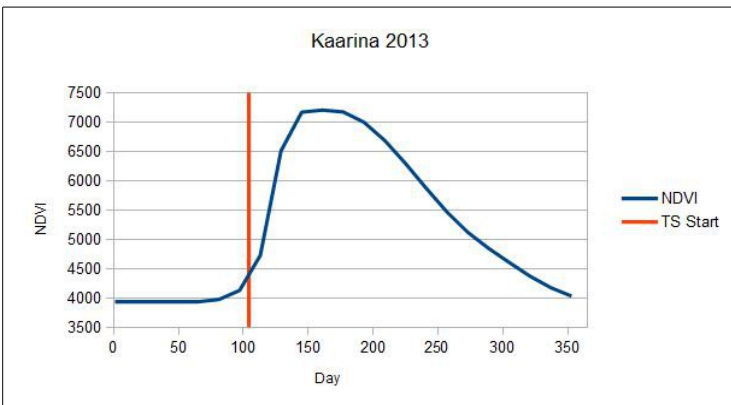
2012			
Day	Adj KG	Adj Day	5 Day Avg
133	23.9	0	0
134	23.8	-0.1	0
135	23.7	-0.1	0
136	23.5	-0.2	-0.08
137	23.5	0	-0.08
138	23.5	0	-0.08
139	23.4	-0.1	-0.02
140	23.3	-0.1	0.02
141	23.4	0.1	0.3
142	23.6	0.2	0.46
143	25	1.4	0.52
144	25.7	0.7	0.52
145	25.9	0.2	0.62
146	26	0.1	0.54
147	26.7	0.7	0.62
148	27.7	1	0.54
149	28.8	1.1	0.52
150	28.6	-0.2	0.38
151	28.6	0	0.14
152	28.6	0	-0.12
153	28.4	-0.2	-0.14
154	28.2	-0.2	-0.2
155	27.9	-0.3	-0.18
156	27.6	-0.3	-0.2
157	27.7	0.1	-0.2
158	27.4	-0.3	-0.16
159	27.2	-0.2	-0.02
160	27.1	-0.1	-0.12
161	27.5	0.4	0
162	27.1	-0.4	0.28
163	27.4	0.3	0.48
164	28.6	1.2	0.72
165	29.5	0.9	1.12
166	31.1	1.6	1.46
167	32.7	1.6	1.58
168	34.7	2	1.32
169	36.5	1.8	1
170	36.1	-0.4	0.62
171	36.1	0	0.18
172	35.8	-0.3	0.02
173	35.6	-0.2	0.56
174	36.6	1	0.54
175	38.9	2.3	0.6
176	38.8	-0.1	0.6
177	38.8	0	0.48
178	38.6	-0.2	-0.08
179	39	0.4	0.04
180	38.5	-0.5	0.22
181	39	0.5	0.22
182	39.9	0.9	0.5
183	39.7	-0.2	0.8
184	41.5	1.8	1.2
185	42.5	1	1.62
186	45	2.5	2.2
187	48	3	2.2
188	50.7	2.7	2.48
189	52.5	1.8	1.94
190	54.9	2.4	1.22
191	54.7	-0.2	0.6
192	54.1	-0.6	0.14
193	53.7	-0.4	-0.24
194	53.2	-0.5	-0.24
195	53.7	0.5	-0.18
196	53.5	-0.2	-0.14

Name	X	Y	Ele. (m)	DMEER
Kaarina	60.4360	22.4323	38	Sarmatic mixed forests

2013 HBNF	Day	Weight (KG)
NF Start	136	34
NF End	199	123.6
NF Duration	63	89.6
Quarter		22.4
25% Flow	178	56.4
50% Flow	187	78.8
75% Flow	191	101.2



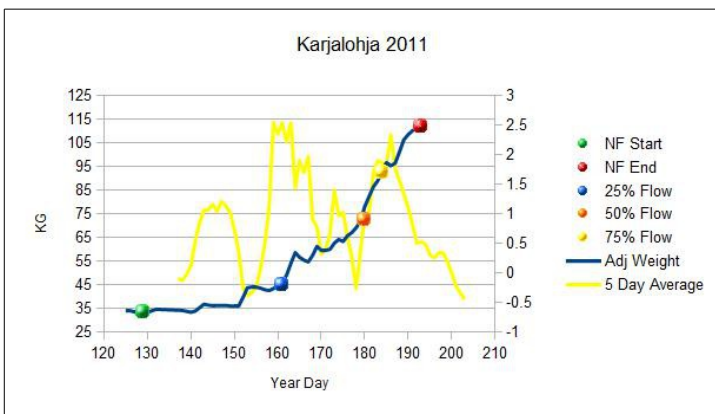
2013 NDVI	Day	Value
SOS	103.84	Base val 3912
End	318.56	Peak val 7202
Length	214.72	Ampl. 3290
Peak t	171.36	L.deriv. 1515
		R.deriv. 339.9
		L.integral 87140
		S.integral 28470



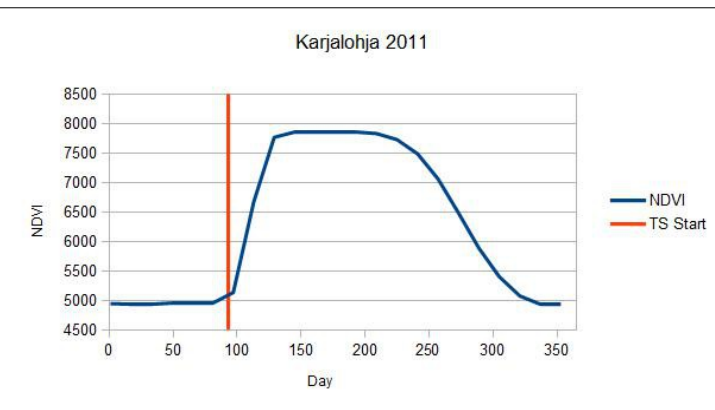
2013			
Day	Adj KG	Adj Day	5 Day Avg
132	34.6	-0.2	-0.02
133	34.4	-0.2	-0.12
134	34.2	-0.2	-0.16
135	34	-0.2	-0.14
136	34	0	-0.06
137	33.9	-0.1	0.12
138	34.1	0.2	0.28
139	34.8	0.7	0.26
140	35.4	0.6	0.36
141	35.3	-0.1	0.26
142	35.7	0.4	0.12
143	35.4	-0.3	-0.02
144	35.4	0	0.12
145	35.3	-0.1	0.1
146	35.9	0.6	0.24
147	36.2	0.3	0.38
148	36.6	0.4	0.7
149	37.3	0.7	1.02
150	38.8	1.5	1.26
151	41	2.2	1.28
152	42.5	1.5	1.24
153	43	0.5	1.04
154	43.5	0.5	0.68
155	44	0.5	0.52
156	44.4	0.4	0.64
157	45.1	0.7	0.64
158	46.2	1.1	0.64
159	46.7	0.5	0.58
160	47.2	0.5	0.44
161	47.3	0.1	0.22
162	47.3	0	0.2
163	47.3	0	0.42
164	47.7	0.4	0.3
165	49.3	1.6	0.44
166	48.8	-0.5	0.28
167	49.5	0.7	0.12
168	48.7	-0.8	-0.1
169	48.3	-0.4	0.18
170	48.8	0.5	0.04
171	49.7	0.9	0.56
172	49.7	0	0.68
173	51.5	1.8	0.76
174	51.7	0.2	0.72
175	52.6	0.9	0.98
176	53.3	0.7	1.2
177	54.6	1.3	1.42
178	57.5	2.9	1.44
179	58.8	1.3	1.14
180	59.8	1	1.88
181	59	-0.8	2.26
182	64	5	2.46
183	68.8	4.8	2.9
184	71.1	2.3	3.96
185	74.3	3.2	4.68
186	78.8	4.5	4.56
187	87.4	8.6	5.1
188	91.6	4.2	5.06
189	96.6	5	5.06
190	99.6	3	3.16
191	104.1	4.5	3.1
192	103.2	-0.9	3.06
193	107.1	3.9	3.2
194	111.9	4.8	3
195	115.6	3.7	3.5
196	119.1	3.5	3
197	120.7	1.6	2.34
198	122.1	1.4	1.78
199	123.6	1.5	1.04
200	124.5	0.9	0.78
201	124.3	-0.2	0.54
202	124.6	0.3	0.2

Name	X	Y	Ele. (m)	DMEER
Karjalohja	60.1834	23.6518	53	Scandinavian and Russian taiga

2011 HBNF	Day	Weight (KG)
NF Start	129	33.26
NF End	193	112.15
NF Duration	64	78.89
Quarter		19.7225
25% Flow	163	52.9825
50% Flow	180	72.705
75% Flow	184	92.4275



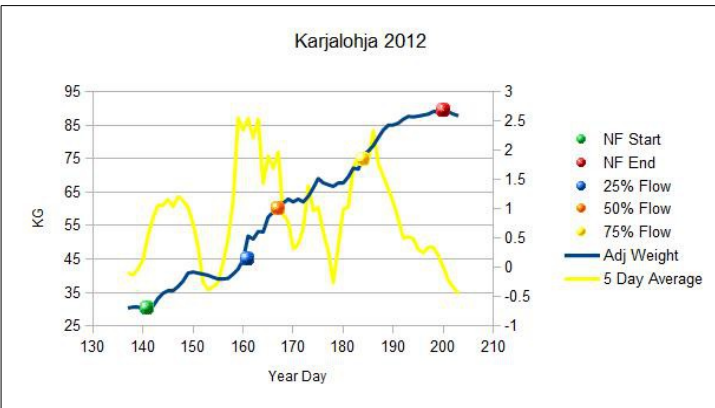
2011 NDVI	Day	Value	
SOS	98.56	Base val	4936
End	305.44	Peak val	7862
Length	206.88	Ampl.	2926
Peak t	184.48	L.deriv.	1348
		R.deriv.	539.3
		L.integral	104000
		S.integral	29910



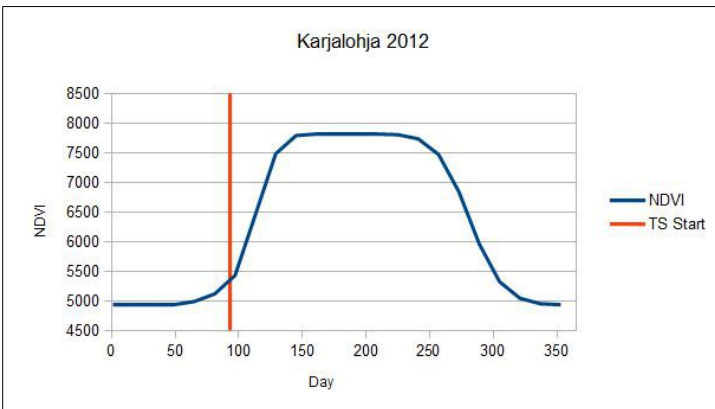
2011			
Day	Adj KG	Adj Day	5 Day Avg
125	34.06	-0.13	-0.19
126	33.84	-0.22	-0.194
127	33.47	-0.37	-0.186
128	33.28	-0.19	-0.144
129	33.26	-0.02	0.028
130	33.34	0.08	0.234
131	33.98	0.64	0.17
132	34.64	0.66	0.024
138	34.13	-0.51	0.106
140	33.38	-0.75	0.266
141	33.87	0.49	0.432
142	35.31	1.44	0.534
143	36.8	1.49	0.6
143	36.8	0	0.458
144	36.38	-0.42	0.198
145	36.16	-0.22	-0.14
148	36.3	0.14	-0.152
149	36.1	-0.2	-0.038
150	36.04	-0.06	0.698
151	36.19	0.15	1.486
152	39.65	3.46	1.566
153	43.73	4.08	1.608
154	43.93	0.2	1.472
155	44.08	0.15	0.652
156	43.55	-0.53	-0.238
157	42.91	-0.64	-0.108
158	42.54	-0.37	0.122
159	43.39	0.85	0.49
160	44.69	1.3	1.216
161	46	1.31	2.294
162	48.99	2.99	3.04
163	54.01	5.02	2.388
164	58.59	4.58	1.882
165	56.63	-1.96	1.132
166	55.41	-1.22	0.688
167	54.65	-0.76	0.526
168	57.45	2.8	0.582
169	61.22	3.77	0.8
170	59.54	-1.68	1.07
171	59.41	-0.13	1.02
172	60	0.59	0.584
173	62.55	2.55	0.752
174	64.14	1.59	1.248
175	63.3	-0.84	1.404
176	65.65	2.35	1.3
177	67.02	1.37	1.524
178	69.05	2.03	2.938
179	71.76	2.71	3.346
180	77.99	6.23	3.888
181	82.38	4.39	3.994
182	86.46	4.08	4.252
183	89.02	2.56	3.744
184	93.02	4	2.59
185	96.71	3.69	1.99
186	95.33	-1.38	2.44
187	96.41	1.08	2.66
188	101.22	4.81	2.366
189	106.32	5.1	2.972
190	108.54	2.22	2.94
191	110.19	1.65	2.186
192	111.11	0.92	1.062
193	112.15	1.04	0.64
194	111.63	-0.52	0.414

Name	X	Y	Ele. (m)	DMEER
Karjalohja	60.1834	23.6518	53	Scandinavian and Russian taiga

2012 HBNF	Day	Weight (KG)
NF Start	141	30.285
NF End	200	89.43
NF Duration	59	59.145
Quarter		14.78625
25% Flow	161	45.07125
50% Flow	167	59.8575
75% Flow	184	74.64375



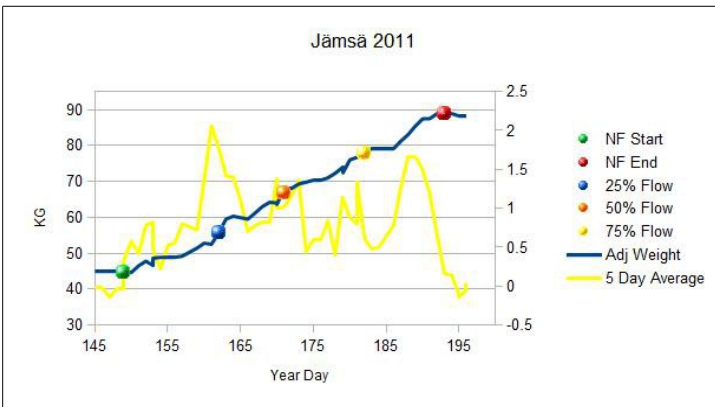
2012 HBNF	Day	Value
SOS	92.64	4928
End	303.04	7822
Length	210.24	2894
Peak t	192.96	1027
		R.deriv. 739.1
		L.integral 104700
		S.integral 30750



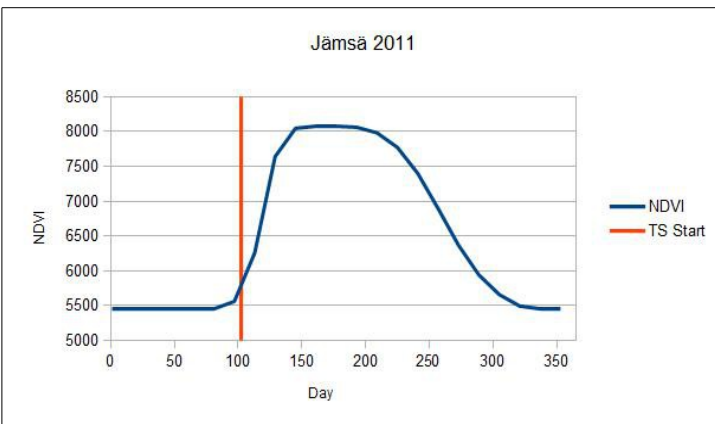
2012			
Day	Adj KG	Adj Day	5 Day Avg
137	30.335	-0.08	-0.094
138	30.48	0.145	-0.129
139	30.5	0.02	-0.026
140	30.075	-0.425	0.126
141	30.285	0.21	0.541
142	30.965	0.68	0.85
143	33.185	2.22	1.067
144	34.75	1.565	1.07
145	35.41	0.66	1.162
146	35.635	0.225	1.04
147	36.775	1.14	1.211
148	38.385	1.61	1.14
149	40.805	2.42	1.028
150	41.11	0.305	0.74
151	40.775	-0.335	0.35
152	40.475	-0.3	-0.251
153	40.135	-0.34	-0.384
154	39.55	-0.585	-0.332
155	39.19	-0.36	-0.251
156	39.115	-0.075	0.076
157	39.22	0.105	0.49
158	40.515	1.295	1.134
159	42	1.485	2.552
160	44.86	2.86	2.347
161	51.875	7.015	2.542
162	50.955	-0.92	2.218
163	53.225	2.27	2.537
164	53.09	-0.135	1.433
165	57.545	4.455	1.905
166	59.04	1.495	1.697
167	60.48	1.44	1.971
168	61.71	1.23	0.908
169	62.945	1.235	0.779
170	62.085	-0.86	0.322
171	62.935	0.85	0.4
172	62.09	-0.845	0.661
173	63.71	1.62	1.399
174	66.25	2.54	0.97
175	69.08	2.83	1.027
176	67.785	-1.295	0.605
177	67.225	-0.56	0.274
178	66.735	-0.49	-0.261
179	67.62	0.885	0.357
180	67.775	0.155	0.993
181	69.57	1.795	1.029
182	72.19	2.62	1.703
183	71.88	-0.31	1.902
184	76.135	4.255	1.868
185	77.285	1.15	1.822
186	78.91	1.625	2.338
187	81.3	2.39	1.774
188	83.57	2.27	1.559
189	85.005	1.435	1.343
190	85.08	0.075	1.103
191	85.625	0.545	0.819
192	86.815	1.19	0.499
193	87.665	0.85	0.528
194	87.5	-0.165	0.483
195	87.72	0.22	0.304
196	88.04	0.32	0.254
197	88.335	0.295	0.344
198	88.935	0.6	0.342
199	89.22	0.285	0.201
200	89.43	0.21	0.001
201	89.045	-0.385	-0.223

Name	X	Y	Ele. (m)	DMEER
Jämsä	61.9642	25.3007	117	Scandinavian and Russian taiga

HBNF 2011		Day	Weight (KG)
NF Start		149	44.7
NF End		193	88.9
NF Duration		44	44.2
Quarter			11.05
25% Flow		162	55.75
50% Flow		171	66.8
75% Flow		182	77.85



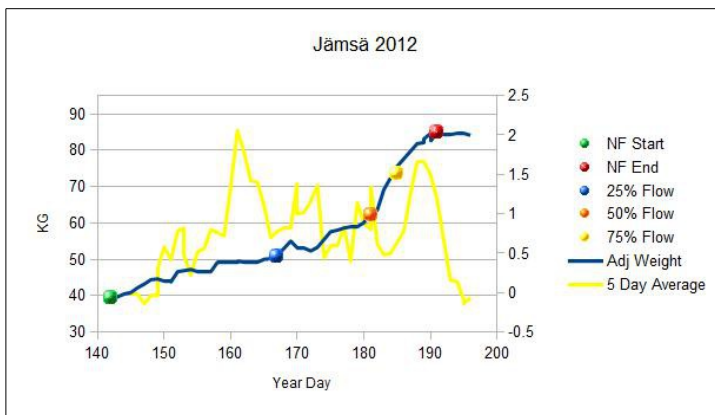
2011 NDVI		Day	Value
SOS		102.56	Base val 5450
End		293.28	Peak val 8075
Length		190.72	Ampl. 2625
Peak t		180.16	L.deriv. 1177
			R.deriv. 474.3
			L.integral 99710
			S.integral 23410



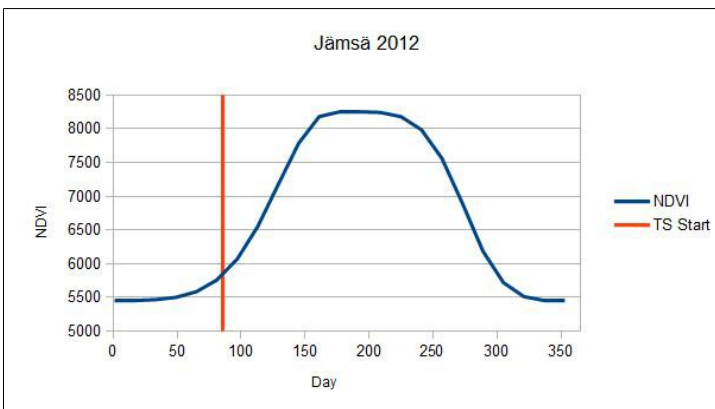
2011			
Day	Adj KG	Adj Day	5 Day Avg
145	44.9	-0.3	-0.02
146	44.9	0	-0.02
147	44.9	0	-0.14
148	44.9	0	-0.04
149	44.5	-0.4	-0.04
149	44.7	0.2	0.32
150	44.7	0	0.58
151	46.5	1.8	0.42
152	47.8	1.3	0.78
153	46.6	-1.2	0.82
153	48.6	2	0.48
154	48.8	0.2	0.22
155	48.9	0.1	0.52
156	48.9	0	0.56
157	49.2	0.3	0.8
159	51.4	2.2	0.72
160	52.8	1.4	1.36
161	52.5	-0.3	2.06
162	55.7	3.2	1.78
163	59.5	3.8	1.42
164	60.3	0.8	1.4
165	59.9	-0.4	1.1
166	59.5	-0.4	0.7
167	61.2	1.7	0.78
168	63	1.8	0.82
169	64.2	1.2	0.82
170	64	-0.2	1.38
170	63.6	-0.4	1
171	68.1	4.5	1.02
172	68	-0.1	1.16
173	69.3	1.3	1.36
174	69.8	0.5	0.44
175	70.4	0.6	0.6
176	70.3	-0.1	0.6
177	71	0.7	0.84
178	72.3	1.3	0.4
179	74	1.7	1.14
179	72.4	-1.6	1.14
180	76	3.6	0.88
181	76.7	0.7	0.8
181	76.7	0	1.34
182	78	1.3	0.62
183	79.1	1.1	0.48
184	79.1	0	0.5
185	79.1	0	0.64
186	79.2	0.1	0.78
187	81.2	2	1.26
188	83	1.8	1.66
189	85.4	2.4	1.66
190	87.4	2	1.5
191	87.5	0.1	1.18
192	88.7	1.2	0.66
193	88.9	0.2	0.16
194	88.7	-0.2	0.14
195	88.2	-0.5	-0.1
196	88.2	0	-0.06

Name	X	Y	Ele. (m)	DMEER
Jämsä	61.9642	25.3007	117	Scandinavian and Russian taiga

2012 HBNF	Day	Weight (KG)
NF Start	142	39.4
NF End	191	85
NF Duration	49	45.6
Quarter		11.4
25% Flow	167	50.8
50% Flow	181	62.2
75% Flow	185	73.6



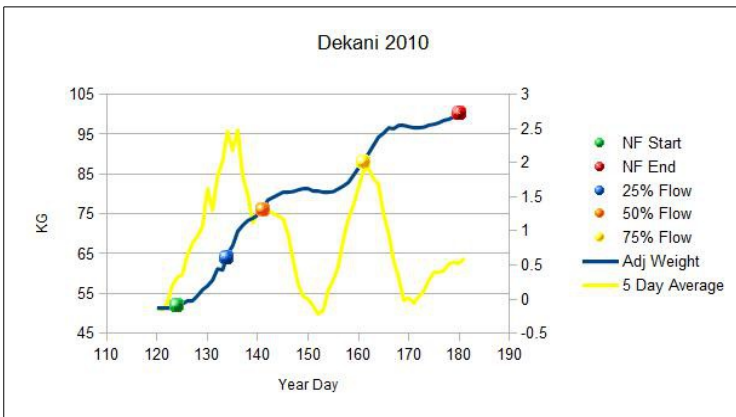
2012 NDVI	Day	Value	
SOS	85.92	Base val	5450
End	298.72	Peak val	8257
Length	212.8	Ampl.	2806
Peak t	196.32	L.deriv.	555
		R.deriv.	625.6
		L.integral	108800
		S.integral	27020



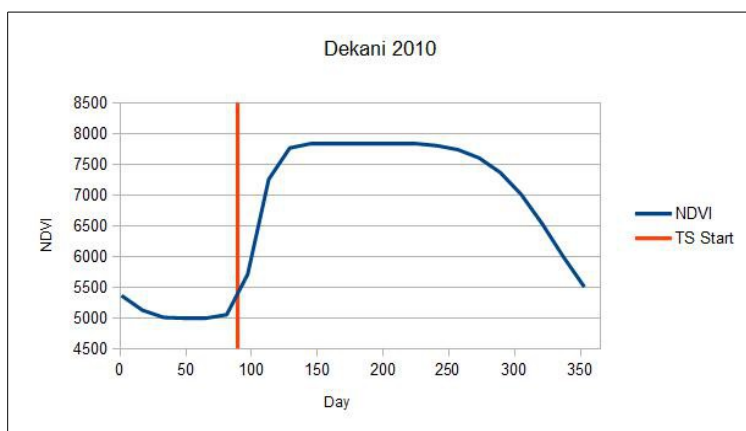
2012			
Day	Adj KG	Adj Day	5 Day Avg
142	39.4	0.8	0.6333333333
143	39.7	0.3	0.575
144	40.5	0.8	0.72
145	40.9	0.4	0.76
146	42.2	1.3	0.94
147	43.2	1	0.82
148	44.4	1.2	0.64
149	44.6	0.2	0.36
150	44.1	-0.5	0.12
151	44	-0.1	0.44
151	43.8	-0.2	0.52
152	46.6	2.8	0.52
154	47.2	0.6	0.54
155	46.7	-0.5	0.58
156	46.7	0	0.54
157	46.7	0	0.42
158	49.3	2.6	0.52
159	49.3	0	0.52
160	49.3	0	0.56
161	49.3	0	0
161	49.5	0.2	0
162	49.3	-0.2	0
163	49.3	0	0.14
164	49.3	0	0.14
165	50	0.7	0.36
166	50.2	0.2	1.14
167	51.1	0.9	0.74
169	55	3.9	0.6
170	53	-2	0.42
171	53	0	0.44
172	52.3	-0.7	0.52
173	53.3	1	1
175	57.6	4.3	1.12
176	58	0.4	1.36
177	58.6	0.6	1.16
178	59.1	0.5	0.5
179	59.1	0	1
180	60.1	1	0.98
181	63	2.9	2.02
182	63.5	0.5	2.66
183	69.2	5.7	3.1
184	72.4	3.2	3.76
185	75.6	3.2	3.72
188	81.8	6.2	2.78
189	82.1	0.3	2.46
189	83.1	1	1.4
190	84.7	1.6	0.64
190	82.6	-2.1	0.46
191	85	2.4	0.24
192	84.4	-0.6	-0.02
193	84.3	-0.1	0.4
194	84.6	0.3	-0.18
195	84.6	0	-0.12
196	84.1	-0.5	0.04

Name	X	Y	Ele. (m)	DMEER
Koper – Dekani	45.5414	13.8330	65	Illyrian deciduous forests

2010 HBNF	Day	Weight (KG)
NF Start	124	51.8
NF End	180	100.1
NF Duration	56	48.3
Quarter		12.075
25% Flow	134	63.875
50% Flow	141	75.95
75% Flow	161	88.025



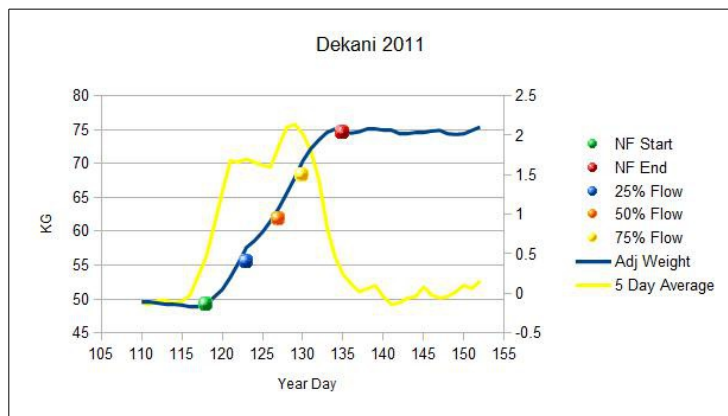
2010 NDVI	Day	Value
SOS	89.12	Base val 4967
End	357.76	Peak val 7837
Length	268.64	Ampl. 2870
Peak t	202.56	L.deriv. 1369
		R.deriv. 474.1
		L.integral 133400
		S.integral 39070



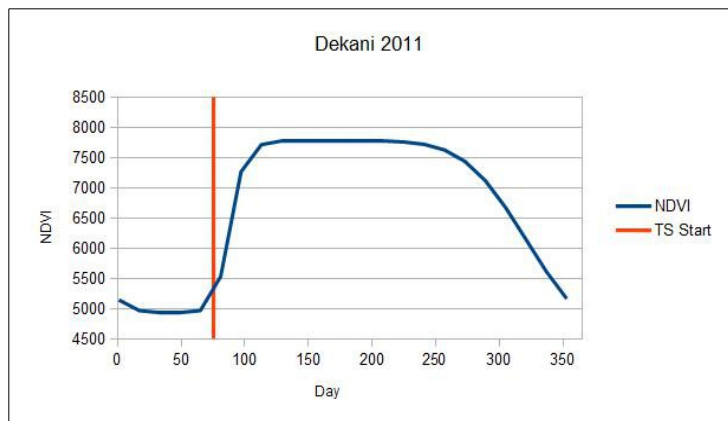
2010			
Day	Adj KG	Adj Day	5 Day Avg
120	51.3	-0.8	-0.12
121	51.4	0.1	-0.16
122	51.3	-0.1	-0.06
123	51.2	-0.1	0.2
124	51.8	0.6	0.32
125	52.3	0.5	0.36
126	53	0.7	0.64
127	53.1	0.1	0.82
128	54.4	1.3	0.92
129	55.9	1.5	1.06
130	56.9	1	1.62
131	58.3	1.4	1.3
132	61.2	2.9	1.8
133	60.9	-0.3	2.02
134	64.9	4	2.46
135	67	2.1	2.18
136	70.6	3.6	2.48
137	72.1	1.5	1.8
138	73.3	1.2	1.54
139	73.9	0.6	1.12
140	74.7	0.8	1.28
141	76.2	1.5	1.4
142	78.5	2.3	1.3
145	80.3	1.8	1.18
146	80.4	0.1	0.96
147	80.6	0.2	0.58
148	81	0.4	0.22
149	81.4	0.4	0.04
150	81.4	0	0
151	80.6	-0.8	-0.1
152	80.6	0	-0.22
153	80.5	-0.1	-0.16
154	80.3	-0.2	0.14
155	80.6	0.3	0.28
156	81.3	0.7	0.48
157	82	0.7	0.88
158	82.9	0.9	1.18
159	84.7	1.8	1.38
160	86.5	1.8	1.64
161	88.2	1.7	1.88
162	90.2	2	1.92
163	92.3	2.1	1.76
164	94.3	2	1.68
165	95.3	1	1.24
166	96.6	1.3	0.96
167	96.4	-0.2	0.56
168	97.1	0.7	0.32
169	97.1	0	-0.02
170	96.9	-0.2	0.02
171	96.5	-0.4	-0.06
172	96.5	0	0.04
173	96.8	0.3	0.12
174	97.3	0.5	0.28
175	97.5	0.2	0.4
176	97.9	0.4	0.4
177	98.5	0.6	0.42
178	98.8	0.3	0.52
179	99.4	0.6	0.54
180	100.1	0.7	0.525

Name	X	Y	Ele. (m)	DMEER
Koper – Dekani	45.5414	13.8330	65	Illyrian deciduous forests

2011 HBNF	Day	Weight (KG)
NF Start	118	49.2
NF End	135	74.6
NF Duration	17	25.4
Quarter		6.35
25% Flow	123	55.55
50% Flow	127	61.9
75% Flow	130	68.25



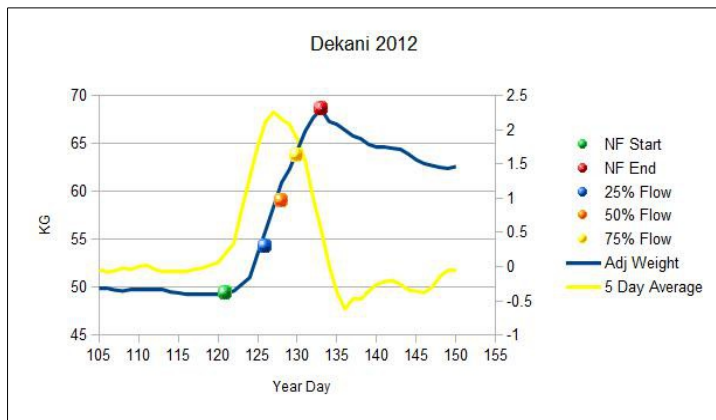
2011 NDVI	Day	Value
SOS	75.2	Base val 4758
End	357.28	Peak val 7774
Length	281.92	Ampl. 3016
Peak t	191.36	L.deriv. 1680
		R.deriv. 487.5
		L.integral 138200
		S.integral 43040



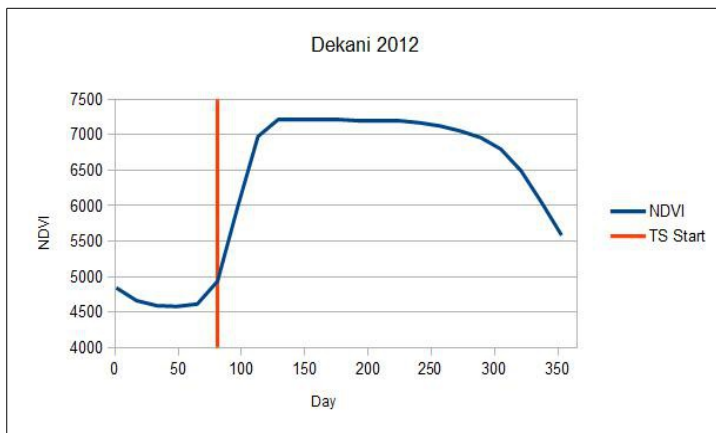
2011			
Day	Adj KG	Adj Day	5 Day Avg
110	49.6	-0.1	-0.12
111	49.5	-0.1	-0.14
112	49.4	-0.1	-0.1
113	49.3	-0.1	-0.1
114	49.2	-0.1	-0.12
115	49.1	-0.1	-0.1
116	48.9	-0.2	-0.02
117	48.9	0	0.22
118	49.2	0.3	0.46
119	50.3	1.1	0.86
120	51.4	1.1	1.28
121	53.2	1.8	1.68
122	55.3	2.1	1.66
123	57.6	2.3	1.7
124	58.6	1	1.66
125	59.9	1.3	1.62
126	61.5	1.6	1.6
127	63.4	1.9	1.86
128	65.6	2.2	2.1
129	67.9	2.3	2.14
130	70.4	2.5	2.02
131	72.2	1.8	1.8
132	73.5	1.3	1.44
133	74.6	1.1	0.84
134	75.1	0.5	0.46
135	74.6	-0.5	0.24
136	74.5	-0.1	0.12
137	74.7	0.2	0.02
138	75.2	0.5	0.06
139	75.2	0	0.1
140	74.9	-0.3	-0.04
141	75	0.1	-0.14
142	74.5	-0.5	-0.12
143	74.5	0	-0.06
144	74.6	0.1	-0.04
145	74.6	0	0.08
146	74.8	0.2	-0.02
147	74.9	0.1	-0.06
148	74.4	-0.5	-0.04
149	74.3	-0.1	0.02
150	74.4	0.1	0.1
151	74.9	0.5	0.06
152	75.4	0.5	0.16

Name	X	Y	Ele. (m)	DMEER
Koper – Dekani	45.5414	13.8330	65	Illyrian deciduous forests

2012 HBNF	Day	Weight (KG)
NF Start	121	49.4
NF End	133	68.6
NF Duration	12	19.2
Quarter		4.8
25% Flow	126	54.2
50% Flow	128	59
75% Flow	130	63.8



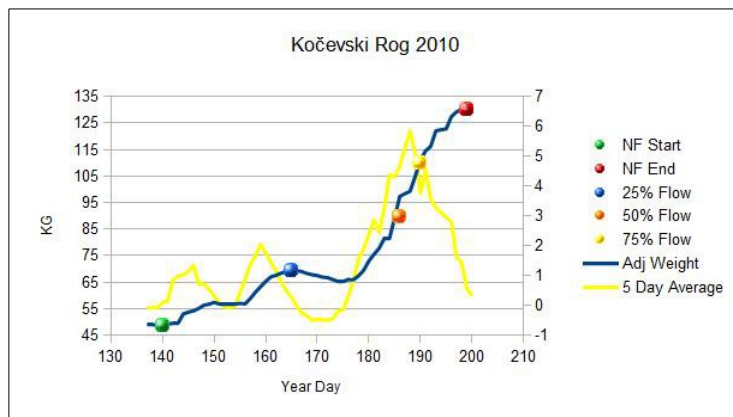
2012 NDVI	Day	Value
SOS	80.64	Base val
End	365.28	Peak val
Length	284.64	Ampl.
Peak t	206.56	L.deriv.
		R.deriv.
		L.integral
		S.integral



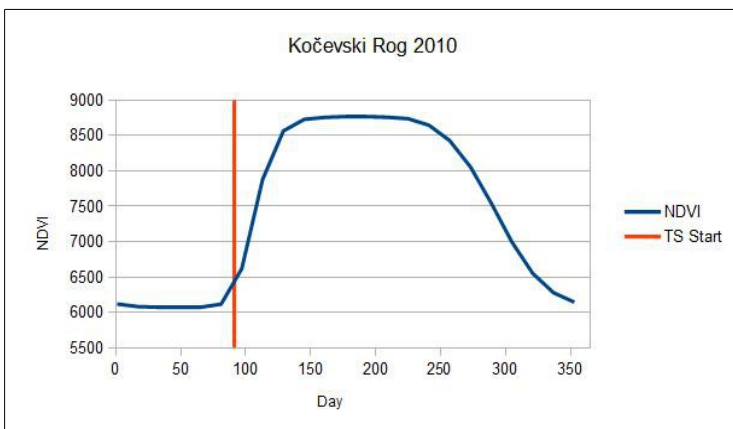
2012			
Day	Adj KG	Adj Day	5 Day Avg
105	49.9	-0.1	-0.04
106	49.9	0	-0.08
107	49.7	-0.2	-0.06
108	49.6	-0.1	-0.02
109	49.7	0.1	-0.04
110	49.8	0.1	0
111	49.7	-0.1	0.02
112	49.7	0	-0.04
113	49.7	0	-0.08
114	49.5	-0.2	-0.08
115	49.4	-0.1	-0.08
116	49.3	-0.1	-0.08
117	49.3	0	-0.04
118	49.3	0	-0.02
119	49.3	0	0.02
120	49.3	0	0.06
121	49.4	0.1	0.2
122	49.6	0.2	0.34
123	50.3	0.7	0.84
124	51	0.7	1.3
125	53.5	2.5	1.76
126	55.9	2.4	2.12
127	58.4	2.5	2.26
128	60.9	2.5	2.16
129	62.3	1.4	2.08
130	64.3	2	1.86
131	66.3	2	1.54
132	67.7	1.4	1
133	68.6	0.9	0.54
134	67.3	-1.3	0.02
135	67	-0.3	-0.38
136	66.4	-0.6	-0.62
137	65.8	-0.6	-0.48
138	65.5	-0.3	-0.48
139	64.9	-0.6	-0.36
140	64.6	-0.3	-0.26
141	64.6	0	-0.22
142	64.5	-0.1	-0.2
143	64.4	-0.1	-0.26
144	63.9	-0.5	-0.34

Name	X	Y	Ele. (m)	DMEER
Kočevski Rog	45.7086	15.0293	535	Pannonian mixed forests

2010 HBNF	Day	Weight (KG)
NF Start	140	48.8
NF End	199	130.2
NF Duration	59	81.4
Quarter		20.35
25% Flow	165	69.15
50% Flow	186	89.5
75% Flow	190	109.85



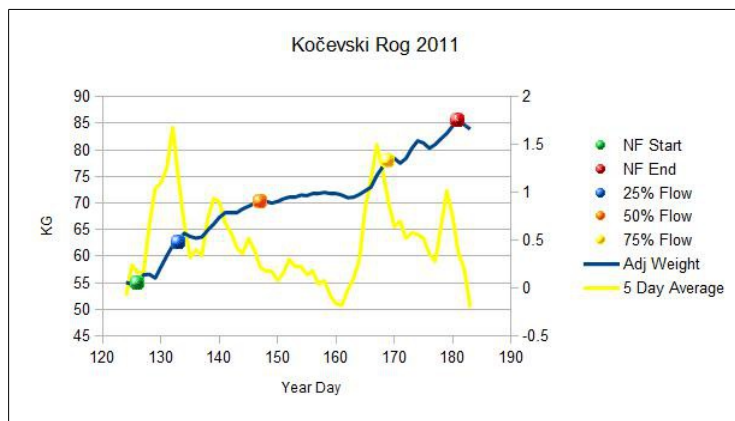
2010 NDVI	Year Day	Value
SOS	91.36	Base val 6075
End	324	Peak val 8760
Length	192.48	Ampl. 2685
Peak t	208.48	L.deriv. 1059
		R.deriv. 487.2
		L.integral 134200
		S.integral 30900



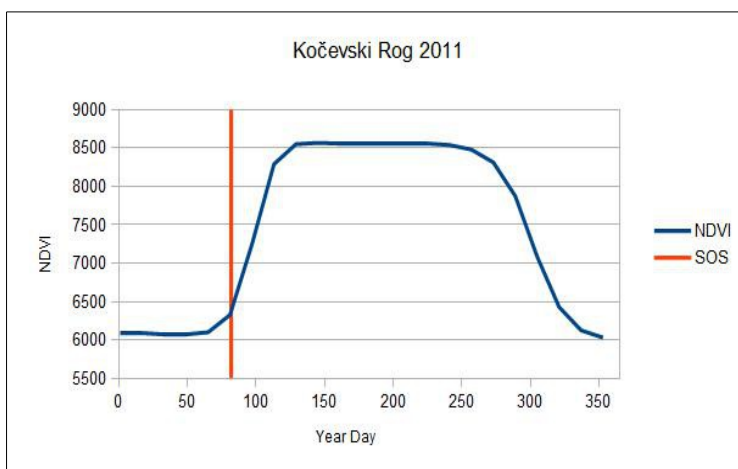
2010			
Day	Adj KG	Adj Day	5 Day Avg
137	48.9	-0.5	-0.1
138	48.9	0	-0.06
139	48.8	-0.1	-0.06
140	48.8	0	0.1
141	49.1	0.3	0.14
142	49.4	0.3	0.84
143	49.6	0.2	0.98
144	53	3.4	1.02
145	53.7	0.7	1.14
146	54.2	0.5	1.34
147	55.1	0.9	0.74
148	56.3	1.2	0.74
149	56.7	0.4	0.54
150	57.4	0.7	0.32
151	56.9	-0.5	0.1
152	56.7	-0.2	-0.04
153	56.8	0.1	-0.08
154	56.5	-0.3	-0.02
155	57	0.5	0.42
156	56.8	-0.2	0.88
157	58.8	2	1.36
158	61.2	2.4	1.66
159	63.3	2.1	2.04
160	65.3	2	1.76
161	67	1.7	1.44
162	67.6	0.6	1.16
163	68.4	0.8	0.78
164	69.1	0.7	0.48
165	69.2	0.1	0.28
166	69.4	0.2	-0.02
167	69	-0.4	-0.26
168	68.3	-0.7	-0.34
169	67.8	-0.5	-0.5
170	67.5	-0.3	-0.46
171	66.9	-0.6	-0.46
172	66.7	-0.2	-0.5
173	66	-0.7	-0.46
174	65.3	-0.7	-0.18
175	65.2	-0.1	-0.16
176	66	0.8	0.28
177	65.9	-0.1	0.84
178	67.4	1.5	1.56
179	69.5	2.1	1.9
180	73	3.5	2.38
181	75.5	2.5	2.86
182	77.8	2.3	2.44
183	81.7	3.9	3.24
184	81.7	0	4.38
185	89.2	7.5	4.3
186	97.4	8.2	4.66
188	99.3	1.9	5.86
189	105	5.7	5.06
190	111	6	3.76
191	114.5	3.5	4.56
192	116.2	1.7	3.56
193	122.1	5.9	3.28
195	122.8	0.7	2.94
196	127.4	4.6	2.8
197	129.2	1.8	1.62
198	130.2	1	1.42
199	130.2	0	0.56
200	129.9	-0.3	0.32

Name	X	Y	Ele. (m)	DMEER
Kočevski Rog	45.7086	15.0293	535	Pannonian mixed forests

2011 HBNF	Day	Weight (KG)
NF Start	126	54.9
NF End	181	85.4
NF Duration	55	30.5
Quarter		7.625
25% Flow	133	62.525
50% Flow	147	70.15
75% Flow	169	77.775



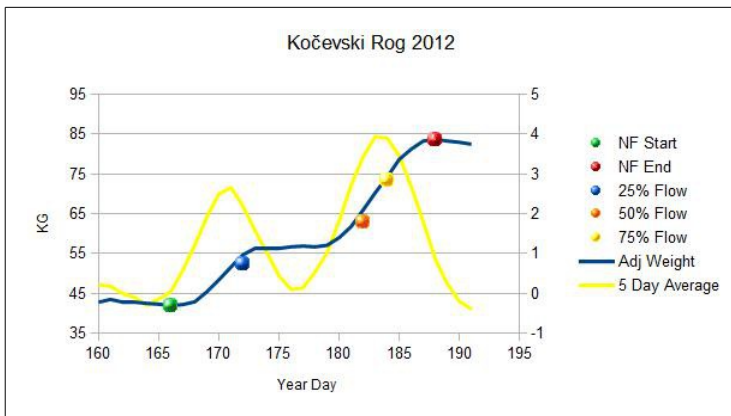
2011 NDVI	Year Day	Value
SOS	82.24	Base val 6042
End	322.08	Peak val 8567
Length	240	Ampl. 2525
Peak t	195.04	L.deriv. 982.2
		R.deriv. 675.7
		L.integral 134600
		S.integral 31910



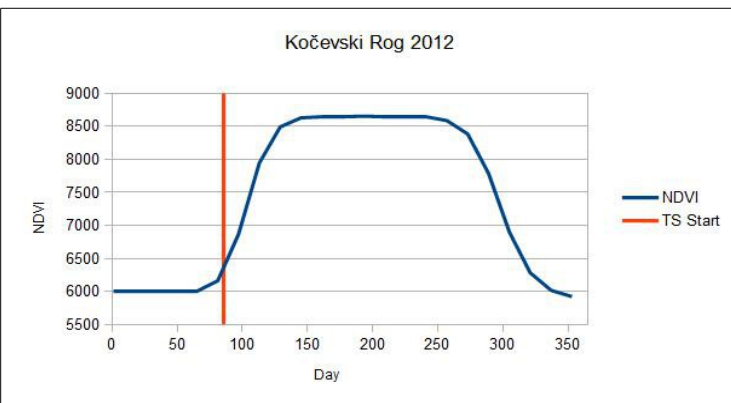
2011			
Day	Adj KG	Adj Day	5 Day Avg
124	55.1	-0.7	-0.08
125	54.7	-0.4	0.24
126	54.9	0.2	0.16
127	56.5	1.6	0.16
128	56.6	0.1	0.66
129	55.9	-0.7	1.04
130	58	2.1	1.1
131	60.1	2.1	1.26
132	62	1.9	1.68
133	62.9	0.9	1.14
134	64.3	1.4	0.66
135	63.7	-0.6	0.32
136	63.4	-0.3	0.4
137	63.6	0.2	0.34
138	64.9	1.3	0.72
139	66	1.1	0.94
140	67.3	1.3	0.9
141	68.1	0.8	0.68
142	68.1	0	0.58
143	68.3	0.2	0.42
144	68.9	0.6	0.36
145	69.4	0.5	0.52
146	69.9	0.5	0.4
147	70.7	0.8	0.22
148	70.3	-0.4	0.18
149	70	-0.3	0.18
150	70.3	0.3	0.08
151	70.8	0.5	0.16
152	71.1	0.3	0.3
153	71.1	0	0.22
154	71.5	0.4	0.22
155	71.4	-0.1	0.14
156	71.9	0.5	0.18
157	71.8	-0.1	0.04
158	72	0.2	0.08
159	71.7	-0.3	-0.08
160	71.8	0.1	-0.16
161	71.5	-0.3	-0.18
162	71	-0.5	-0.02
163	71.1	0.1	0.1
164	71.6	0.5	0.3
165	72.3	0.7	0.84
166	73	0.7	1.14
167	75.2	2.2	1.5
168	76.8	1.6	1.22
169	79.1	2.3	0.9
170	78.4	-0.7	0.64
171	77.5	-0.9	0.7
172	78.4	0.9	0.52
173	80.3	1.9	0.58
174	81.7	1.4	0.56
175	81.3	-0.4	0.52
176	80.3	-1	0.36
177	81	0.7	0.28
178	82.1	1.1	0.64
179	83.1	1	1.02
180	84.5	1.4	0.74
181	85.4	0.9	0.36
182	84.7	-0.7	0.2

Name	X	Y	Ele. (m)	DMEER
Kočevski Rog	45.7086	15.0293	535	Pannonian mixed forests

2012 HBNF	Day	Weight (KG)
NF Start	166	42
NF End	188	83.7
NF Duration	22	41.7
Quarter		10.425
25% Flow	172	52.425
50% Flow	182	62.85
75% Flow	184	73.275



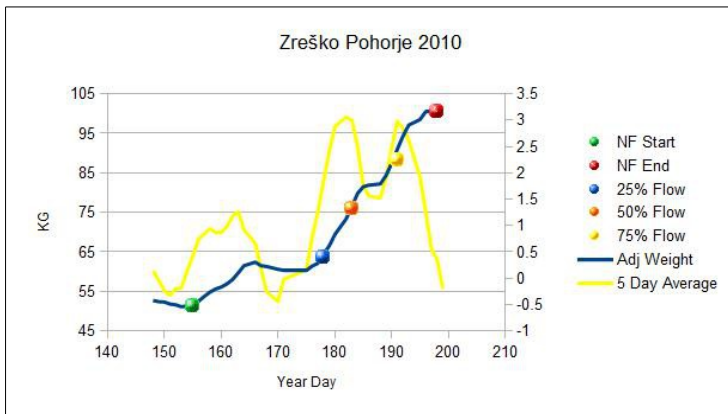
2012 NDVI	Day	Value
SOS	85.44	Base val 5942
End	319.68	Peak val 8654
Length	234.24	Ampl. 2712
Peak t	198.4	L.deriv. 883.9
		R.deriv. 731.3
		L.integral 127900
		S.integral 32870



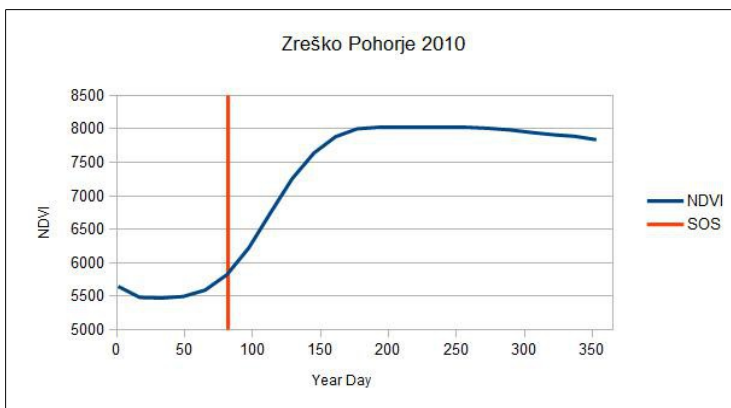
2012			
Day	Adj KG	Adj Day	5 Day Avg
150	41.6	0	0.08
151	41.7	0.1	0.06
152	42	0.3	0
153	41.9	-0.1	0.04
154	41.6	-0.3	0.04
155	41.8	0.2	-0.04
156	41.9	0.1	-0.02
157	41.8	-0.1	0.18
158	41.8	0	0.2
159	42.5	0.7	0.32
160	42.8	0.3	0.22
161	43.5	0.7	0.18
162	42.9	-0.6	0
163	42.7	-0.2	-0.1
164	42.5	-0.2	-0.3
165	42.3	-0.2	-0.14
166	42	-0.3	0.04
167	42.2	0.2	0.58
168	42.9	0.7	1.22
169	45.4	2.5	1.92
170	48.4	3	2.5
171	51.6	3.2	2.66
172	54.7	3.1	2.2
173	56.2	1.5	1.58
174	56.4	0.2	1.02
175	56.3	-0.1	0.44
176	56.7	0.4	0.1
177	56.9	0.2	0.14
178	56.7	-0.2	0.54
179	57.1	0.4	1.02
180	59	1.9	1.82
181	61.8	2.8	2.72
182	66	4.2	3.44
183	70.3	4.3	3.94
184	74.3	4	3.9
185	78.7	4.4	3.46
186	81.3	2.6	2.68
187	83.3	2	1.8
188	83.7	0.4	0.86
189	83.3	-0.4	0.24
190	83	-0.3	-0.2
191	82.5	-0.5	-0.4

Name	X	Y	Ele. (m)	DMEER
Zreško Pohorje	46.440	15.351	1143	Alps conifer and mixed forests

2010 HBNF	Day	Weight (KG)
NF Start	155	51.4
NF End	198	100.6
NF Duration	43	49.2
Quarter		12.3
25% Flow	178	63.7
50% Flow	183	76
75% Flow	191	88.3



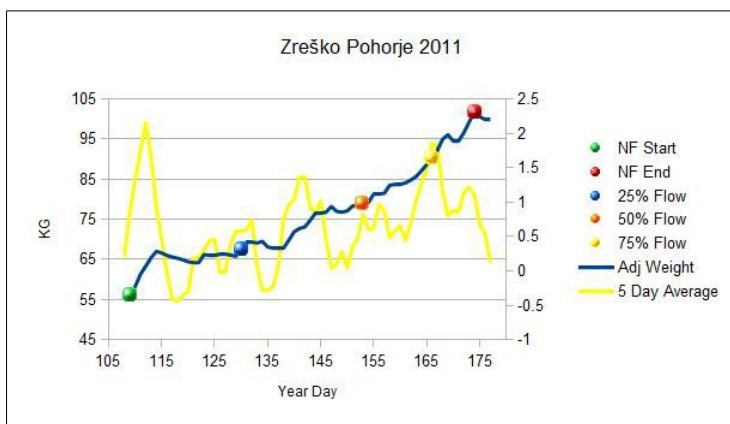
2010 NDVI	Year Day	Value
SOS	81.44	Base val
End	405.28	Peak val
Length	324	Ampl.
Peak t	254.08	L.deriv.
		R.deriv.
		L.integral
		S.integral



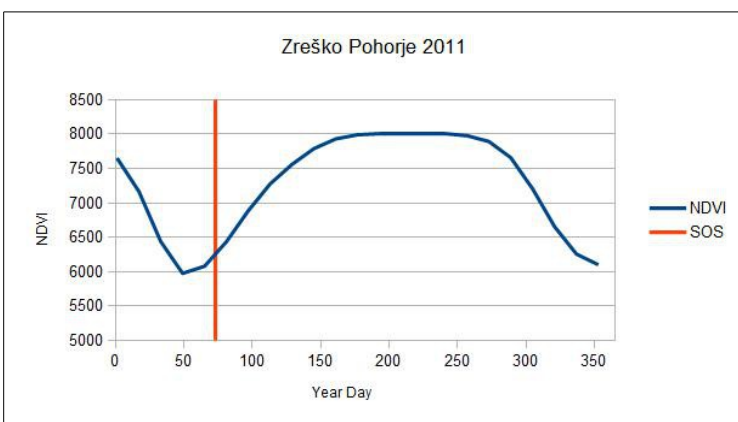
Day	Adj KG	Adj Day	5 Day Avg
148	52.7	-0.1	0.14
149	52.4	-0.3	-0.04
150	52.3	-0.1	-0.24
151	51.8	-0.5	-0.32
152	51.6	-0.2	-0.2
153	51.1	-0.5	-0.18
154	51.4	0.3	0.14
155	51.4	0	0.42
156	52.5	1.1	0.74
157	53.7	1.2	0.84
158	54.8	1.1	0.94
159	55.6	0.8	0.88
160	56.1	0.5	0.86
161	56.9	0.8	0.98
162	58	1.1	1.18
163	59.7	1.7	1.26
164	61.5	1.8	0.92
166	62.4	0.9	0.66
167	61.5	-0.9	0.18
168	61.3	-0.2	-0.26
170	60.6	-0.7	-0.44
171	60.2	-0.4	-0.02
175	60.2	0	0.16
176	61.4	1.2	0.78
177	62.1	0.7	1.26
178	64.5	2.4	1.84
179	66.5	2	2.4
180	69.4	2.9	2.88
182	73.4	4	3.06
183	76.5	3.1	3
184	79.8	3.3	2.5
185	81.5	1.7	1.76
186	81.9	0.4	1.56
188	82.2	0.3	1.52
189	84.3	2.1	1.9
190	87.4	3.1	2.48
191	91	3.6	2.98
192	94.3	3.3	2.84
193	97.1	2.8	2.62
195	98.5	1.4	1.92
196	100.5	2	1.26
197	100.6	0.1	0.56
198	100.6	0	0.35
199	99.9	-0.7	-0.2

Name	X	Y	Ele. (m)	DMEER
Zreško Pohorje	46.440	15.351	1143	Alps conifer and mixed forests

2011 HBNF	Year Day	Weight (KG)
NF Start	109	56.2
NF End	174	101.8
NF Duration	65	45.6
Quarter		11.4
25% Flow	130	67.6
50% Flow	153	79
75% Flow	166	90.4



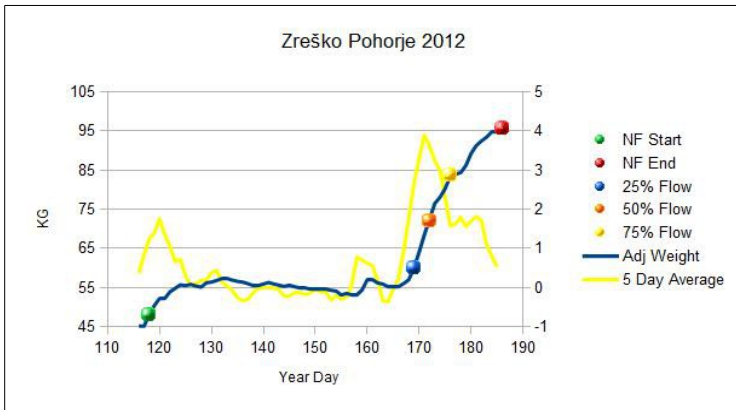
2011 NDVI	Year Day	Value
SOS	72.96	Base val 6031
End	331.04	Peak val 8002
Length	258.08	Ampl. 1971
Peak t	209.92	L.deriv. 367.1
		R.deriv. 483.4
		L.integral 133600
		S.integral 25010



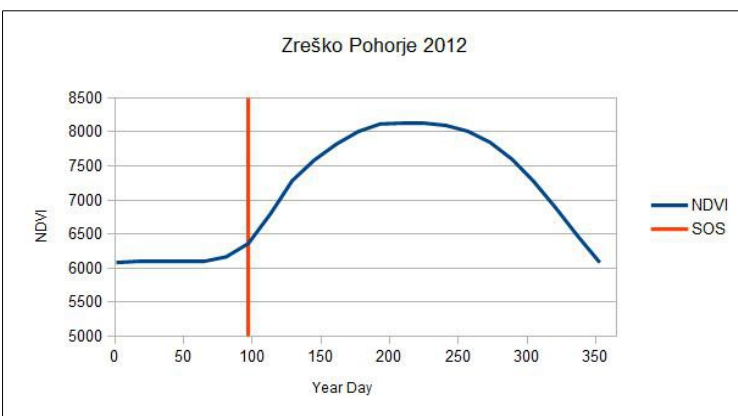
2011			
Day	Adj KG	Adj Day	5 Day Avg
108	56.7	0	0.2
109	56.2	-0.5	0.86
110	58.2	2	1.32
111	61.3	3.1	1.74
112	63.3	2	2.16
113	65.4	2.1	1.68
114	67	1.6	0.94
115	66.6	-0.4	0.46
116	66	-0.6	-0.02
117	65.6	-0.4	-0.42
118	65.3	-0.3	-0.44
119	64.9	-0.4	-0.36
120	64.4	-0.5	-0.3
121	64.2	-0.2	0.18
122	64.1	-0.1	0.2
123	66.2	2.1	0.3
124	65.9	-0.3	0.44
125	65.9	0	0.46
126	66.4	0.5	-0.02
127	66.4	0	-0.02
128	66.1	-0.3	0.38
129	65.8	-0.3	0.58
130	67.8	2	0.58
131	69.3	1.5	0.6
132	69.3	0	0.74
133	69.1	-0.2	0.06
134	69.5	0.4	-0.28
135	68.1	-1.4	-0.28
136	67.9	-0.2	-0.24
137	67.9	0	0.06
138	67.9	0	0.76
139	69.8	1.9	0.96
140	71.9	2.1	1.04
141	72.7	0.8	1.36
142	73.1	0.4	1.36
143	74.7	1.6	0.94
144	76.6	1.9	0.82
145	76.6	0	1.02
146	76.8	0.2	0.46
147	78.2	1.4	0.04
148	77	-1.2	0.1
149	76.8	-0.2	0.28
150	77.1	0.3	0.04
151	78.2	1.1	0.34
152	78.4	0.2	0.48
153	78.7	0.3	0.82
154	79.2	0.5	0.6
155	81.2	2	0.62
156	81.2	0	0.96
157	81.5	0.3	0.88
158	83.5	2	0.48
159	83.6	0.1	0.58
160	83.6	0	0.66
161	84.1	0.5	0.44
162	84.8	0.7	0.7
163	85.7	0.9	1.02
164	87.1	1.4	1.28
165	88.7	1.6	1.48
166	90.5	1.8	1.86
167	92.2	1.7	1.8
168	95	2.8	1.16
169	96.1	1.1	0.8
170	94.5	-1.6	0.88
171	94.5	0	0.86
172	96.6	2.1	1.14
173	99.3	2.7	1.22
174	101.8	2.5	1.1
175	100.6	-1.2	0.68

Name	X	Y	Ele. (m)	DMEER
Zreško Pohorje	46.440	15.351	1143	Alps conifer and mixed forests

2012 HBNF	Day	Weight (KG)
NF Start	118	48
NF End	186	95.8
NF Duration	68	47.8
Quarter		11.95
25% Flow	169	59.95
50% Flow	172	71.9
75% Flow	176	83.85



2012 NDVI	Year Day	Value
SOS	97.28	Base val 5784
End	363.36	Peak val 8136
Length	265.92	Ampl. 2353
Peak t	220.64	L.deriv. 373.6
		R.deriv. 372.2
		L.integral 132300
		S.integral 28170

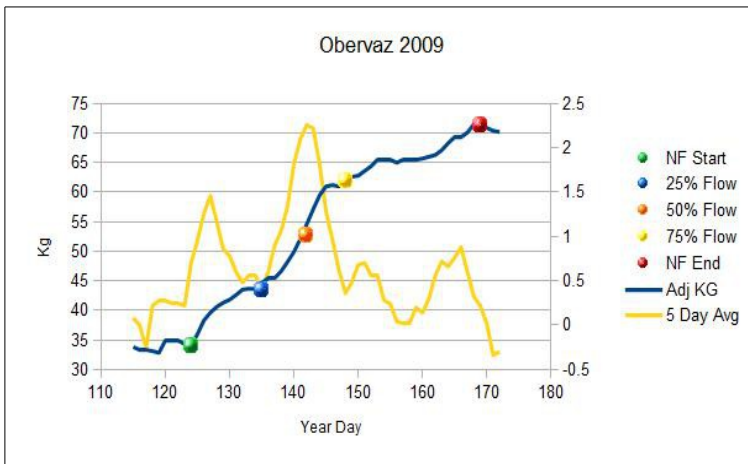


2012			
Day	Adj KG	Adj Day	5 Day Avg
117	45.1	-0.1	0.84
118	48	2.9	1.24
119	50.4	2.4	1.4
120	52.2	1.8	1.76
121	52.2	0	1.36

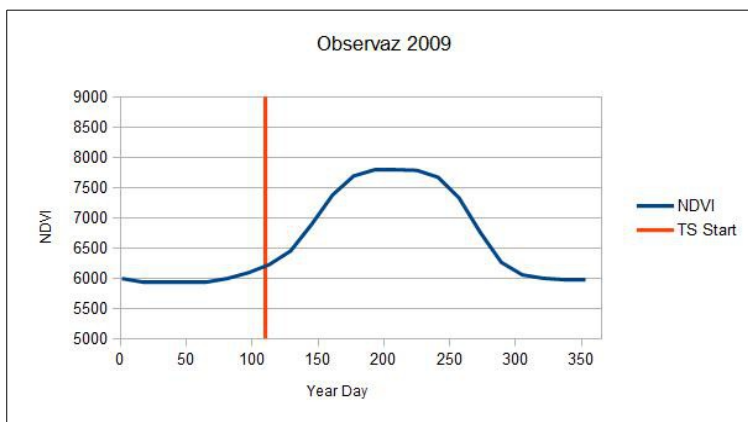
122	53.9	1.7	1.06
123	54.8	0.9	0.66
124	55.7	0.9	0.72
125	55.5	-0.2	0.3
126	55.8	0.3	0.06
127	55.4	-0.4	0.1
128	55.1	-0.3	0.18
129	56.2	1.1	0.2
130	56.4	0.2	0.38
131	56.8	0.4	0.44
132	57.3	0.5	0.14
133	57.3	0	0.04
134	56.9	-0.4	-0.08
135	56.6	-0.3	-0.26
136	56.4	-0.2	-0.34
137	56	-0.4	-0.3
138	55.6	-0.4	-0.14
139	55.4	-0.2	-0.02
140	55.9	0.5	-0.02
141	56.3	0.4	0
142	55.9	-0.4	-0.02
143	55.6	-0.3	-0.06
144	55.3	-0.3	-0.22
145	55.6	0.3	-0.22
146	55.2	-0.4	-0.14
147	54.8	-0.4	-0.14
148	54.9	0.1	-0.18
149	54.6	-0.3	-0.14
150	54.7	0.1	-0.04
151	54.5	-0.2	-0.12
152	54.6	0.1	-0.1
153	54.3	-0.3	-0.32
154	54.1	-0.2	-0.2
155	53.1	-1	-0.3
156	53.5	0.4	-0.24
157	53.1	-0.4	0.06
158	53.1	0	0.78
159	54.4	1.3	0.7
160	57	2.6	0.62
161	57	0	0.56
162	56.2	-0.8	0.18
163	55.9	-0.3	-0.34
164	55.3	-0.6	-0.36
165	55.3	0	-0.04
166	55.2	-0.1	0.22
167	56	0.8	0.94
168	57	1	1.76
169	60	3	2.66
170	64.1	4.1	3.3
171	68.5	4.4	3.9
172	72.5	4	3.62
173	76.5	4	3.24
174	78.1	1.6	3
175	80.3	2.2	2.3
176	83.5	3.2	1.58
177	84	0.5	1.62
178	84.4	0.4	1.8
179	86.2	1.8	1.56
180	89.3	3.1	1.7
181	91.3	2	1.82
182	92.5	1.2	1.7
183	93.5	1	1.08
184	94.7	1.2	0.8
185	94.7	0	0.54
186	95.3	0.6	0.28

Name	X	Y	Ele. (m)	DMEER
Vaz/Obervaz	46.7151	9.5376	1162	Alps conifer and mixed forests

2009 HBNF		Day	Weight (KG)
NF Start		124	34
NF End		169	71.3
NF Duration		45	37.3
Quarter			9.325
25% Flow		132	43.325
50% Flow		142	52.65
75% Flow		148	61.975



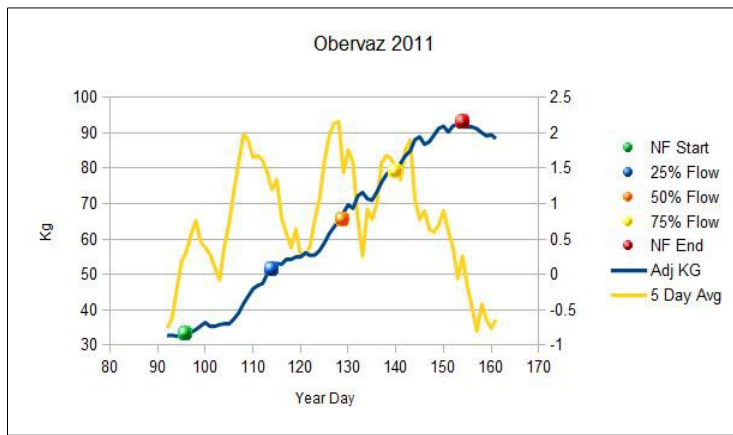
2009 NDVI		Year Day	Value
TS Start 15%		110.032	Base val 5947
End 15%		289.12	Peak val 7797
Length		11.2	Ampl. 1850
Peak t		206.72	L.deriv. 400.1
			R.deriv. 507.4
			L.integral 98130
			S.integral 14870



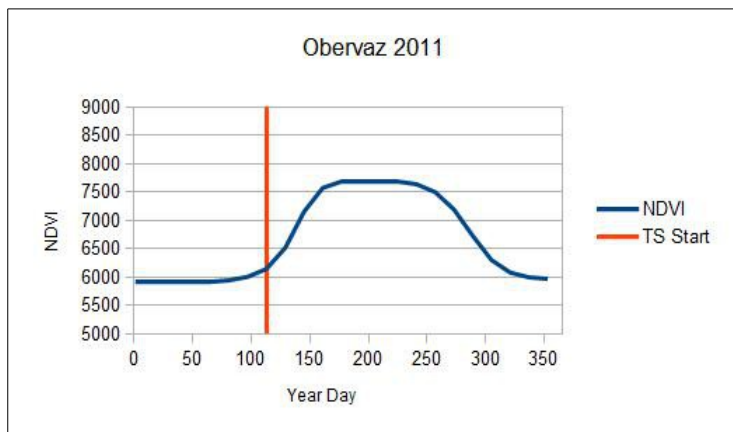
2009			
Day	Adj KG	Adj Day	5 Day Avg
109	33.1	0	-0.08
110	33.1	0	-0.04
111	33.1	0	0
112	33	-0.1	0.2
113	33.1	0.1	0.14
114	34.1	1	0.06
115	33.8	-0.3	0.08
116	33.4	-0.4	0
117	33.4	0	-0.26
118	33.1	-0.3	0.22
119	32.8	-0.3	0.28
120	34.9	2.1	0.28
121	34.8	-0.1	0.24
122	34.8	0	0.24
123	34.3	-0.5	0.22
124	34	-0.3	0.7
125	36	2	0.96
126	38.3	2.3	1.26
127	39.6	1.3	1.46
128	40.6	1	1.16
129	41.3	0.7	0.86
130	41.8	0.5	0.78
131	42.6	0.8	0.6
132	43.5	0.9	0.48
133	43.6	0.1	0.56
134	43.7	0.1	0.56
135	44.6	0.9	0.4
136	45.4	0.8	0.6
137	45.5	0.1	0.9
138	46.6	1.1	1.06
139	48.2	1.6	1.34
140	49.9	1.7	1.82
141	52.1	2.2	2.1
142	54.6	2.5	2.26
143	57.1	2.5	2.22
144	59.5	2.4	1.82
145	61	1.5	1.28
146	61.2	0.2	0.96
147	61	-0.2	0.62
148	61.9	0.9	0.36
149	62.6	0.7	0.48
150	62.8	0.2	0.68
151	63.6	0.8	0.7
152	64.4	0.8	0.56
153	65.4	1	0.56
154	65.4	0	0.28
155	65.6	0.2	0.24
156	65	-0.6	0.04
157	65.6	0.6	0.02
158	65.6	0	0.02
159	65.5	-0.1	0.2
160	65.7	0.2	0.14
161	66	0.3	0.3
162	66.3	0.3	0.56
163	67.1	0.8	0.72
164	68.3	1.2	0.66
165	69.3	1	0.76
166	69.3	0	0.88
167	70.1	0.8	0.6
168	71.5	1.4	0.32
169	71.3	-0.2	0.22
170	70.9	-0.4	0.02
171	70.4	-0.5	-0.34
172	70.2	-0.2	-0.3

Name	X	Y	Ele. (m)	DMEER
Vaz/Obervaz	46.715	9.538	1162	Alps conifer and mixed forests

2011 HBNF	Day	Weight (KG)
NF Start	96	33.1
NF End	154	93.2
NF Duration	48	55.8
Quarter		13.95
25% Flow	114	51.35
50% Flow	129	65.3
75% Flow	140	79.25



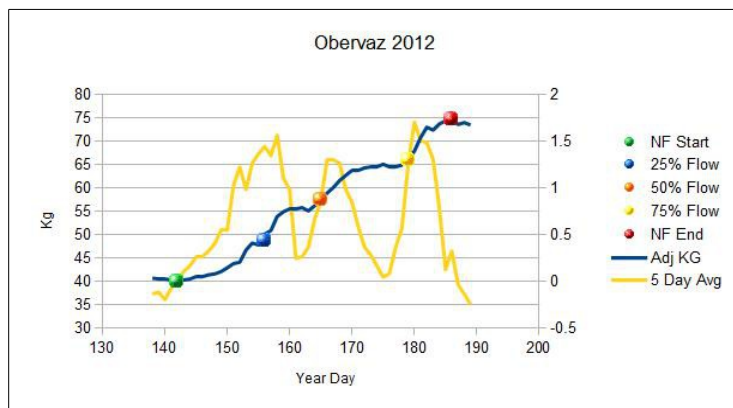
2011 NDVI	Year Day	Value
SOS	113.6	Base val 5934
End	309.92	Peak val 7690
Length	196.32	Ampl. 1756
Peak t	207.52	L.deriv. 508
		R.deriv. 417.8
		L.integral 99550
		S.integral 16470



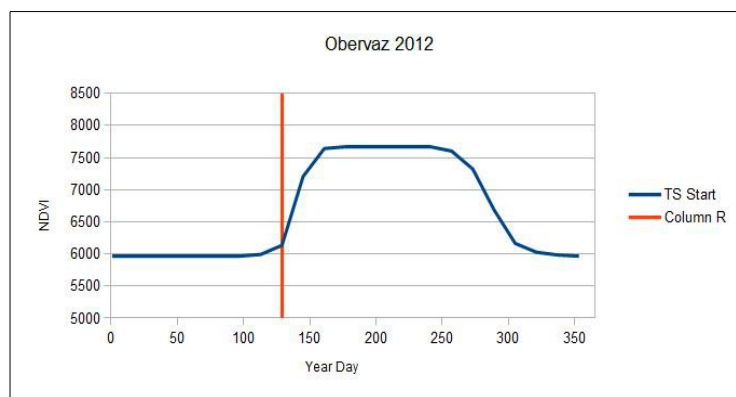
2011				
Day	Adj KG	Adj Day	5 Day Avg	
90	35.7	-0.7	-0.82	
91	34.2	-1.5	-0.78	
92	32.7	-1.5	-0.76	
93	32.8	0.1	-0.62	
94	32.6	-0.2	-0.22	
95	32.6	0	0.18	
96	33.1	0.5	0.32	
97	33.6	0.5	0.56	
98	34.4	0.8	0.76	
99	35.4	1	0.46	
100	36.4	1	0.38	
101	35.4	-1	0.28	
102	35.5	0.1	0.1	
103	35.8	0.3	-0.08	
104	35.9	0.1	0.4	
105	36	0.1	0.72	
106	37.4	1.4	1.18	
107	39.1	1.7	1.58	
108	41.7	2.6	1.98	
109	43.8	2.1	1.9	
110	45.9	2.1	1.66	
111	46.9	1	1.68	
112	47.4	0.5	1.62	
113	50.1	2.7	1.44	
114	51.9	1.8	1.2	
115	53.1	1.2	1.34	
116	52.9	-0.2	0.8	
117	54.1	1.2	0.58	
118	54.1	0	0.38	
119	54.8	0.7	0.64	
120	55	0.2	0.26	
121	56.1	1.1	0.28	
122	55.4	-0.7	0.4	
123	55.5	0.1	0.78	
124	56.8	1.3	1.08	
125	58.9	2.1	1.6	
126	61.5	2.6	1.96	
127	63.4	1.9	2.14	
128	65.3	1.9	2.16	
129	67.5	2.2	1.44	
130	69.7	2.2	1.76	
131	68.7	-1	1.58	
132	72.2	3.5	0.78	
133	73.2	1	0.26	
134	71.4	-1.8	0.92	
135	71	-0.4	0.78	
136	73.3	2.3	1	
137	76.1	2.8	1.58	
138	78.2	2.1	1.68	
139	79.3	1.1	1.64	
140	79.4	0.1	1.5	
141	81.5	2.1	1.34	
142	83.6	2.1	1.76	
143	84.9	1.3	1.9	
144	88.1	3.2	1.06	
145	88.9	0.8	0.78	
146	86.8	-2.1	0.9	
147	87.5	0.7	0.64	
148	89.4	1.9	0.6	
149	91.3	1.9	0.7	
150	91.9	0.6	0.9	
151	90.3	-1.6	0.62	
152	92	1.7	0.38	
153	92.5	0.5	-0.06	
154	93.2	0.7	0.26	
155	91.6	-1.6	-0.16	
156	91.6	0	-0.48	
157	91.2	-0.4	-0.8	

Name	X	Y	Ele. (m)	DMEER
Vaz/Obervaz	46.715	9.538	1162	Alps conifer and mixed forests

2012 HBNF	Day	Weight (KG)
NF Start	142	40
NF End	186	74.6
NF Duration	44	34.6
Quarter		8.65
25% Flow	156	48.65
50% Flow	165	57.3
75% Flow	179	65.95



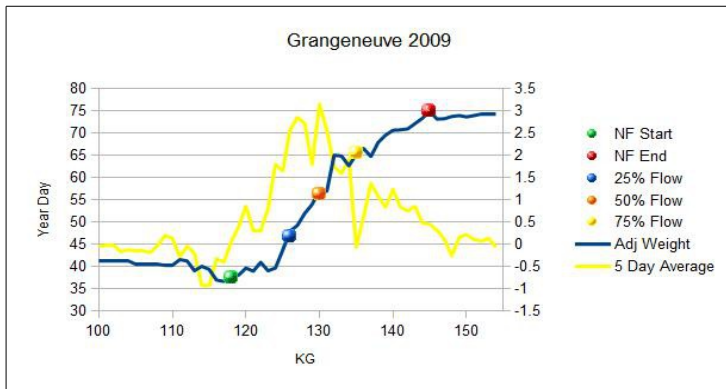
2012 NDVI	Year Day	Value
TS Start 15%	129.12	Base val 5934
End 15%	302.24	Peak val 7690
Length	172.96	Ampl. 1756
Peak t	225.92	L.deriv. 508
		R.deriv. 417.8
		L.integral 99550
		S.integral 16470



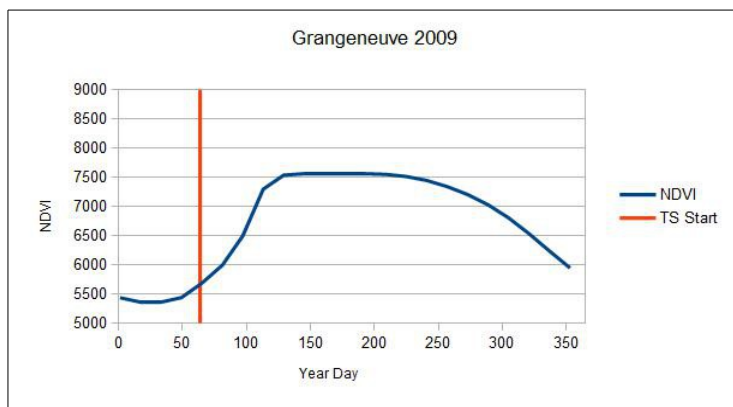
2012			
Day	Adj KG	Adj Day	5 Day Avg
124	41.4	0	0.02
125	41.5	0.1	0
126	41.4	-0.1	-0.04
127	41.3	-0.1	0
128	41.2	-0.1	0
129	41.4	0.2	0.04
130	41.5	0.1	0
131	41.6	0.1	0
132	41.3	-0.3	-0.06
133	41.2	-0.1	-0.1
134	41.1	-0.1	-0.16
135	41	-0.1	-0.06
136	40.8	-0.2	-0.12
137	41	0.2	-0.14
138	40.6	-0.4	-0.14
139	40.4	-0.2	-0.12
140	40.3	-0.1	-0.2
141	40.2	-0.1	-0.08
142	40	-0.2	0
143	40.2	0.2	0.1
144	40.4	0.2	0.16
145	40.8	0.4	0.26
146	41	0.2	0.26
147	41.3	0.3	0.32
148	41.5	0.2	0.4
149	42	0.5	0.54
150	42.8	0.8	0.54
151	43.7	0.9	1.02
152	44	0.3	1.22
153	46.6	2.6	0.98
154	48.1	1.5	1.26
155	47.7	-0.4	1.36
156	50	2.3	1.44
157	50.8	0.8	1.34
158	53.8	3	1.56
159	54.8	1	1.1
160	55.5	0.7	0.98
161	55.5	0	0.24
162	55.7	0.2	0.26
163	55	-0.7	0.36
164	56.1	1.1	0.66
165	57.3	1.2	0.86
166	58.8	1.5	1.3
167	60	1.2	1.3
168	61.5	1.5	1.26
169	62.6	1.1	0.98
170	63.6	1	0.84
171	63.7	0.1	0.58
172	64.2	0.5	0.36
173	64.4	0.2	0.28
174	64.4	0	0.16
175	65	0.6	0.04
176	64.5	-0.5	0.08
177	64.4	-0.1	0.36
178	64.8	0.4	0.56
179	66.2	1.4	1.24
180	67.8	1.6	1.7
181	70.7	2.9	1.5
182	72.9	2.2	1.48
183	72.3	-0.6	1.3
184	73.6	1.3	0.78
185	74.3	0.7	0.12
186	74.6	0.3	0.32
187	73.5	-1.1	-0.04
188	73.9	0.4	-0.14
189	73.4	-0.5	-0.25
190	73.6	0.2	0.0333333333

Name	X	Y	Ele. (m)	DMEER
Posieux (Grangeneuve)	46.7643	7.0977	670	Western European Broadleaf forests

2009 HBNF	Day	Weight (KG)
NF Start	118	37.5
NF End	145	75
NF Duration	27	37.5
Quarter		9.375
25% Flow	126	46.875
50% Flow	130	56.25
75% Flow	135	65.625



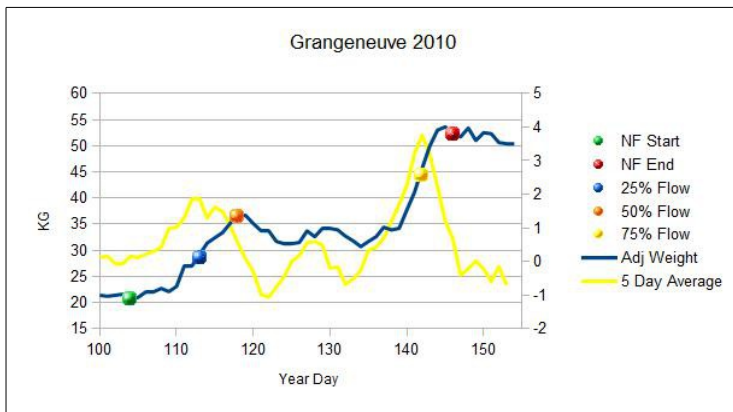
2009 NDVI	Year Day	Value
SOS	64.032	Base val 5430
End	360.64	Peak val 7565
Length	296.64	Ampl. 2135
Peak t	192.48	L.deriv. 547.3
		R.deriv. 255.3
		L.integral 138500
		S.integral 29940



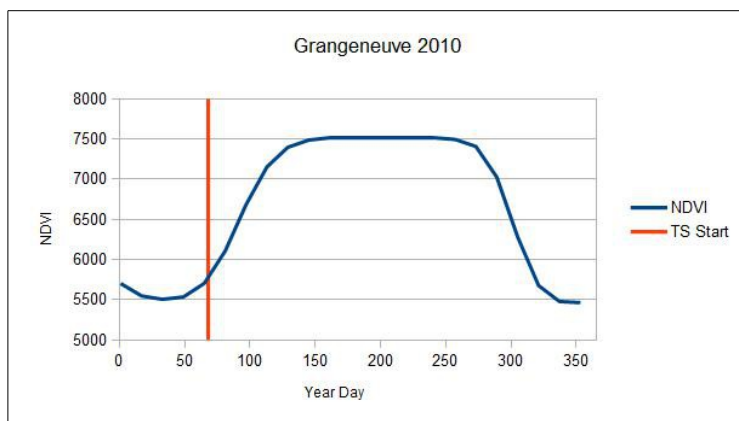
2009			
Day	Adj KG	Adj Day	5 Day Avg
99	41.3	0	-0.075
100	41.3	0	-0.04
101	41.2	-0.1	-0.02
102	41.3	0.1	-0.02
103	41.2	-0.1	-0.16
104	41.2	0	-0.12
105	40.5	-0.7	-0.14
106	40.6	0.1	-0.14
107	40.6	0	-0.18
108	40.5	-0.1	-0.02
109	40.3	-0.2	0.2
110	40.4	0.1	0.14
111	41.6	1.2	-0.28
112	41.3	-0.3	-0.04
113	39.1	-2.2	-0.2
114	40.1	1	-0.92
115	39.4	-0.7	-0.92
116	37	-2.4	-0.32
117	36.7	-0.3	-0.4
118	37.5	0.8	0.06
119	38.1	0.6	0.4
120	39.7	1.6	0.86
121	39	-0.7	0.32
122	41	2	0.32
123	39.1	-1.9	0.8
124	39.7	0.6	1.8
125	43.7	4	1.66
126	48	4.3	2.58
127	49.3	1.3	2.86
128	52	2.7	2.72
129	54	2	1.8
130	57.3	3.3	3.16
131	57	-0.3	2.58
132	65.1	8.1	1.74
133	64.9	-0.2	1.6
134	62.7	-2.2	1.92
135	65.3	2.6	-0.06
136	66.6	1.3	0.62
137	64.8	-1.8	1.38
138	68	3.2	1.08
139	69.6	1.6	0.84
140	70.7	1.1	1.24
141	70.8	0.1	0.84
142	71	0.2	0.76
143	72.2	1.2	0.86
144	73.4	1.2	0.48
145	75	1.6	0.46
146	73.2	-1.8	0.32
147	73.3	0.1	0.12
148	73.8	0.5	-0.26
149	74	0.2	0.16
150	73.7	-0.3	0.22
151	74	0.3	0.12
152	74.4	0.4	0.08
153	74.4	0	0.14

Name	X	Y	Ele. (m)	DMEER
Posieux (Grangeneuve)	46.7643	7.0977	670	Western European Broadleaf forests

2010 HBNF	Day	Weight (KG)
NF Start	104	20.6
NF End	146	52.2
NF Duration	42	31.6
Quarter		7.9
25% Flow	113	28.5
50% Flow	118	36.4
75% Flow	142	44.3



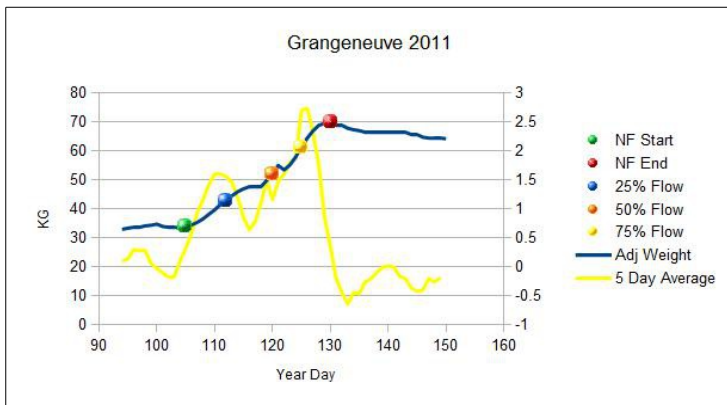
2010 NDVI	Year Day	Value
SOS	68	Base val 5485
End	317.44	Peak val 7513
Length	249.44	Ampl. 2027
Peak t	197.6	L.deriv. 500.3
		R.deriv. 655
		L.integral 119500
		S.integral 26240



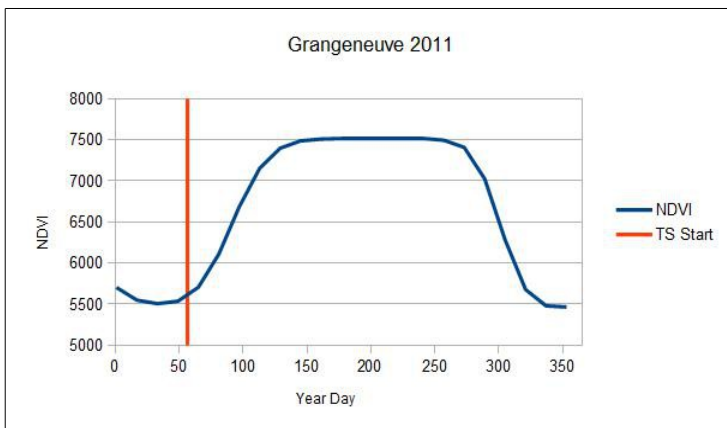
2010			
Day	Adj KG	Adj Day	5 Day Avg
98	20.8	0	-0.16
99	20.9	0.1	-0.12
100	21.4	0.5	0.12
101	21.2	-0.2	0.16
102	21.4	0.2	-0.06
103	21.6	0.2	-0.08
104	20.6	-1	0.16
105	21	0.4	0.12
106	22	1	0.22
107	22	0	0.3
108	22.7	0.7	0.42
109	22.1	-0.6	0.98
110	23.1	1	1.02
111	26.9	3.8	1.3
112	27.1	0.2	1.86
113	29.2	2.1	1.86
114	31.4	2.2	1.3
115	32.4	1	1.62
116	33.4	1	1.48
117	35.2	1.8	1.04
118	36.6	1.4	0.54
119	36.6	0	0.08
120	35.1	-1.5	-0.3
121	33.8	-1.3	-0.98
122	33.7	-0.1	-1.06
123	31.7	-2	-0.76
124	31.3	-0.4	-0.46
125	31.3	0	0
126	31.5	0.2	0.18
127	33.7	2.2	0.56
128	32.6	-1.1	0.6
129	34.1	1.5	0.48
130	34.3	0.2	-0.2
131	33.9	-0.4	-0.16
132	32.7	-1.2	-0.68
133	31.8	-0.9	-0.52
134	30.7	-1.1	-0.26
135	31.7	1	0.34
136	32.6	0.9	0.42
137	34.4	1.8	0.7
138	33.9	-0.5	1.2
139	34.2	0.3	1.7
140	37.7	3.5	2.26
141	41.1	3.4	3.22
142	45.7	4.6	3.76
143	50	4.3	3.18
144	53	3	2.22
145	53.6	0.6	1.2
146	52.2	-1.4	0.68
147	51.7	-0.5	-0.4
148	53.4	1.7	-0.22
149	51	-2.4	0.02
150	52.5	1.5	-0.22
151	52.3	-0.2	-0.6
152	50.6	-1.7	-0.15
153	50.4	-0.2	-0.7

Name	X	Y	Ele. (m)	DMEER
Posieux (Grangeneuve)	46.7643	7.0977	670	Western European Broadleaf forests

2011 HBNF	Day	Weight (KG)
NF Start	105	33.9
NF End	130	70.3
NF Duration	25	36.4
Quarter		9.1
25% Flow	112	43
50% Flow	120	52.1
75% Flow	125	61.2



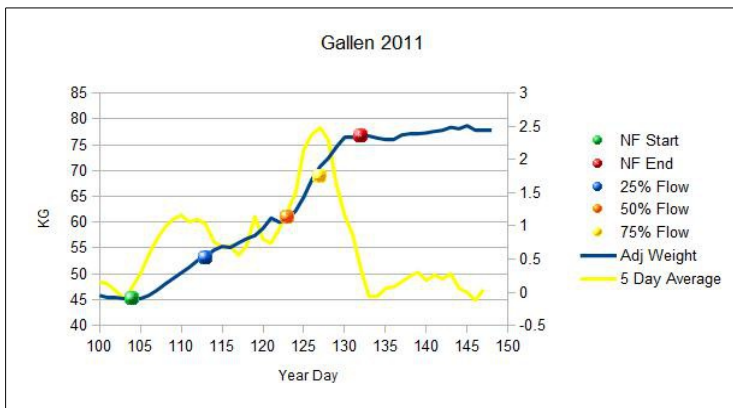
2011 NDVI	Year Day	Value
SOS	56.16	Base val 5461
End	333.28	Peak val 7496
Length	277.12	Ampl. 2035
Peak t	198.24	L.deriv. 715.9
		R.deriv. 866.7
		L.integral 134900
		S.integral 31190



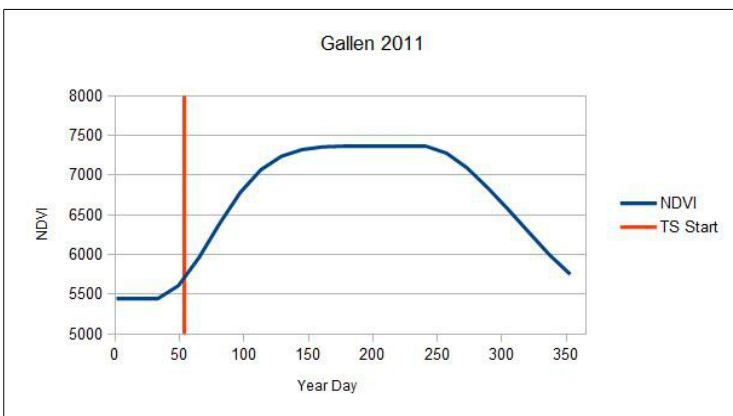
2011			
Day	Adj KG	Adj Day	5 Day Avg
92	33.2	0	0.04
93	32.7	-0.5	0.08
94	33	0.3	0.1
95	33.4	0.4	0.14
96	33.7	0.3	0.3
97	33.9	0.2	0.28
98	34.2	0.3	0.28
99	34.4	0.2	0.06
100	34.8	0.4	-0.02
101	34	-0.8	-0.1
102	33.8	-0.2	-0.18
103	33.7	-0.1	-0.18
104	33.5	-0.2	0.1
105	33.9	0.4	0.32
106	34.5	0.6	0.58
107	35.4	0.9	0.94
108	36.6	1.2	1.16
109	38.2	1.6	1.42
110	39.7	1.5	1.6
111	41.6	1.9	1.6
112	43.4	1.8	1.56
113	44.6	1.2	1.46
114	46	1.4	1.2
115	47	1	0.86
116	47.6	0.6	0.64
117	47.7	0.1	0.78
118	47.8	0.1	1.1
119	49.9	2.1	1.5
120	52.5	2.6	1.16
121	55.1	2.6	1.48
122	53.5	-1.6	1.6
123	55.2	1.7	1.8
124	57.9	2.7	1.88
125	61.5	3.6	2.7
126	64.5	3	2.74
127	67	2.5	2.34
128	68.9	1.9	1.76
129	69.6	0.7	0.86
130	70.3	0.7	0.36
131	68.8	-1.5	-0.2
132	68.8	0	-0.44
133	67.9	-0.9	-0.64
134	67.4	-0.5	-0.44
135	67.1	-0.3	-0.46
136	66.6	-0.5	-0.26
137	66.5	-0.1	-0.2
138	66.6	0.1	-0.1
139	66.4	-0.2	0
140	66.6	0.2	0.02
141	66.6	0	0
142	66.6	0	-0.16
143	66.6	0	-0.2
144	65.6	-1	-0.36
145	65.6	0	-0.42
146	64.8	-0.8	-0.4
147	64.5	-0.3	-0.2

Name	X	Y	Ele. (m)	DMEER
St. Gallen	47.4251	9.3766	671	Western European Broadleaf forests

2011 HBNF	Day	Weight (KG)
NF Start	104	45.1
NF End	132	76.6
NF Duration	28	31.5
Quarter		7.875
25% Flow	113	52.975
50% Flow	123	60.85
75% Flow	127	68.725



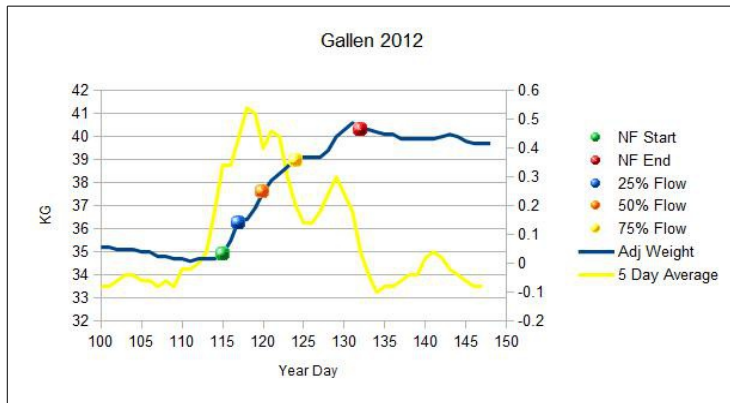
2011 NDVI	Year Day	Value
TS Start 15%	56.16	Base val 5442
End 15%	333.28	Peak val 7373
Length	277.12	Ampl. 1931
Peak t	198.24	L.deriv. 374.6
		R.deriv. 271.2
		L.integral 142000
		S.integral 27690



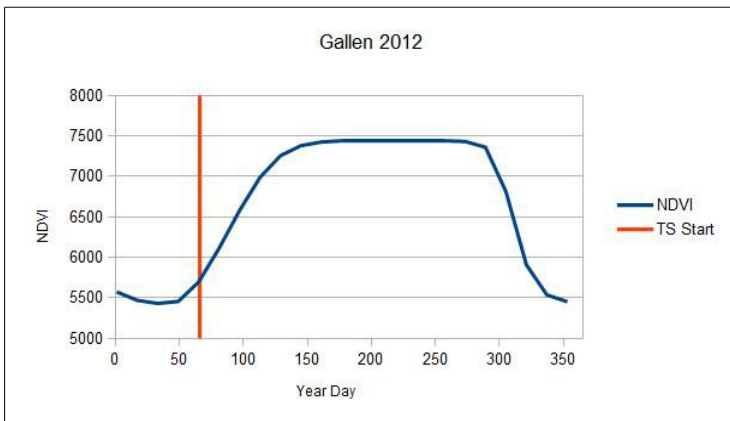
2011			
Day	Adj KG	Adj Day	5 Day Avg
90	44.5	0	
91	44.5	0	-0.025
92	44.4	-0.1	-0.02
93	44.4	0	-0.04
94	44.4	0	-0.04
95	44.3	-0.1	0.04
96	44.3	0	0.04
97	44.6	0.3	0.12
98	44.6	0	0.3
99	45	0.4	0.22
100	45.8	0.8	0.16
101	45.4	-0.4	0.12
102	45.4	0	0.02
103	45.2	-0.2	-0.1
104	45.1	-0.1	0.08
105	45.3	0.2	0.28
106	45.8	0.5	0.56
107	46.8	1	0.8
108	48	1.2	0.98
109	49.1	1.1	1.1
110	50.2	1.1	1.16
111	51.3	1.1	1.06
112	52.6	1.3	1.1
113	53.3	0.7	1.02
114	54.6	1.3	0.76
115	55.3	0.7	0.68
116	55.1	-0.2	0.7
117	56	0.9	0.56
118	56.8	0.8	0.7
119	57.4	0.6	1.14
120	58.8	1.4	0.8
121	60.8	2	0.74
122	60	-0.8	0.96
123	60.5	0.5	1.22
124	62.2	1.7	1.5
125	64.9	2.7	2.16
126	68.3	3.4	2.38
127	70.8	2.5	2.48
128	72.4	1.6	2.3
129	74.6	2.2	1.62
130	76.4	1.8	1.16
131	76.4	0	0.86
132	76.6	0.2	0.34
133	76.7	0.1	-0.06
134	76.3	-0.4	-0.06
135	76.1	-0.2	0.06
136	76.1	0	0.08
137	76.9	0.8	0.16
138	77.1	0.2	0.24
139	77.1	0	0.3
140	77.3	0.2	0.18
141	77.6	0.3	0.26
142	77.8	0.2	0.2
143	78.4	0.6	0.28
144	78.1	-0.3	0.06
145	78.7	0.6	0
146	77.9	-0.8	-0.12
147	77.8	-0.1	0.04
148	77.8	0	-0.06
149	78.3	0.5	-0.02
150	78.4	0.1	-0.02
151	77.8	-0.6	0.02
152	77.7	-0.1	0.02
153	77.9	0.2	-0.04
154	78.4	0.5	0.04
155	78.2	-0.2	0.18
156	78	-0.2	0.06
157	78.6	0.6	-0.1

Name	X	Y	Ele. (m)	DMEER
St. Gallen	47.4251	9.3766	671	Western European Broadleaf forests

2012 HBNF	Day	Weight (KG)
NF Start	115	34.9
NF End	132	40.3
NF Duration	17	5.4
Quarter		1.35
25% Flow	117	36.25
50% Flow	120	37.6
75% Flow	124	38.95



2012 NDVI	Year Day	Value	
Start	65.44	Base val	5436
End	327.2	Peak val	7441
Length	261.92	Ampl.	2005
Peak t	206.08	L.deriv.	422.6
		R.deriv.	750.6
		L.integral	125100
		S.integral	27290



2012			
Day	Adj KG	Adj Day	5 Day Avg
90	35.7	-0.1	-0.06
91	35.6	-0.1	-0.06
92	35.6	0	-0.06
93	35.5	-0.1	-0.02
94	35.5	0	0
95	35.6	0.1	-0.02
96	35.6	0	0
97	35.5	-0.1	-0.02
98	35.5	0	-0.08
99	35.4	-0.1	-0.08
100	35.2	-0.2	-0.08
101	35.2	0	-0.08
102	35.1	-0.1	-0.06
103	35.1	0	-0.04
104	35.1	0	-0.04
105	35	-0.1	-0.06
106	35	0	-0.06
107	34.8	-0.2	-0.08
108	34.8	0	-0.06
109	34.7	-0.1	-0.08
110	34.7	0	-0.02
111	34.6	-0.1	-0.02
112	34.7	0.1	0
113	34.7	0	0.04
114	34.7	0	0.18
115	34.9	0.2	0.34
116	35.5	0.6	0.34
117	36.4	0.9	0.44
118	36.4	0	0.54
119	36.9	0.5	0.52
120	37.6	0.7	0.4
121	38.1	0.5	0.46
122	38.4	0.3	0.44
123	38.7	0.3	0.3
124	39.1	0.4	0.2
125	39.1	0	0.14
126	39.1	0	0.14
127	39.1	0	0.18
128	39.4	0.3	0.24
129	40	0.6	0.3
130	40.3	0.3	0.24
131	40.6	0.3	0.18
132	40.3	-0.3	0.04
133	40.3	0	-0.04
134	40.2	-0.1	-0.1
135	40.1	-0.1	-0.08
136	40.1	0	-0.08
137	39.9	-0.2	-0.06
138	39.9	0	-0.04
139	39.9	0	-0.04
140	39.9	0	0.02
141	39.9	0	0.04
142	40	0.1	0.02
143	40.1	0.1	-0.02
144	40	-0.1	-0.04
145	39.8	-0.2	-0.06
146	39.7	-0.1	-0.08

All Locations/Years - HBNF 25%

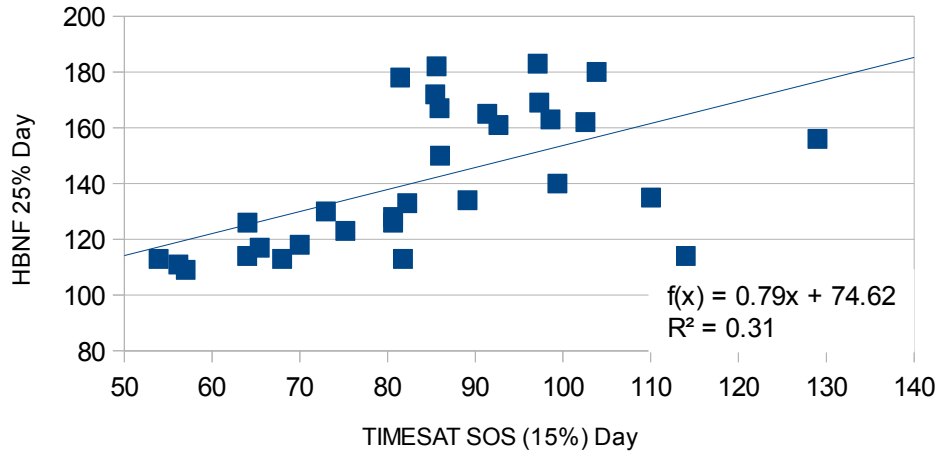


Figure 1: All Locations/Years – HBNF 25%, n=31

All Locations/Years - 75% HBNF

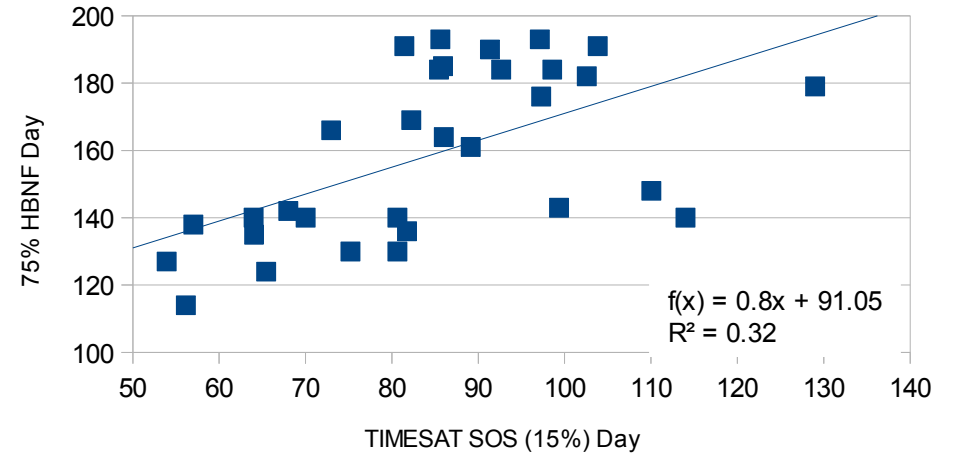


Figure 2: All Locations/Years – HBNF 75%, n=31

All Locations 2011 - HBNF Start

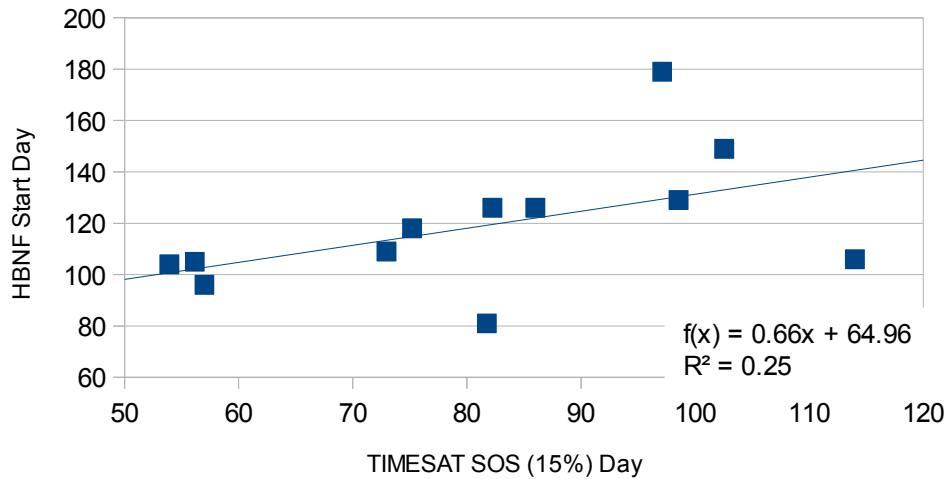


Figure 3: All Locations 2011 – HBNF Start, n=12

All Locations 2011 - HBNF 25%

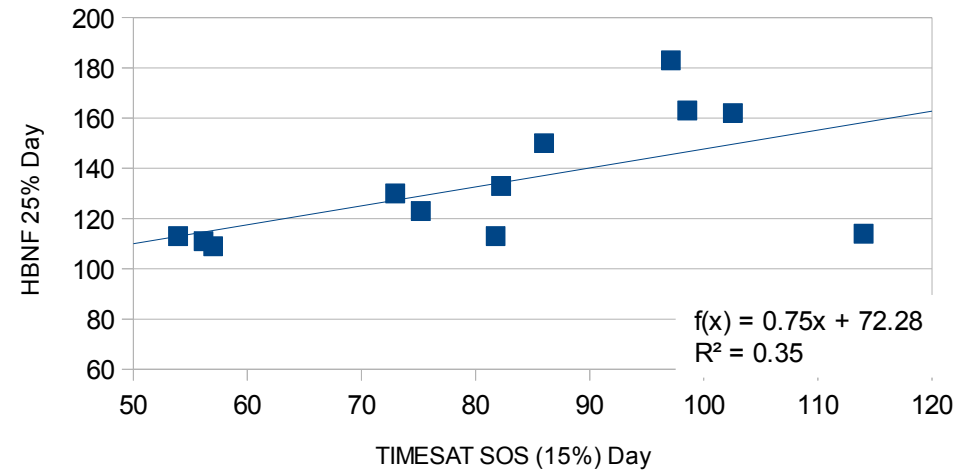


Figure 4: All Locations 2011 – HBNF 25%, n=12

All Locations 2011 - HBNF 50%

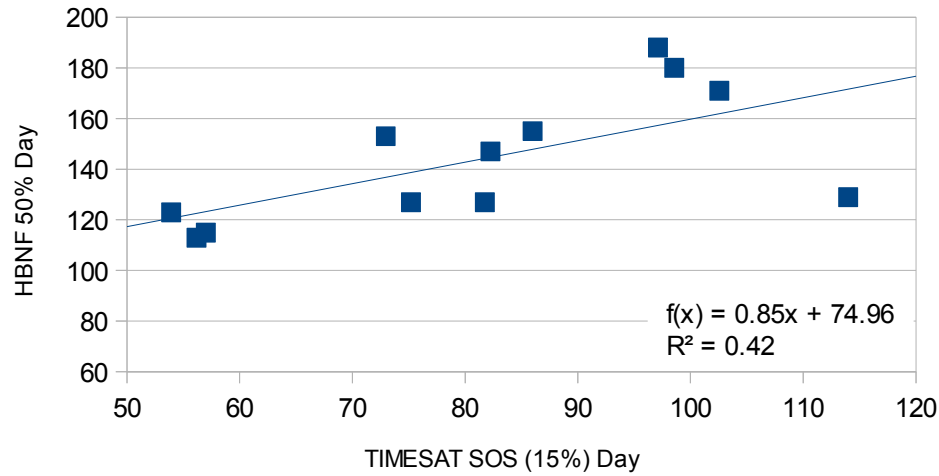


Figure 5: All Locations 2011 - HBNF 50%

All Locations 2011 - HBNF 75%

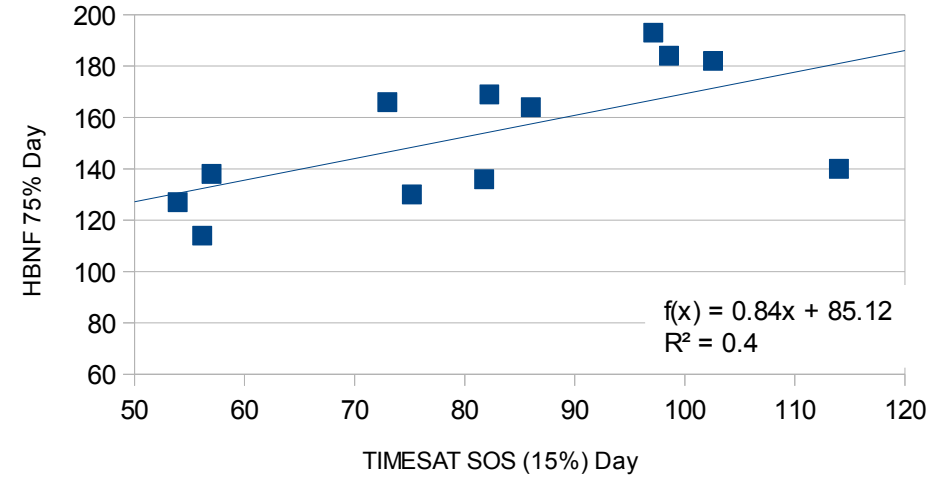


Figure 6: All Locations/Years – HBNF 75%, n=31

Slovenia - All Years HBNF 50%

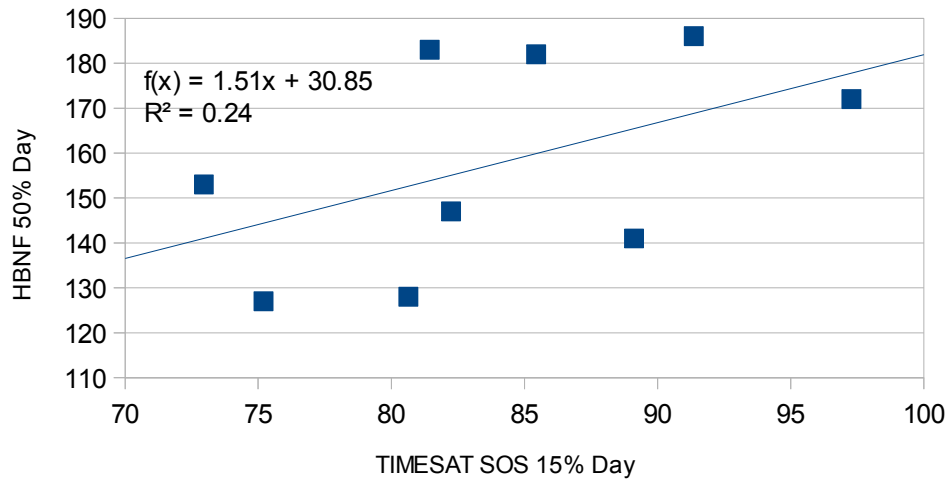


Figure 7: Slovenia – All Years HBNF 50%, n=9

Finland - All Years HBNF 50%

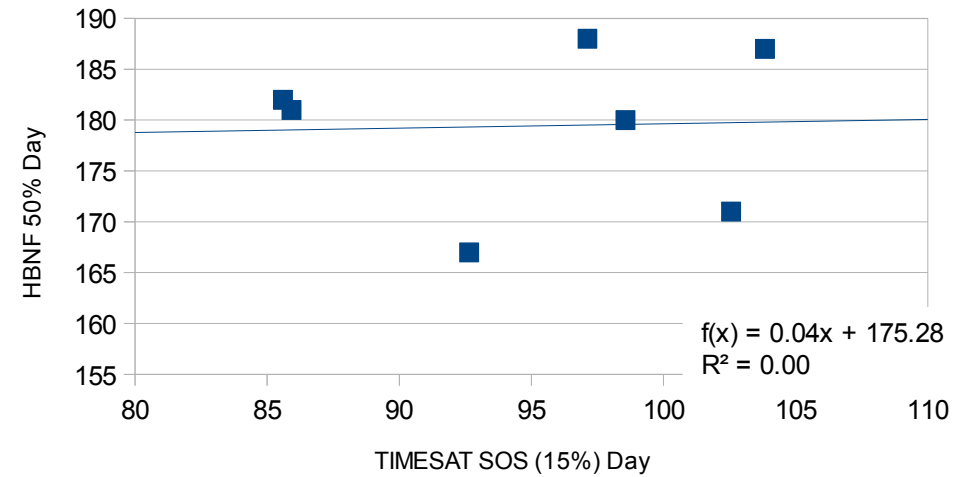


Figure 8: Finland – All Years HBNF 50%, n=7

<u>Data</u>	<u>File Type</u>	<u>Location</u>
HBNF Totals	LibreOffice Spreadsheet	M:\diss_final\hbnf_totals.ods
Scale-Hive	LibreOffice Spreadsheet	M:\diss_final\hbnf\
NDVI Data	ASCII	M:\diss_final\ndvi
LST Data	ASCII	M:\diss_final\lst
Hive Locations	Shapefile	M:\diss_final\gis\hivepoints.shp
DMEER	MS Database	M:\diss_final\gis\dmeereea4074i.mdb
<u>Program</u>		
TIMESAT	ZIP	M:\diss_final\timesat311_nostandalone.zip